DOE/ER/04447--187

DE85 006381

SPECTROSCOPIC AND ELECTROCHEMICAL STUDIES OF SELECTED LANTHANIDES AND ACTINIDES IN CONCENTRATED AQUEOUS CARBONATE AND CARBONATE-HYDROXIDE SOLUTIONS AND IN MOLTEN DIMETHYL SULFONE

A Dissertation

Presented for the

Doctor of Philosophy

Degree

The University of Tennessee, Knoxville

Peter Gregory Varlashkin

March 1985

LEGIBILITY NOTICE

A major purpose of the Technical Information Center is to provide the broadest dissemination possible of information contained in DOE's Research and Development Reports to business, industry, the academic community, and federal, state and local governments.

Although a small portion of this report is not reproducible, it is being made available to expedite the availability of information on the research discussed herein.

1

DEDICATION

The author dedicates this work to his parents, Dr. Paul G. and Charlotte D. Varlashkin.

ACKNOWLEDGMENTS

Suffice it to say that the successful completion of any doctoral research project is not possible without the help of many people. First, the author wishes to thank Dr. Joseph R. Peterson, research advisor, for financial, scientific, and moral support during the course of this research. Special thanks go to Dr. Richard G. Haire for technical assistance. The author has relied on Dr. Haire's chemical expertise on numerous occasions. The technical support and friendship of Dr. Haire are greatly appreciated.

Additional thanks are due Dr. George M. Begun for his technical expertise and support in obtaining the Raman spectroscopic data presented in this work. Thanks also go to Mr. W. Wilmarth, Mr. E. Earley, Mr. A. Massey, Mr. K. Sowder, Mr. J. H. Oliver, Mr. W. D. Carden, Mr. D. R. Simpson, Mr. C. Haynes, Dr. J. P. Young, Dr. R. L. Hahn, Dr. G. D. O'Kelley, Dr. O. L. Keller, Dr. C. Madic, Dr. K. Samhoun, Dr. H. E. Hellwege, Dr. J. Q. Chambers, Dr. M. J. Sepaniak, Dr. P. G. Huray, and Ms. S. A. Morris.

The outstanding glassblowing services of Mr. R. W. Poole and his staff are acknowledged. The secretarial services of Ms. A. Scott, Ms. B. Mercer, and Ms. R. Collins are gratefully acknowledged. Special thanks go to Ms. Carol Proaps for typing this dissertation.

The author expresses his appreciation for financial support provided by the Division of Chemical Sciences, Office of Basic Energy Sciences, U.S. Department of Energy under contracts DE-AS05-76ER04447 with The University of Tennessee (Knoxville), DE-AC05-84OR21400 with

Martin Marietta Energy Systems, Inc., and W-7405-eng-26 with Union Carbide Corporation. Additional thanks are due the Chemistry Division, Oak Ridge National Laboratory (operated by Martin Marietta Energy Systems, Inc.) and the Chemistry Department, The University of Tennessee.

Under the guidance of Dr. David E. Hobart, the author learned the necessary techniques for performing spectroscopic and electrochemical experiments in a gloved box environment. The author gained an immeasurable amount of practical experience working with Dr. Hobart. Just as importantly, the author gained a valued friend in David.

The author would like to thank his parents, Dr. Paul G. and Charlotte D. Varlashkin for instilling in the author the personal qualities necessary to see a research project such as this through to completion. The loving support of the author's parents is a constant driving and renewing force in both the personal and professional life of the author. Finally, the author would like to thank his father for being an individual to emulate. In his lifetime the author hopes to attain the same level of personal and professional integrity, honesty, and character exhibited by his father.

ABSTRACT

Electrochemical and spectroscopic studies of neptunium, plutonium, americium, californium, and terbium in concentrated aqueous carbonate and carbonate-hydroxide solutions have been carried out. Changes in the absorption spectra of Np(VII), Np(V), Pu(VI), Pu(V), Am(VI), and Am(V) in concentrated Na_2CO_3 solution and in the formal potentials of the Np(VI)/Np(V) and Pu(VI)/Pu(V) couples as a function of pH were observed. Heptavalent neptunium in concentrated Na_2CO_3 solution could only be produced at pH values close to or greater than 14. Plutonium(VII) in 2 M Na_2CO_3 solution could only be produced at hydroxide ion concentrations in excess of about 2.5 M. The Raman spectra of Np(VII) and Pu(VII) in Na_2CO_3-NaOH solution exhibit a single actinide ion vibration at 734 ± 2 cm^{-1} and 703 ± 6 cm^{-1}, respectively. The complexation of Np(VII) and Pu(VII) in Na_2CO_3-NaOH solution seems to be mainly by hydroxide ions. Neptunium(IV) and plutonium(IV) are insoluble in Na_2CO_3 solution above ca. pH 11-12. Neptunium(III) in carbonate solution is rapidly oxidized by water to Np(IV). Plutonium(III) is insoluble in Na_2CO_3 solution. In K_2CO_3 solution Pu(III) is stable to oxidation by water but is very sensitive to air oxidation.

The redox properties of Cf(III) in Na_2CO_3 and K_2CO_3 solutions at pH values from 8 to 14 were investigated. Californium(III) in bicarbonate-carbonate-hydroxide solution could not be oxidized to Cf(IV) chemically or electrochemically.

The oxidation of terbium(III) in K_2CO_3-KOH solution was studied. The concentrations of terbium, carbonate, and hydroxide ions

for generation and stabilization of Tb(IV) are critical. Redox titrations of Tb(IV) with $Fe(CN)_6^{4-}$ ion and analysis of Tb(IV) precipitates indicate that the Tb(IV) complex in solution is clustered in nature.

Spectroscopic and electrochemical studies of cerium, samarium, europium, ytterbium, uranium, neptunium, plutonium, and americium in molten dimethyl sulfone ($DMSO_2$) at 400 K were performed. Differences in the $DMSO_2$ solution absorption spectra of trivalent Sm, Eu, and Yb and divalent Eu compared with those in aqueous solution were observed. Complexation effects on the spectra of Ce(III), Ce(IV), U(VI), Np(VI), Pu(VI), and Am(VI) are more noticeable in poorly coordinating $DMSO_2$ than they are in water.

TABLE OF CONTENTS

CHAPTER PAGE

LIST OF TABLES

LIST OF FIGURES

CHAPTER I

INTRODUCTION

A. Background

There is a great deal of interest in the solution chemistry of the lanthanides and actinides. Solution studies of the f-transition elements are necessary in the development of separation and purification schemes for these elements. Applications in nuclear energy and technology depend on fundamental studies of the behavior of lanthanides and actinides in solution. The presence of actinides such as plutonium in the environment and problems in nuclear waste disposal are motivation enough for performing detailed solution studies in a controlled laboratory environment. Thus the literature contains numerous reports concerning the solution chemistry of the lanthanides and actinides in aqueous and, to a lesser extent, nonaqueous solutions.

The primary limiting factors involving research with actinides are their radioactive and toxic natures and the limited quantities available. Experimentation needs to be performed in ventilated hoods and/or air-flow gloved boxes. Containment of the activity is always of primary concern. The limited amounts of actinides (especially the transamericium elements) places limitations on the locations and types of experimentation. The Transuranium Research Laboratory (TRL) at the Oak Ridge National Laboratory, Oak Ridge, TN, is equipped for actinide solution research and is conveniently located near sources of the transuranium elements [e.g., the High Flux Isotope Reactor (HFIR), and the Transuranium Processing Plant (TRU)].

B. Oxidation States in Solution

1. Lanthanides

The most stable oxidation state of the lanthanides in aqueous solution is the trivalent state. The reason for the stability of the Ln(III) (Ln = lanthanide) state does not lie with the electronic configuration of the trivalent lanthanide ions but rather in the thermodynamics of such hydrated species. The ionization and hydration energies are of appropriate magnitude and sign such that the trivalent state is the most stable species in solution.[1] As seen in Table I, some of the lanthanide elements also exist in solution in the dipositive and tetrapositive states. These species are Eu(II), Yb(II), Sm(II), Ce(IV), Tb(IV), and Pr(IV). The appearance of these species in solution is related in part to the electronic configuration of these ions. Added stability is obtained when an empty, half-filled, or filled 4f shell occurs. For example, Ce(IV) is the most stable tetravalent lanthanide, and it has a $4f^0$ electronic configuration. Divalent europium is the most stable divalent lanthanide ion, and it has a $4f^7$ electronic configuration. Listed in Table II are the electronic configurations of the lanthanide atoms and their ions.

a. Ln(II). The divalent state is known for Sm, Eu, and Yb both in solution and in the solid state.[1] Divalent Eu is stable in

TABLE I

OXIDATION STATES OF THE LANTHANIDE ELEMENTS IN SOLUTION

Element	Symbol	Oxidation States[a]
Cerium	Ce	3 4
Praseodymium	Pr	3 (4)
Neodymium	Nd	3
Promethium	Pm	3
Samarium	Sm	2 3
Europium	Eu	2 3
Gadolinium	Gd	3
Terbium	Tb	3 (4)
Dysprosium	Dy	3
Holmium	Ho	3
Erbium	Er	3
Thulium	Tm	3
Ytterbium	Yb	2 3
Lutetium	Lu	3

[a]The species in parentheses are known only in carbonate-hydroxide solution. The most stable oxidation states are underlined.

TABLE II

ELECTRONIC CONFIGURATIONS OF LANTHANIDE ATOMS AND IONS[a]

Atomic number	Symbol	Electronic configuration Atom	M(II)	M(III)	M(IV)
58	Ce	$4f^1 5d^1 6s^2$	$4f^2$	$4f^1$	$4f^0$
59	Pr	$4f^3 \quad 6s^2$	$4f^3$	$4f^2$	$4f^1$
60	Nd	$4f^4 \quad 6s^2$	$4f^4$	$4f^3$	–
61	Pm	$4f^5 \quad 6s^2$	–	$4f^4$	–
62	Sm	$4f^6 \quad 6s^2$	$4f^6$	$4f^5$	–
63	Eu	$4f^7 \quad 6s^2$	$4f^7$	$4f^6$	–
64	Gd	$4f^7 5d^1 6s^2$	$4f^7 5d^1$	$4f^7$	–
65	Tb	$4f^9 \quad 6s^2$	$4f^9$	$4f^8$	$4f^7$
66	Dy	$4f^{10} \quad 6s^2$	$4f^{10}$	$4f^9$	$4f^8$
67	Ho	$4f^{11} \quad 6s^2$	$4f^{11}$	$4f^{10}$	–
68	Er	$4f^{12} \quad 6s^2$	$4f^{12}$	$4f^{11}$	–
69	Tm	$4f^{13} \quad 6s^2$	$4f^{13}$	$4f^{12}$	–
70	Yb	$4f^{14} \quad 6s^2$	$4f^{14}$	$4f^{13}$	–
71	Lu	$4f^{14} 5d^1 6s^2$	–	$4f^{14}$	–

[a]Only the valence-shell electrons (those outside the [Xe] core) are given. A dash indicates that this oxidation state is not known.

aqueous solution, but Sm(II) and Yb(II) are unstable to oxidation by water and by air.[2] The standard reduction potentials of the Ln(III)/Ln(II) couple for Sm, Eu, and Yb are −1.55, −0.35, and −1.15 V/NHE (normal hydrogen electrode), respectively.[3]

b. Ln(III). This is the most stable oxidation state for all the lanthanides in aqueous solution.

c. Ln(IV). Tetravalent Ce, Pr, and Tb have been found in aqueous solution.[1,4] In aqueous solution Ce(IV) is a strong oxidant and is a well known analytical reagent. Both Tb(IV) and Pr(IV) oxidize water quite rapidly and require complexing agents to stabilize them in solution.[4] As will be discussed later, complexing agents can be used to shift reduction potentials negatively and thereby stabilize otherwise unstable oxidation states. The standard reduction potentials of the Ln(IV)/Ln(III) couple for Ce, Pr, and Tb are +1.74, ca. +3.2, and +3.1 V/NHE, respectively, in noncomplexing solution.[1,5]

2. Actinides

As seen in Table III, the actinides exhibit a wider range of oxidation states than do the lanthanides. After Am, the onset of lanthanide-like behavior occurs. For Am-Lr, excluding No, the trivalent state is the most stable oxidation state. In contrast, the most stable oxidation state of U is U(VI), which has a $5f^0$ electronic configuration. The electronic configurations of the An (An = actinide) atoms and their ions are listed in Table IV.

TABLE III

OXIDATION STATES OF THE ACTINIDE ELEMENTS IN SOLUTION

Element	Symbol	Oxidation states[a]
Thorium	Th	_4_
Protactinium	Pa	4 _5_
Uranium	U	3 4 5 _6_
Neptunium	Np	3 4 _5_ 6 7
Plutonium	Pu	3 _4_ 5 6 7
Americium	Am	(2) _3_ 4 5 6
Curium	Cm	(2) _3_ 4
Berkelium	Bk	_3_ 4
Californium	Cf	(2) _3_
Einsteinium	Es	2 _3_
Fermium	Fm	2 _3_
Mendelevium	Md	2 _3_
Nobelium	No	_2_ 3
Lawrencium	Lr	_3_

[a]The species in parentheses were produced by pulse radiolysis (10–100 ms lifetimes). The most stable oxidation states are underlined.

TABLE IV

ELECTRONIC CONFIGURATIONS OF ACTINIDE ATOMS AND IONS[a]

Atomic number	Element	Electronic configuration						
		Atom	M(II)	M(III)	M(IV)	M(V)	M(VI)	M(VII)
90	Th	$5f^0 6d^2 7s^2$	–	–	$5f^0$	–	–	–
91	Pa	$5f^2 6d^1 7s^2$	–	–	$5f^1$	$5f^0$	–	–
92	U	$5f^3 6d^1 7s^2$	–	$5f^3$	$5f^2$	$5f^1$	$5f^0$	–
93	Np	$5f^4 6d^1 7s^2$	–	$5f^4$	$5f^3$	$5f^2$	$5f^1$	$5f^0$
94	Pu	$5f^6 \; 7s^2$	–	$5f^5$	$5f^4$	$5f^3$	$5f^2$	–
95	Am	$5f^7 \; 7s^2$	$5f^7$	$5f^6$	$5f^5$	$5f^4$	$5f^3$	–
96	Cm	$5f^7 6d^1 7s^2$	–	$5f^7$	$5f^6$	–	–	–
97	Bk	$5f^9 \; 7s^2$	–	$5f^8$	$5f^7$	–	–	–
98	Cf	$5f^{10} \; 7s^2$	$5f^{10}$	$5f^9$	$5f^8$	–	–	–
99	Es	$5f^{11} \; 7s^2$	$5f^{11}$	$5f^{10}$	–	–	–	–
100	Fm	$5f^{12} \; 7s^2$	$5f^{12}$	$5f^{11}$	–	–	–	–
101	Md	$5f^{13} \; 7s^2$	$5f^{13}$	$5f^{12}$	–	–	–	–
102	No	$5f^{14} \; 7s^2$	$5f^{14}$	$5f^{13}$	–	–	–	–
103	Lr	$5f^{14} 6d^1 7s^2$	–	$5f^{14}$	–	–	–	–

[a]Only the valence-shell electrons (those outside the [Rn] core) are given. A dash indicates that this oxidation state is not known, or the configuration of this oxidation state is not known.

a. An(II). Nobelium(II) is the most stable oxidation state for No. Mendelevium(II) is fairly stable. The other known divalent actinides are very unstable in solution.[6,7]

b. An(III). All the actinides except for Th and Pa exhibit this oxidation state in solution.[7] Uranium(III) is a strong reducing agent and the least stable of the trivalent actinides.

c. An(IV). This is the most stable oxidation state for Th[6] and Pu.[7] Einsteinium through lawrencium do not exhibit the tetravalent state in solution. Curium(IV) has been generated in aqueous solution by pulse radiolysis.[8] Claims have been made for the generation of bulk Cm(IV) and Cf(IV) in solution by oxidizing their corresponding trivalent species in phosphotungstate, $K_{10}P_2W_{17}O_{61}$ solutions.[9] However, the reported shift in potential of the An(IV)/An(III) couple should not be sufficient to stabilize Cm(IV) and Cf(IV) in aqueous solution. Keenan[10] prepared a solution of tetravalent Cm by dissolving CmF_4 in concentrated CsF solution.

d. An(V). The dioxy cation AnO_2^+ is found in solution for Pa-Am.[7] The pentavalent state is the most stable state for Pa and Np. Uranium(V), plutonium(V), and americium(V) tend to disproportionate in solution, but they can be stabilized under the proper conditions.[7]

e. An(VI). The hexavalent state for U, Np, Pu, and Am exists in solution as AnO_2^{2+} ions.[7] Uranium(VI) is the most stable oxidation state of this element.

f. An(VII). Both Np(VII) and Pu(VII) can exist in strongly alkaline media, probably in the form $AnO_2(OH)_n^{(3-n)+}$.[6] Heptavalent Np has the $5f^0$ electronic configuration. Am(VII) has been claimed,[11] but other researchers[6] have failed to reproduce this work.

C. Solution Absorption Spectra

There are three types of electronic absorption bands seen for the lanthanides and actinides. Transitions between electronic states involving only the 4f (lanthanide) or 5f (actinide) orbitals are known as f-f transitions. These bands are sharp, Laporte-forbidden ($\Delta J = 0$) and exhibit absorption coefficients of 0-10 $\underline{M}^{-1}$ cm^{-1} for the lanthanides[12] and approximately an order of magnitude larger for the actinides.[13] Due to the reduced shielding of the 5f orbitals in comparison to the 4f orbitals, the f-f absorption bands of the actinides are more intense (more allowed) and broader than those of the lanthanides.

Transitions from the 4f to 5d (lanthanides) or the 5f to 6d (actinides) orbitals are called f-d transitions. These bands are Laporte allowed ($\Delta J = \pm 1$) and exhibit molar absorptivity coefficients several orders of magnitude larger than those for the f-f transitions.[13]

Charge-transfer absorption bands involving transfer of an electron from a ligand orbital to a metal orbital or vice-versa are similar to f-d absorption bands in intensity. Both the charge-transfer and the f-d absorption bands of the lanthanides and actinides are quite broad due to the increased interaction of the participating orbitals with perturbing fields.[13] The frequencies of these absorption bands are affected by the complexing agents and solvents used, while the f–f absorption bands are much less affected by the species' environment.[13]

D. Complexing Agents and Their Effect on Redox Chemistry

The values of the reduction potentials of the various redox couples give an indication of the relative stabilities of the various lanthanide and actinide oxidation states. Some potentials are sufficiently high that the higher oxidation state species oxidizes the solvent. Complexing agents can be used to shift negatively the formal potential, thereby stabilizing the higher oxidation state. In a metal ion solution containing a mixture of oxidation states, ligands preferentially complex species with the higher charge-to-radius ratio[14] which is usually (but not always) the species in the higher oxidation state. The negative potential shift is due to the increased complexation of the higher oxidation state over the lower oxidation state. For example, the reduction potential of the Ce(IV)/Ce(III) couple in noncomplexing 1 M $HClO_4$ is +1.70 V/NHE.[2] In 1 M H_2SO_4 the reduction potential is +1.44 V/NHE, a negative potential shift of −0.26 V, indicating sulfate complexation.[2] In strongly complexing aqueous carbonate media, the Ce(IV)/Ce(III) reduction potential is shifted to +0.05 V/NHE.[4] Terbium(IV) is unstable in aqueous acid solution due to the high reduction potential of the Tb(IV)/Tb(III) couple. Thus, Tb(III) cannot be oxidized in bulk to Tb(IV) in aqueous acid solution. However, in aqueous carbonate-hydroxide solution, Tb(III) can be oxidized (chemically or electrolytically) to form a stable Tb(IV) species.[4]

For the actinides, the sequence of complexing strength of a ligand for the various oxidation states of a particular actinide is[6]

$$An^{4+} > AnO_2^{2+} > An^{3+} > AnO_2^{+}.$$

The AnO_2^{2+} cation has an effective charge greater than +3.[6] Since the ligand(s) bonds in the equatorial positions of the linear AnO_2^{2+} cation, the ligand(s) sees a charge greater than +3. Thus AnO_2^{2+} is complexed somewhat more strongly than is An^{3+}.

Lanthanides and actinides form two major types of complexes: inner sphere and outer sphere.[6,15] In outer sphere complexes, the metal ion and the ligand(s) are separated by a solvent molecule. Weak complexing agents such as halides (except F^-), nitrates, and sulfonates form outer sphere complexes. Fluoride, iodate, and sulfate ions (strong complexing agents) are examples of ligands that tend to form inner sphere complexes where there is no solvent molecule between the metal ion and the ligand.

For aqueous solutions the most important ligand is probably the hydroxide ion.[16] Thus pH is an important factor in complexation. Large H^+ concentrations are needed to suppress the hydrolysis (OH^- complexation) of lanthanide and actinide ions. The hydrolysis of some actinide ions is complicated by the formation of polymers. For example, in aged solutions Pa(V) can form irreversible hydrolysis products [Pa(V) colloids].[16] The stability of some actinides in solution is affected by pH, even in the presence of large concentrations of other complexing agents. For example, U(V) disproportionates rapidly to U(VI) and U(IV), but it can be stabilized to a certain degree at pH 2-4.[16] In 2 M Na_2CO_3, U(V) is stable when the pH = 11-12.[17] Below pH 11, disproportionation occurs, and above pH 12, a black amorphous precipitate forms.

E. The Use of Nonaqueous Solvents in Electrochemistry

The use of nonaqueous solvents for characterizing the solution chemistry of the lanthanides and actinides encompasses a wide range of studies. One advantage of nonaqueous solvents over water is the more extended electrochemical working range. Bulk reduction in water at potentials more negative than ca. -2 V/NHE is not possible due to the reduction of water to form hydrogen gas and hydroxide ions. Organic solvents such as dimethylsulfoxide (DMSO), dimethylformamide (DMF), and acetonitrile have voltammetric ranges down to about -2.6 V/NHE.[18] Reduction of Sm(III) to Sm(II) is not possible in aqueous solution. Divalent Sm is quickly oxidized by water but can be stabilized in purified (water free) nonaqueous solvents [e.g., hexamethylphosphoramide (HMPA)[19]]. Thus, spectroscopic and other physicochemical solution studies of Sm(II) can be performed in nonaqueous media that could not be performed (or at least without extreme difficulty) in aqueous solution.

Some common difficulties with nonaqueous media are lack of solubility of the lanthanide and actinide species of interest, inability to dry completely polar organic solvents, and complicating interactions of the solvents with electrochemical cells (e.g., surface passivation of working electrodes). Nevertheless, the diversity of media available provides a wide range of solution environments. For example, solvents may be liquid at low temperatures, such as NH_3, or at high temperatures, such as molten salts.

F. Proposed Research

Bulk electrolysis is a chemically "clean" and selective method of converting a solution containing a mixture of lanthanide or actinide oxidation states to a solution containing a single oxidation state species. Techniques such as cyclic voltammetry, coulometry, UV-Vis-IR spectroscopy, and spectroelectrochemistry can be used to characterize the various oxidation states (produced by bulk electrolysis or by chemical means). Two different media are used in this work to study the electrochemical and spectroscopic properties of selected lanthanides and actinides. The solution chemistry of certain lanthanide and actinide ions in concentrated aqueous carbonate media is explored. Dimethyl sulfone, $(CH_3)_2SO_2$, is used as a nonaqueous medium for additional solution studies.

1. Aqueous Carbonate Studies

There is considerable interest in the solution chemistry of the actinides in aqueous carbonate media for practical applications as well as for purely basic research. Certain separation/purification schemes involve the use of carbonate solution. In the Purex process for the separation of plutonium from irradiated uranium fuels, tributyl phosphate (TBP) is used as an extractant.[20] At one point in the purification process, the organic phase is washed with sodium carbonate solution to remove hydrolysis products such as monobutyl and dibutyl phosphates and U(VI) and Pu(IV) ions. Separation of Am from Cm and the lanthanides in irradiated plutonium targets can be achieved by oxidizing Am(III) to Am(V) in carbonate solution.[21] The Am(V) forms insoluble "double-carbonate" compounds which can be isolated from the soluble Cm and lanthanide species by filtration. Carbonate and bicarbonate ions have been shown to be environmentally important ions.[22,23] Due to the existence of actinides in the environment from nuclear detonations and nuclear waste storage problems (leakage into the environment), studies of actinides in carbonate media are vitally important.

The wide range of oxidation states available gives the actinides a diverse solution chemistry. The properties of the actinides in acid solution differ from those in carbonate solution. Thus, the solution chemistry of the actinides in carbonate media cannot be inferred from known acidic solution chemistry. Direct studies in carbonate media are required.

Due to the radioactivity, toxic nature, and limited availability of the actinides, precursor studies of the lanthanides in solution are important. Work with the lanthanides in carbonate solution also leads to a better understanding of their chemistry.

Various reports of the chemistry of the lanthanides and actinides in aqueous carbonate and bicarbonate solutions have appeared in the literature.[4,17,24-29] To date solution studies involving actinides in carbonate media have placed emphasis on solutions less basic than pH 12. In order to characterize more completely the actinides in carbonate media, the solution chemistry of carbonate-hydroxide solutions of Np, Pu, Am, Cf, and Tb were investigated. Standard electrochemical and spectroscopic techniques were employed.

2. Molten Dimethyl Sulfone Studies

The unique properties of dimethyl sulfone ($DMSO_2$) make it an interesting solvent for the lanthanides and actinides (as well as the transition metals). $DMSO_2$ is a highly polar molecule and is a poor co-ordinator.[50-52] $DMSO_2$ has a wide electrochemical range from about +2 V to approximately -3.5 V vs an Ag/Ag^+ reference electrode.[50] $DMSO_2$ is spectrally transparent in the UV-VIS region.

One of the principal difficulties encountered in electrochemical studies with organic solvents such as DMSO, DMF, and acetonitrile is the lack of adequate (and simple) drying procedures. Elaborate and time consuming drying techniques involving distillations, drying agents, and molecular sieves are not always sufficient to remove water contamination. $DMSO_2$ is a solid at room temperature (m.p. 108°C) and is easily dried in a vacuum oven. Work involving bulk electrolysis of species in $DMSO_2$ has not been reported in the literature for any element (to the knowledge of this author). Cyclic voltammetry, bulk electrolysis/coulometry, chemical oxidation, and spectroscopy of lanthanides and actinides in molten dimethyl sulfone were performed. The results obtained are compared with those from similar studies in aqueous solutions.

CHAPTER II

EXPERIMENTAL TECHNIQUES

A. Background

Consider the general electrochemical reaction (half-cell)

$$Ox + ne^- \rightleftarrows Red \quad (1)$$

where Ox and Red represent the oxidized and reduced forms of an electroactive species. The measured potential of the half-cell is related to the concentrations of Ox and Red by the Nernst equation.

$$E = E° + (RT/nF)\ln([Ox]/[Red]) + (RT/nF)\ln K_{act}, \quad (2)$$

where E is the electrode potential, E° is the standard reduction potential of the half-cell, R is the gas constant, T is the absolute temperature, n is the number of moles of electrons exchanged, F is the Faraday, [Ox] and [Red] are the molar concentrations of Ox and Red, respectively, and K_{act} is a constant incorporating the activity coefficients of Ox and Red. Since activity coefficients are rarely known, the formal potential, E°', instead of E° is used where

$$E = E°' + (RT/nF)\ln([Ox]/[Red] \quad (3)$$

and

$$E°' = E° + (RT/nF)\ln K_{act}. \quad (4)$$

The formal potential of an oxidation-reduction (redox) couple is dependent on the nature of the medium. For example, the formal potential can vary with changes in ionic strength and complexation.[53]

The principal electrochemical experiments used in this research were controlled potential bulk electrolysis/coulometry and cyclic voltammetry. In controlled potential coulometry,[54] a suitably positive or negative applied potential with respect to a reference potential is maintained at a working electrode (the electrode where the electrochemical reaction of interest is carried out) to drive an electrochemical reaction to completion. The charge passed in an exhaustive electrolysis is related by Faraday's law to the equivalents of the electroactive species.[55]

In cyclic voltammetry,[56] a quiescent solution is electrochemically probed by sweeping the applied potential of a small working electrode (e.g., a Pt disc electrode or a hanging mercury drop electrode) around the formal potential of a redox couple. Electrochemical information concerning the nature of a redox couple can be obtained quickly. Experimentally, the potential at the working electrode, E(t), is varied linearly with time such that

$$E(t) = E_i \pm vt, \qquad (5)$$

where E_i is the initial applied potential, v is the potential sweep rate (V/s), and t is the sweep time. At some potential E(λ), the direction of the potential sweep is reversed (at t = λ). The applied potential is then swept back to E_i.

A cyclic voltammogram of an idealized reversible (nernstian) couple is shown in Figure 1. If on applying a certain potential to a working electrode, the concentration ratio of Ox and Red around the electrode quickly approaches the value predicted by the Nernst

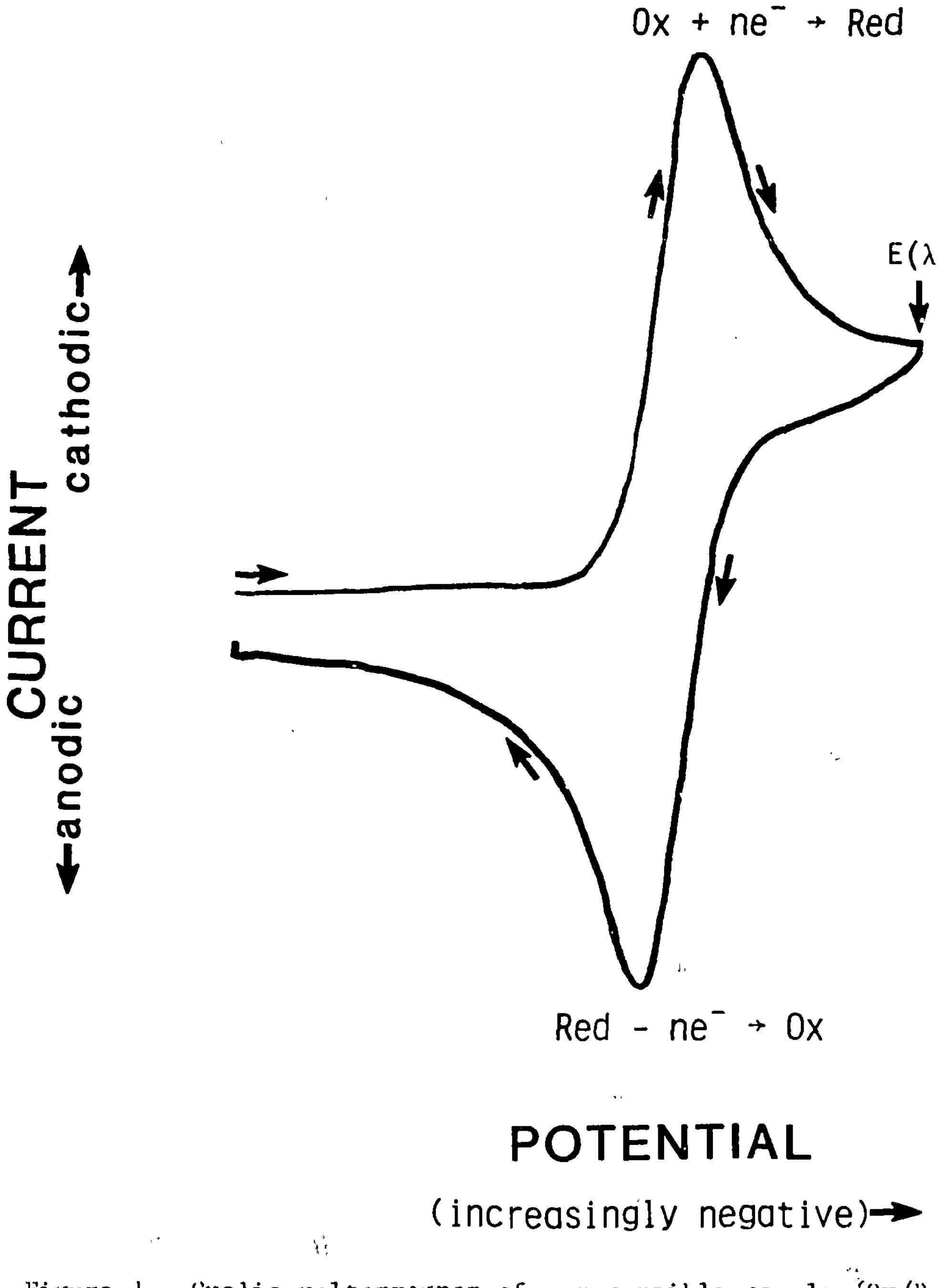

Figure 1. Cyclic voltammogram of a reversible couple (Ox/Red). E(λ) is the switching potential (the point where the scan direction is reversed).

equation (see Equation 3), the system is said to be reversible. For a nernstian system [e.g., Fe(III)/Fe(II) in 1 M KCl], the formal potential of the redox couple can be approximated as the midpoint between the cathodic (positive) and the anodic (negative) current peak potentials. Notice the current and potential sign conventions used in Figure 1 and in all cyclic voltammograms presented in this work.

Instead of monitoring the current in a controlled potential experiment, the absorbance of Ox and/or Red can be monitored. The simplest type of spectroelectrochemical experiment involves the use of an optically transparent electrode (OTE) through which the optical light source beam is transmitted. The absorbance of an electroactive species at the electrode surface or in the bulk solution is monitored while a potential is applied to the OTE. Extensive reviews of spectroelectrochemistry are available in the literature.[57,58]

B. Equipment

1. Radioactivity Containment

All manipulations involving radioactive materials (except uranium) were performed in a gloved box. For procedures requiring an inert atmosphere, a He-filled gloved box was used. All other manipulations were performed in conventional three-foot, air-flow gloved boxes. Two air-flow gloved boxes were modified with an appendage to allow coupling to a spectrophotometer. Two different designs were used. In one gloved box, a side compartment of the gloved box is equipped with quartz windows, and it slides into the sample/reference compartment of a Cary Model 14-H spectrophotometer (see Figure 2). This box is also equipped with a centrifuge. The other gloved box has an appendage that lowers into the sample compartment of a Cary Model 14-L spectrophotometer (see Figures 3 and 4). This box is equipped with water lines (for input and drain) for cooling a resistively-heated absorption cell. Both boxes are equipped with electrical and gas connections. Solution preparations involving uranium were performed in a hood.

2. Spectrophotometers

Solution absorption and solid state reflectance spectra were recorded with Cary Model 14-H and Cary Model 14-L spectrophotometers. Quartz cuvets of 0.5, 1, and 2 cm path lengths were used. For the aqueous solution absorption spectra, the reference cuvet was filled with the solvent. The $DMSO_2$ solution absorption spectra were referenced versus an empty quartz cuvet. Infrared spectra of solids were obtained from mineral oil mulls using a Perkin-Elmer 521 spectrophotometer equipped with AgCl windows.

Raman spectra were recorded using a Ramanor HG-2S spectrophotometer (Jobin Yvon-Instruments S. A.) equipped with concave, aberration corrected, holographic gratings, photoelectric detection, and pulse counting electronics. Excitation for the Raman spectra was achieved using the 488.0 or 514.5 nm line of a Spectra-Physics Model 164 argon ion laser, the 647.1 nm line of a Spectra-Physics Model 164-01 krypton ion laser, or the 633 nm line of a CW dye laser (Coherent Radiation Model 590). Both solids and

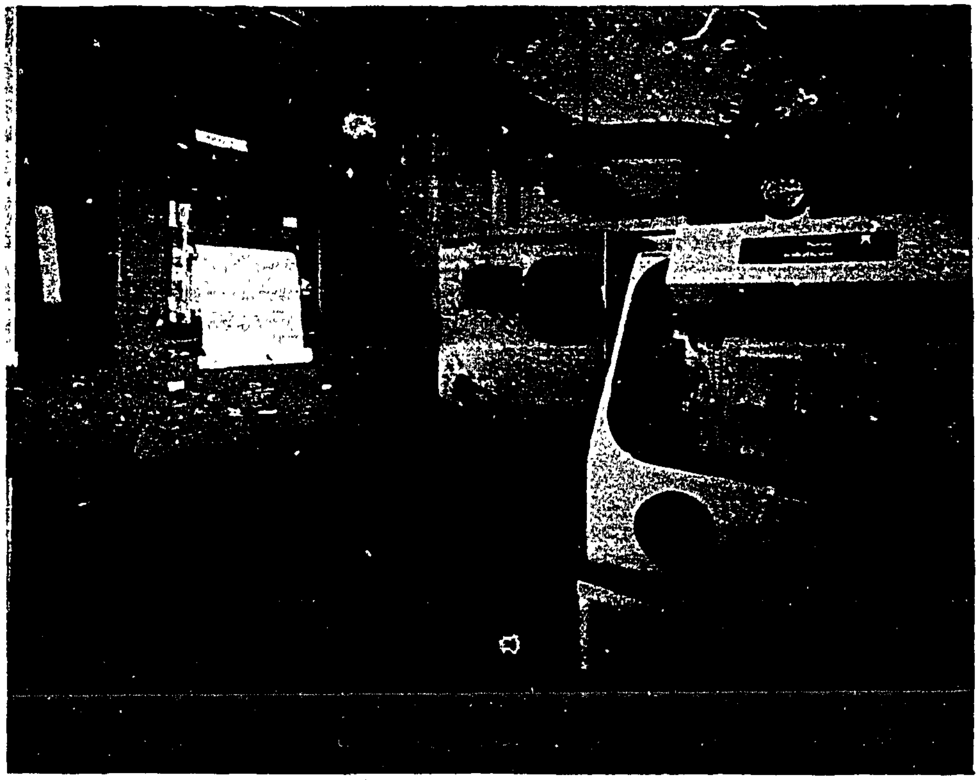

Figure 2. Spectrophotometer/gloved box assembly #1. Appendage on left side of the gloved box slides into the sample/reference compartment of the spectrophotometer.

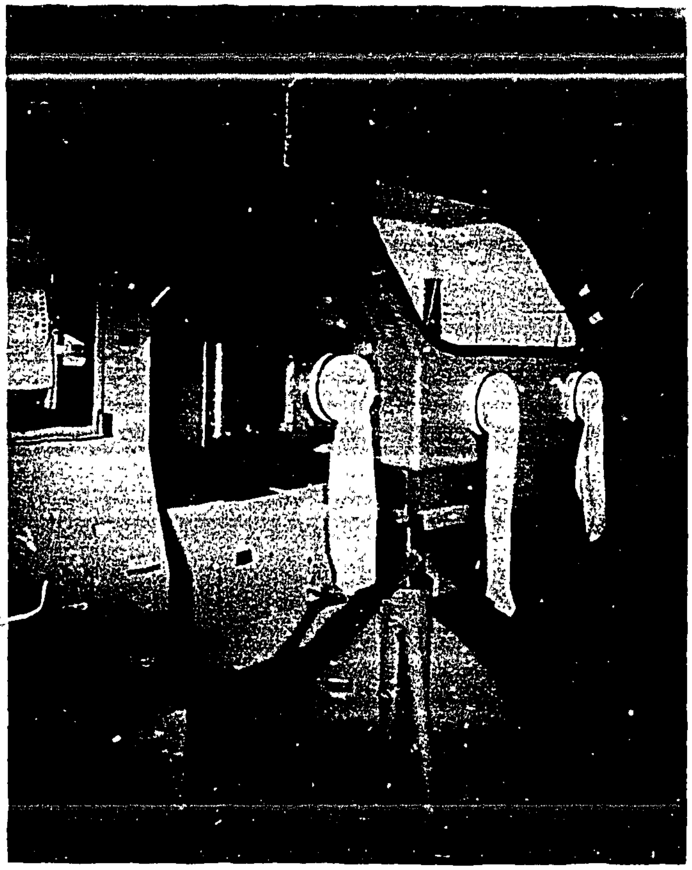

Figure 3. Spectrophotometer/gloved box assembly #2. Glove box is raised and lowered by a hydraulic jack. See also Figure 4.

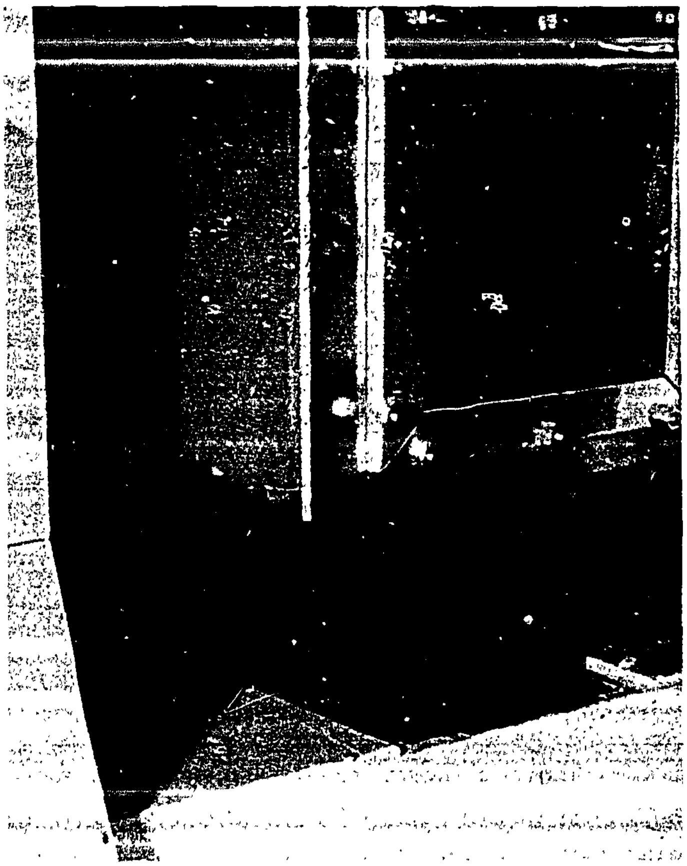

Figure 4. Absorption cell appendage of gloved box (see Figure 3). Appendage lowers into the sample compartment of the spectrophotometer.

solutions were doubly contained to prevent radioactive contamination of the spectrophotometer by mounting capillaries (for solids) or 0.5 cm path length pyrex solution cells in stoppered test tubes.

3. Resistively-Heated Absorption Cell

A schematic drawing of the resistively-heated absorption cell used in the $DMSO_2$ studies is presented in Figure 5. Essentially, the cell consists of an outer Teflon body (painted black) with coiled copper tubing, water cooling lines placed inside the cell block. Within the cooling coils is an aluminum cell holder wrapped with insulated Nichrome wire (for resistive heating). An autotransformer controls the voltage applied to the heating wire. A 1 cm path length quartz cuvet that fits inside the aluminum cell holder has a Teflon cap with a hole in it for placement of a thermocouple. The whole assembly fits inside the sample compartment appendage of the gloved box (see Figure 4).

4. Voltammeter

Electrochemical measurements were performed with an EG&G PARC Model 173D/179D/175 potentiostat/coulometer/universal programmer. Voltammograms were recorded using an Esterline Angus Model XY 530 recorder.

5. X-ray Spectrometer

A General Electric Model XRD-6 X-ray generator provided copper X radiation, and a nickel foil was used to filter out the Cu K_β radiation. Debye-Scherrer-type cameras (57.3 mm diameter)

ORNL-DWG 84-15154

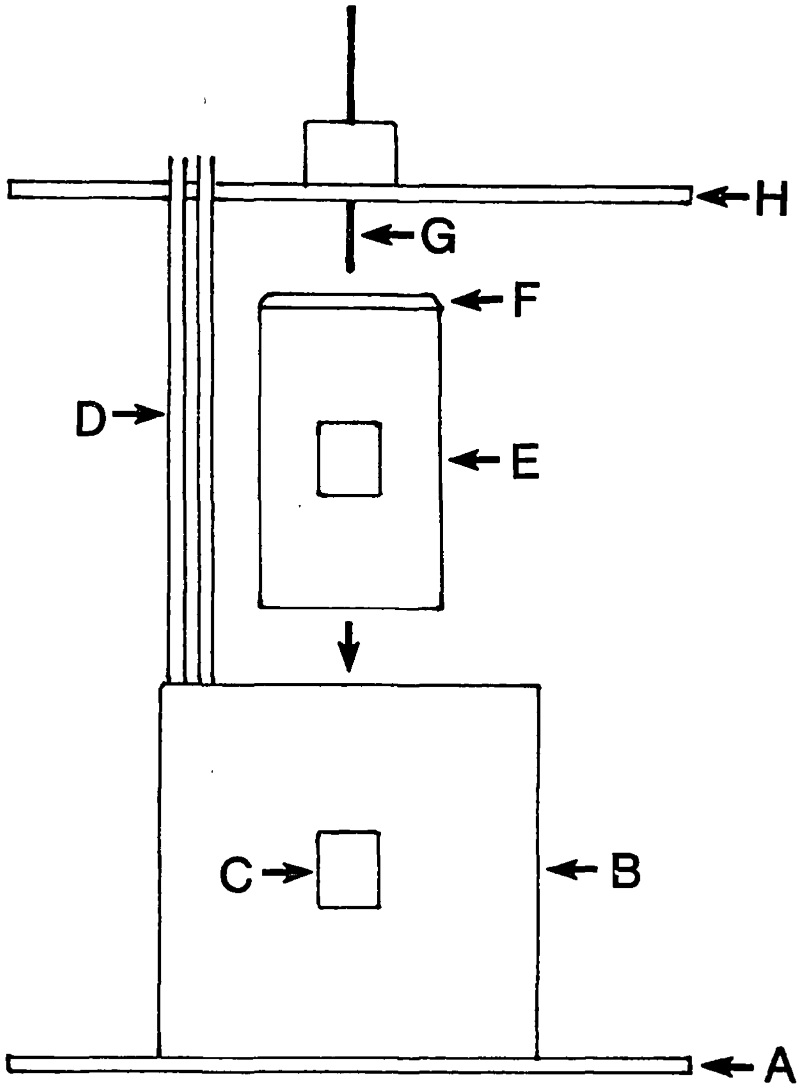

Figure 5. Resistively-heated absorption cell. (A) aluminum base plate; (B) Teflon block; (C) hole for optical path; (D) cooling lines; (E) aluminum cell holder; (F) Teflon cap; (G) thermocouple; (H) aluminum lid. Not shown are the support rods that hold H in place and the Nichrome wire wrapping around E.

manufactured by Philips-Norelco were used. All exposures were made at room temperature.

6. Alpha Particle Detection Equipment

Alpha counting was achieved using a gas flow (10% methane in argon) proportional counter (2π geometry).

7. pH Meter

A Corning Model 130 pH meter with a Fisher Model E-5A combination electrode with a silver/silver chloride reference was used for pH measurements.

8. Electrochemical Cells and Electrodes

Three-electrode configurations were used where the electrochemical cell current passes between a working electrode and a counter (auxiliary) electrode. The potential difference between the working electrode and a reference electrode is controlled with a potentiostat. Negligible current flows between the working electrode and the reference electrode. The advantages of a three-electrode configuration compared to a two-electrode configuration have been discussed.[59,60]

a. Electrochemical cells. For aqueous work, the electrochemical cells consisted of a working electrode compartment and two side compartments for the counter and the reference electrodes, the latter two separated from the former by asbestos fiber junctions (see Figure 6). Stirring was accomplished with a magnetic stirring bar or by a gas bubbler (nitrogen or argon).

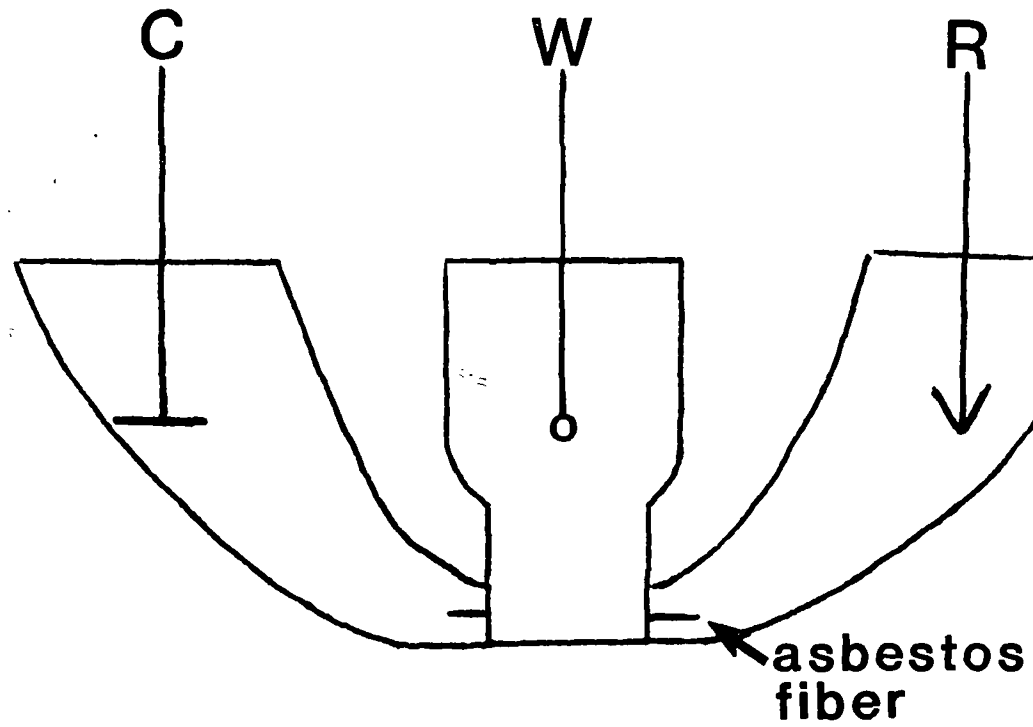

Figure 6. Electrochemical cell. (C) counterelectrode; (W) working electrode; (R) reference (miniature saturated calomel) electrode. The working electrode compartment (middle compartment) volume is ca. 1 mL. The compartments are separated by asbestos fiber junctions.

For molten dimethyl sulfone studies, the electrochemical cells consisted of a small beaker wrapped with Nichrome wire for resistive heating and held in place with epoxy resin. An outer glass cylinder filled with glass wool served as a thermal insulation jacket for the electrochemical cell. A rubber stopper with holes for fritted glass (or asbestos fiber junction) tubes which contained the reference electrode and the counterelectrode, a bubbler and a thermocouple probe sealed the top of the cell.

b. Spectroelectrochemical cell. The 5 mm path length spectroelectrochemical cell used to obtain the spectrum of Pu(III) in K_2CO_3 solution is shown schematically in Figure 7. The cell consists of an optical quartz cell body with pyrex side compartments for the counter and reference electrodes. The side compartments, each equipped with a glass frit junction, were sealed to the quartz cell with epoxy. The optically transparent electrode was amalgamated nickel porous metal foam (PMF) (obtained from Astro Met Associates, Inc., Cincinnati, Ohio).[61] Porous metal foam is a metal matrix electrode with a three-dimensional construction similar to that of reticulated vitreous carbon (RVC).[62] Porous metal foam is available in various pore sizes. The amount of light transmitted through PMF is dependent upon the pore size and the electrode thickness. For the OTE cell shown in Figure 7, a 4 mm section of Series 260 Ni-PMF, which has a light transmittance of about 25%, was used.

c. Electrodes. The working electrodes used for bulk electrolysis/coulometry were 40 mesh Pt screen, RVC (RVC is sold by Chemotronics International Inc., Ann Arbor, Michigan), almagamated nickel porous metal foam, or mercury pool. For cyclic voltammetry,

ORNL-DWG 82-19870

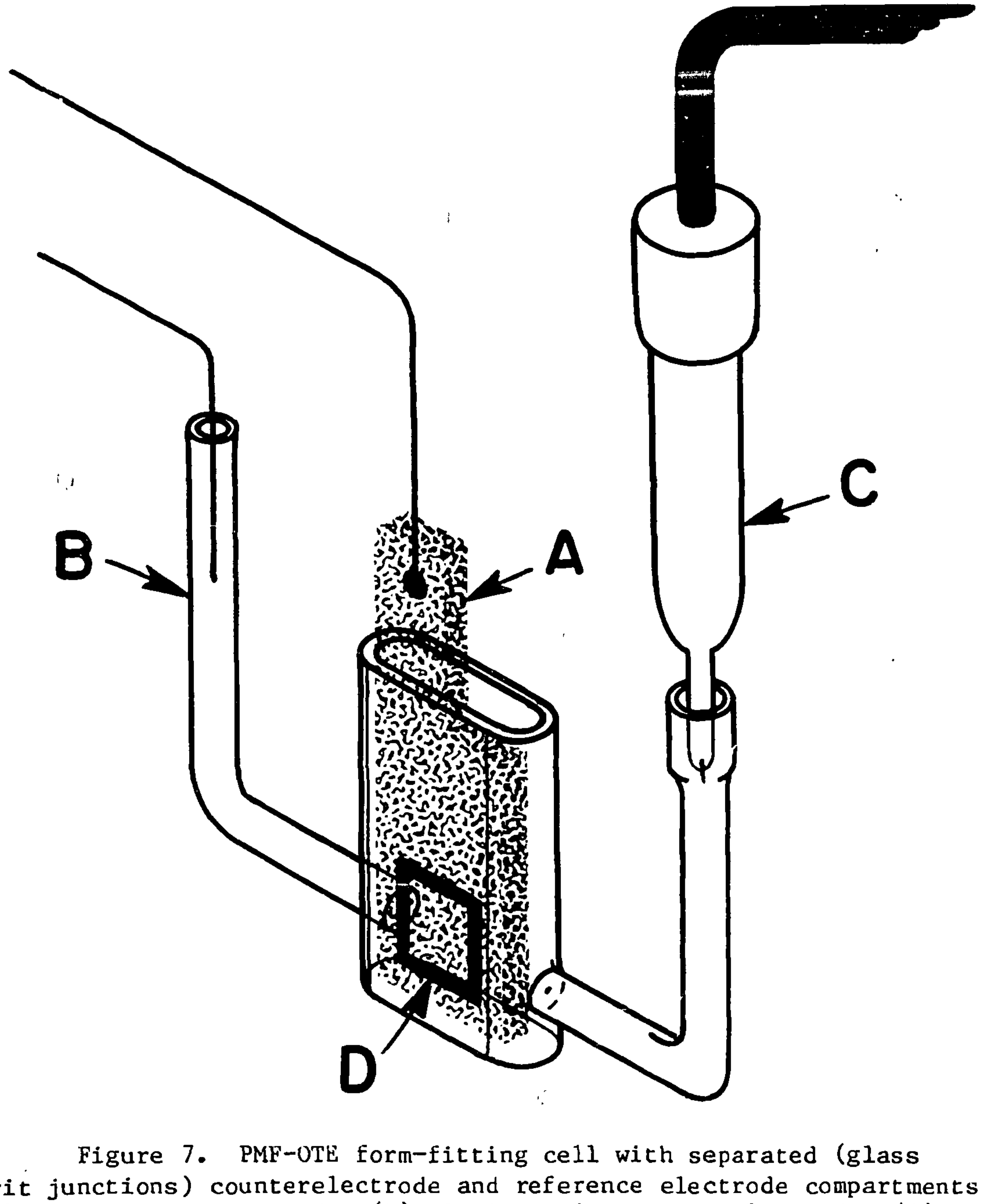

Figure 7. PMF-OTE form-fitting cell with separated (glass frit junctions) counterelectrode and reference electrode compartments. (A) PMF working electrode; (B) platinum wire counterelectrode; (C) miniature saturated calomel electrode; (D) optical window.

the working electrodes were an 18 gauge Pt wire, a hanging mercury drop (HMDE), a RVC strand, or an 18 gauge amalgamated nickel wire. An 18 gauge Pt wire was used for the counterelectrode.

For aqueous work, a miniature KCl saturated calomel electrode (SCE) (Fisher Scientific, Norcross, Georgia) served as the reference electrode. For $DMSO_2$ studies, the reference electrode consisted of Pt or Ag wire in a fritted glass tube filled with the supporting electrolyte. In some cases the silver wire was anodized in 1 M KCl to produce a thin coating of AgCl on the wire. Other Ag reference electrodes consisted of a silver wire in contact with a solution containing the supporting electrolyte and 0.01 M $AgClO_4$. For potentials more negative than 0 V, the latter reference electrode was avoided owing to the diffusion of Ag^+ ions into the working solution where Ag^+ ions would be reduced and form a black coating on the working electrode.

d. Pt wire pretreatment. Platinum wire working electrodes used for cyclic voltammetry were pretreated before use. Due to the necessity of working in a gloved box, a simple electrode pretreatment procedure was used. This procedure consisted of soaking the electrode in 1 M HNO_3 followed by polishing with 1551 AB Alpha polishing alumina No. 2 (Buehler Ltd., Evanston, Illinois). Then, sufficiently negative potentials were applied to the Pt electrode in 1 M KCl to evolve H_2 gas. Finally, the electrode potential was raised to 0 V/SCE to remove adsorbed H_2 gas, and then the electrode was rinsed with deionized distilled water.

e. Mercury electroplating procedure. Nickel wire and Ni-PMF were electroplated with mercury by the same method. The Ni electrode was first rinsed with ethanol or acetone to remove any surface organic impurities and then with distilled water. The electrode was cathodized in 1 M KCl for about 5 minutes at potentials where hydrogen gas evolution was visibly apparent. The electrode was again rinsed with water and electroplated at −1.15 V/SCE in a Hg-plating solution saturated with nitrogen gas. The Hg-plating solution consisted of 10^{-2} M $HgCl_2$, 0.1 M KCl, and 0.01 M HCl. The electrode was electroplated for 10 minutes or longer (depending on the size of the electrode) with occasional solution stirring with N_2 gas. The electrode was then rinsed with water and with ethanol or acetone and left to dry in air. The Ni(Hg) electrode was then immersed in a pool of mercury for a minute or two and then removed (with shaking to dislodge the excess Hg).

C. Reagents

General reagents were standard ACS-certified reagent grade and were used without additional purification. Reagent grade dimethyl sulfone was obtained from Aldrich and Fisher Scientific and was recrystallized once with water and once with methanol. Further recrystallizations did not improve the electrochemical "background." The recrystallized $DMSO_2$ was dried in vacuo at 30°C overnight.

Lanthanide salts were obtained from Research Chemicals-NUCOR, Phoenix, Arizona, and Cerac, Inc., Milwaukee, Wisconsin, and were used without additional purification.

Uranyl nitrate hexahydrate, $UO_2(NO_3)_2 \cdot 6H_2O$, was obtained from City Chemical Corp., New York, New York. The isotopes ^{237}Np, ^{242}Pu, ^{243}Am, and ^{249}Cf were obtained from the Oak Ridge National Laboratory under the Department of Energy's program for transuranium element production and research.

Neptunium-237 and plutonium-242 were obtained as stock solutions of Np(V) in 2-3 M HNO_3 and Pu(VI) in 0.9 M $HClO_4$. These stock solutions were previously prepared by dissolving the oxides (NpO_2 and PuO_2) in acid and electrolyzing to obtain solutions of 100% Np(V) and 100% Pu(VI).

Approximately 6 mg of ^{243}Am were obtained from a recovery solution of previous experiments.[45] This recovery solution contained $Fe(CN)_6^{3-}$ ions and was purified by ion-exchange. Americium(III) in 0.2 M HCl was loaded onto a cation exchange column (400 mesh Dowex 50W). The column was washed successively with 0.5 M, 1 M, and 1.5 M HCl. Iron was eluted off the column with 2 M HCl. Finally, Am(III) was stripped off the column with 6 M HCl as a pink solution.

Multimilligram amounts of ^{249}Cf were purified at TRU/ORNL as discussed elsewhere.[63] The ^{249}Cf was obtained as a stock solution of Cf(III) in 1 M HCl. In Table V is a listing of the isotopes used in this work, along with their half-lives (alpha decay).

Nitrogen and argon gases (both 99.997%) were obtained from Linde/Union Carbide Corporation, New York, New York. Oxygen gas (99.5%) (Tennessee Welding Supply, Knoxville, Tennessee) was passed through a high-voltage arc-discharge apparatus to produce ozone (ca. 5-10% by volume).

TABLE V

ACTINIDE ISOTOPES USED IN THIS WORK

Isotope	Half-life[a]
^{238}U[b]	4.51×10^9 y
^{237}Np	2.14×10^6 y
^{242}Pu	3.79×10^5 y
^{243}Am	7.37×10^3 y
^{249}Cf	351 y

[a]Alpha decay.

[b]Natural uranium was used; it is predominantly ^{238}U.

D. Procedures

1. Aqueous Carbonate-Hydroxide Solution Work

a. Preparation of neptunium solutions. Neptunium-in-carbonate solutions were prepared from a stock solution of $^{237}Np(V)$ in 2-3 M HNO_3. Red-brown neptunium [probably Np(VI)] hydroxide was precipitated from the stock solution by the addition of 6 M NaOH. The precipitate was washed three times with water and then dissolved in 2 M Na_2CO_3.

In order to obtain sufficient concentrations of Np(VII) and Np(V) in Na_2CO_3 solutions for Raman spectroscopy, the precipitated neptunium hydroxide was first dissolved in a minimal amount of HCl. The acid solution was then introduced into freshly prepared 2.5 M Na_2CO_3 (2.5 M Na_2CO_3 is an unstable, supersaturated solution) to give a 2 M Na_2CO_3 solution. The resulting solution, containing a mixture of Np(VI) and (V), was then electrochemically reduced to Np(V) at a platinum screen. Heptavalent neptunium solutions for Raman spectroscopy were prepared by adjusting the pH of Np(V) in Na_2CO_3 solutions and then electrolyzing to 100% Np(VII). This procedure eliminated Raman scattering signals due to nitrate ion (originating from the neptunium stock solution). Heptavalent Np was produced by oxidizing Np(V) rather than Np(VI) since Np(VI) precipitates from Na_2CO_3-NaOH solution.

b. Preparation of plutonium solutions. Carbonate solutions containing plutonium were prepared from a stock solution of $^{242}Pu(VI)$

in ca. 0.9 M $HClO_4$. Plutonium hydroxide was precipitated from the stock solution by the addition of 6 M NaOH. The precipitate was washed three times with water and then dissolved in sodium or potassium carbonate solution.

For Raman spectroscopy of Pu(VII), the precipitated plutonium hydroxide was first dissolved in a minimal amount of hydrochloric acid. The acid solution was then introduced into 2 M Na_2CO_3 solution to give a Pu(VI) solution. This Pu(VI) solution was then saturated with ozone, made basic with NaOH solution, and finally oxidized to Pu(VII) with additional ozone. This procedure eliminated Raman scattering signals due to perchlorate ion (originating from the plutonium stock solution).

c. Preparation of americium solutions. Americium was precipitated from a stock solution of ^{243}Am(III) in 6 M HCl with 6 M NaOH. The hydroxide precipitate was washed three times with water and then dissolved in sodium carbonate solution.

d. Preparation of californium solutions. Californium-in-carbonate solutions were prepared from a stock solution of ^{249}Cf(III) in 1 M HCl. Californium(III) hydroxide was precipitated with 6 M NaOH and washed thrice with water. The washed precipitates were dissolved in Na_2CO_3 or K_2CO_3 solution.

e. Preparation of terbium solutions. The $TbCl_3 \cdot 6H_2O$ was dissolved directly in carbonate solution. Trivalent solutions of Tb were oxidized electrochemically or with ozone to produce Tb(IV) solutions. Hexamminecobalt(III) chloride [used to co-precipitate

Tb(IV)] was prepared by a procedure described previously.[64] Essentially, this procedure involves oxidizing $CoCl_2$ (with air) in an ammoniacal solution.

f. Actinide assay procedures. Controlled potential coulometry was used to determine the concentrations of Np(V), Np(VI), Pu(V), and Pu(VI) in 2 M Na_2CO_3 solutions for molar absorptivity determinations. The molar absorptivity determinations of Np(VII) were performed by adding an aliquot of NaOH solution to a known concentration of Np(V) in Na_2CO_3 solution and then electrochemically oxidizing to Np(VII). Due to the instability of Pu(VII) in Na_2CO_3–NaOH solution, only an estimate of the molar absorptivity of the most intense Pu(VII) visible absorption peak could be made. Conventional α-counting techniques using 2π geometry detectors were employed to determine the concentrations of Np(IV), Pu(IV), and Cf(III) solutions. Americium concentrations were estimated from absorbance measurements using literature molar absorptivity values.

g. Terbium solids assay procedures. Precipitates of Tb(IV) solutions were separated by centrifugation, washed thrice with water and twice with methanol. The samples were dried in vacuum at room temperature for one day. The dried solids were analyzed for terbium and carbonate content. For the Tb analysis the solids were dissolved in a minimal amount of 1 M HCl and then diluted with water. Hexamethylenetetramine was used to adjust the pH to 6. The solutions were then titrated with 0.01 M EDTA[65] using Xylenol Orange (City Chemical Corporation, New York, New York) as the indicator. A gravimetric method was used to determine the CO_3^{2-} ion content.[66] A weighed portion of solid was placed in a 100-mL distilling flask. Approximately 20 mL of water was added [the Tb(IV) solids are insoluble in water] followed by a few milliliters of 5 M HNO_3 solution. The solution was purged with Ar gas, and the evolved CO_2 was passed through a $Mg(ClO_4)_2$ column to remove water and then through a column containing $Mg(ClO_4)_2$ and ascarite. The weight gain of the ascarite column was used to determine the CO_3^{2-} ion content in the Tb(IV) sample. This procedure was proven reliable using known amounts of Na_2CO_3.

h. pH measurements. The pH meter was calibrated with pH 7.00 (KH_2PO_4-NaOH) and pH 10.00 (K_2CO_3-$K_2B_4O_7$-KOH) buffer solutions in the pH range 7 to 10. In the pH range 10 to 12, the same pH 10.00 buffer and 2.0 M Na_2CO_3 solutions were used as the calibration standards. In the pH range 12 to 13, 2.0 M Na_2CO_3 and 5.0 M K_2CO_3 solutions were used to calibrate the pH meter. The pH values of the 2.0 M Na_2CO_3 and 5.0 M K_2CO_3 standard solutions were calculated using the computer program CARBEX.[67] The error in the pH values given in this work is ca. ± 0.2 pH unit. Above pH 13, all hydroxide ion concentrations are reported in formal concentration units (M).

2. Dimethyl Sulfone Work

a. Preparation of lanthanide solutions. The trichloride hexahydrate salts of Ce, Pr, Sm, Eu, Tb, and Yb were dissolved directly in molten $DMSO_2$. Ytterbium and samarium solutions for bulk electrolysis were prepared by dissolving a dimethyl sulfoxide (DMSO) adduct of $YbCl_3$ and $SmCl_3$ in $DMSO_2$. The DMSO adducts of $YbCl_3$ and $SmCl_3$ were prepared using a procedure similar to that given elsewhere.[68] Enough $YbCl_3 \cdot 6H_2O$ or $SmCl_3 \cdot 6H_2O$ was weighed into a small beaker to produce the desired concentration. The hydrated salts were then dissolved in minimal amounts of DMSO and the solutions were then placed in a vacuum oven at approximately 30°C and left overnight. The resulting $YbCl_3 \cdot n(DMSO)$ and $SmCl_3 \cdot n(DMSO)$ crystals were quickly dissolved in molten dimethyl sulfone to minimize moisture absorption.

Anhydrous $YbCl_3$, $SmCl_3$, and $SmCl_2$ were purchased from Cerac Inc., Milwaukee, Wisconsin. Anhydrous $YbCl_2$ was prepared by reacting Yb_2O_3 with HCl at ca. 500°C (to form $YbCl_3$) and then reacting $YbCl_3$ with H_2 at 600°C.

The supporting electrolytes used for cyclic voltammetry and bulk electrolysis of $DMSO_2$ solutions containing (separately) Sm(III), Eu(III), and Yb(III) were tetrabutylammonium perchlorate (TBAP), tetraethylammonium perchlorate (TEAP), lithium perchlorate [only for Eu(III) solutions], tetramethylammonium chloride (TMAC), and lithium chloride [only for Eu(III) solutions]. For applied potentials more negative than −1 V vs. a Pt reference electrode, lithium-containing electrolytes were purposely not used to avoid the reduction of Li^+ ions.

b. <u>Preparation of actinide(VI) solutions</u>. Solutions of U(VI) in $DMSO_2$ were prepared by dissolving $UO_2(NO_3)_2 \cdot 6H_2O$ in molten $DMSO_2$ (m.p. 108°C) or by injecting an aliquot of U(VI) in 0.5 <u>M</u> HCl solution into $DMSO_2$ (see next paragraph for this solution preparation procedure) and distilling off the water.

Neptunium-237 and plutonium-242 were obtained as stock solutions of Np(V) in 2–3 M HNO_3 and Pu(VI) in 0.9 M $HClO_4$. Dimethyl sulfone solutions of Np(VI) and Pu(VI) [and U(VI)-Cl^-] were prepared as follows. The actinide hydroxides were precipitated from the stock solutions with 6 M NaOH. The precipitates were washed thrice with water and then dissolved in acid solution. For Np(VI) and Pu(VI), the hydroxides were dissolved separately in 0.5 M HCl, 0.5 M HNO_3, and 0.5 M $HClO_4$. The Np and Pu acid solutions were oxidized to the hexavalent state using ozone. Aliquots of the solutions were then injected into molten dimethyl sulfone, and the water was distilled off with the aid of ozone gas bubbling (this also insured that the An(VI) oxidation state was maintained). After the solutions visibly stopped "boiling," the solutions were bubbled with ozone gas for an additional two hours. Voltammograms of such $DMSO_2$ solutions did reveal some residual water (probably ca. 10^{-2} M). No attempt was made to determine the minimum concentration of water that could be produced by this method. The $DMSO_2$ solutions of U(VI)-Cl^- were bubbled with argon gas rather than with ozone.

Dimethyl sulfone solutions of Np(VI) and Pu(VI) with Cl^-, NO_3^-, and ClO_4^- as the anions tended to precipitate with time. The rate of precipitation of Np(VI) with ClO_4^- and NO_3^- anions and Pu(VI) with ClO_4^- and Cl^- anions was slow enough not to interfere with the absorption and Raman studies. However, Np(VI) with Cl^- anion and

Pu(VI) with NO_3^- anion precipitated much faster (within hours). A small amount of precipitation occurred for Np(VI) with Cl^- ion solutions and added a light scattering background to the solution absorption spectrum of Np(VI). Plutonium(VI) with NO_3^- anion precipitated too fast to obtain suitable solutions (stable solutions were produced only when significant amounts of water remained in solution) for absorption spectroscopy.

Raman spectra of some of these $DMSO_2$ solutions revealed (by monitoring the intensity of the NO_3^- ion Raman signal) that approximately all the excess HNO_3 was driven off. However, ca. 1-1/2 to 2 times as much ClO_4^- ion was evident (from the intensities of the ClO_4^- ion Raman signals) in the $DMSO_2$ solutions as would be calculated from the formula $AnO_2(ClO_4)_2 \cdot nH_2O$ (An = actinide). The amount of excess ClO_4^- ion depends on the concentration and volume of the aqueous $HClO_4$ aliquots added to molten $DMSO_2$. Due to the Raman inactivity of Cl^- ion, no determination was made for residual HCl in $DMSO_2$. If none of the HCl was driven off by the procedure described previously, the concentration of HCl in the $DMSO_2$ solutions presented herein would be about 0.1 M HCl (as determined by dilution). For aqueous actinide solutions, evidence for chloro complexation (as compared to noncomplexing perchlorate ion solution) is not observed until the Cl^- ion concentration is much higher than that used in this work.

c. Preparation of americium(III) solution. Americium-243 was obtained as a stock solution of Am(III) in 6 M HCl. Americium(III) hydroxide was precipitated from the stock solution with 6 M NaOH. The $Am(OH)_3$ was washed three times with water and then dissolved in 0.5 M HCl.

When 0.5 M HCl was injected into $DMSO_2$, oxidized Cl^- ion (as Cl_2 and/or Cl_3^- ion) was slowly produced. If ozone was applied to the $DMSO_2$ solutions, the amount of oxidized Cl^- ion increased. For the absorption spectra of U(VI), Np(VI), and Pu(VI), the amount of oxidized Cl^- ion contributing to the actinide UV-Vis absorption spectra was negligible. However, for Am(III) [which absorbs much less UV light than do U(VI), Np(VI), and Pu(VI)], the presence of Cl_2 and/or Cl_3^- ion interferes with the UV spectrum of Am(III). Thus Am(III) was introduced into molten dimethyl sulfone as the salt $AmCl_3 \cdot nH_2O$ rather than as an aqueous solution of Am(III). The hydrated salt of Am(III) was prepared by evaporating to dryness with a heat lamp a solution of Am(III) in 0.5 M HCl.

d. Actinide(VI) solutions for Raman spectroscopy. Dimethyl sulfone solutions were loaded (while molten) into 0.5 cm path length pyrex solution cells. The samples were placed in test tubes with rubber stoppers for double containment. A hypodermic syringe needle pierced the test tube stopper and allowed for the expansion of the heated air. The syringe was filled with glass wool (to collect $DMSO_2$ vapor in case of cell breakage). The test tube was then placed in a glass tube wrapped with Nichrome wire (for resistive heating). A thermocouple probe monitored the air temperature around the Raman solution cell (between 115 to 130°C). The laser excitation beam passed through all three walls of glass.

E. Error Limits

1. Cyclic Voltammetry

The error given in the formal potentials of the various couples determined by cyclic voltammetry (in this work) is not the error in $E^{\circ'}$ itself. The error limits listed are the error in the potential midpoint value between the cathodic and anodic current peaks. These reported error limits are conservative estimates that are larger than those determined statistically (95% confidence limits). These conservative error limits are reported due to the approximations involved in determining $E^{\circ'}$.

For a reversible system, the half-wave potential $E_{1/2}$ is calculated as[69]

$$E_{1/2} = (E_p{}^c + E_p{}^a)/2 \qquad (6)$$

where $E_p{}^c$ and $E_p{}^a$ are the cathodic and anodic current peak potentials, respectively. Equation 6 assumes that the switching potential (see page 19) is at least 35 mV/n (n = number of moles of electrons exchanged) past the first current peak ($E_p{}^c$ or $E_p{}^a$ depending upon the initial potential and scan direction).[70] The half-wave potential is related to $E^{\circ'}$ by the relation[71]

$$E_{1/2} = E^{\circ'} - (RT/nF)\ln(D_O/D_R)^{1/2}, \qquad (7)$$

where D_O and D_R are the diffusion coefficients for the oxidized species Ox and the reduced species Red, respectively. When D_O is approximately equal to D_R (which it is for reversible systems), then $E^{\circ'}$ is close to $E_{1/2}$. Equation 6 does not hold for quasi-reversible and irreversible couples. However, for couples that are nearly reversible, the approximation that $E^{\circ\prime}$ is equal to the average of E_p^c and E_p^a is fairly good. The term "quasi-reversible" couple, as used in this work, refers to a couple that is almost (but not exactly) a nernstian system.

Tests used to indicate quasi-reversibility are deviation of the value of the anodic peak current/cathodic peak current ratio from one[70] and deviation from a linear relationship between the square root of the potential scan rate and the anodic or cathodic peak current.[72] With the Pt electrode pretreatment method used in this work, the reversible Fe(III)/Fe(II) couple in 1 M KCl exhibited a linear relationship between the peak current and the square root of the potential scan rate, and the Fe anodic peak current to cathodic peak current ratio was 1.0 (for scan rates = 10-200 mV/sec). The potential current peak separation, ΔE_p, between E_p^c and E_p^a is another test for reversibility.[73] This test, however, was not used as a reliable gauge of reversibility since ΔE_p is strongly dependent on external factors such as electrode pretreatment[74] and uncompensated resistance.[75] For example, with the Pt wire electrode pretreatment procedure used in this work (see page 31), ΔE_p for the reversible couple Fe(III)/Fe(II) in 1 M KCl is ca. 70 mV. Ideally, ΔE_p (with planar diffusion) should equal about 60 mV/n (n = number of moles of electrons exchanged) for a reversible couple.[73] Thus, the observed magnitudes of ΔE_p are somewhat larger than the ΔE_p values due to purely kinetic effects.

Other uncalculated errors in the determination of $E^{\circ\prime}$ are due to liquid junction potentials.[76] All potentials reported in this work are not corrected for liquid junction potentials. No correction for uncompensated resistance using positive feedback[77] was performed in the electrochemical experiments. Errors in the reference potential of the SCE due to fluctuations in room temperature were small enough to be ignored.

2. Absorption Spectra

The error in the molar absorptivity values presented in the aqueous solution absorption spectra is about ± 5% (relative standard deviation). The error is primarily due to uncertainties in the solution concentration determinations (by coulometry or α-counting analysis).

For molten $DMSO_2$ (as well as molten salts), it is more convenient to use molal (m) concentration units instead of formal (M) concentration units. However, for dilute solutions, the formal (or molar) concentration is approximately equal to the product of the molal concentration and the density of $DMSO_2$ (1.11 g/mL at 127°C).[50] All molar absorptivity values derived from the $DMSO_2$ solution absorption spectra are actually based on the product (m)(1.11). Molar absorptivity values ($DMSO_2$ solutions) for wavelengths lower than 230 nm are too high due to uncorrected background absorption/scattering from the $DMSO_2$ and the absorption cell. The error in the molar absorptivity values derived from $DMSO_2$ spectra (above 230 nm) is about ± 10-20%; the molar absorptivity values are only meant to be semi-quantitative.

3. Raman Spectra

The error in the reported Raman signal frequencies is ca. ± 2 cm^{-1}. This error is based on the lack of frequent recalibration of the spectrometer with known frequency standards. The Raman system described (see page 21) is capable of higher accuracy (to ± 0.25 cm^{-1}).

CHAPTER III

RESULTS AND DISCUSSION: AQUEOUS CARBONATE STUDIES

A. Neptunium[78]

As in aqueous acid solution, neptunium in aqueous carbonate media exhibits a wide range of oxidation states. The solution chemistry of Np in carbonate media varies with OH^- ion concentration. The stabilities and colors of ^{237}Np(VII), (VI), (V), (IV), and (III) in 2 M Na_2CO_3 solution are listed in Table VI as a guide for the reader in absorbing and comprehending the descriptive chemistry to be presented here. The discussion begins with the Np(VI)/Np(V) couple and then moves to the less stable or less accessible oxidation states.

1. Np(VI) and (V)

The Np(VI)/Np(V) couple in 2 M Na_2CO_3 solution is quasi-reversible at a Pt electrode, and the formal potential of the couple, as determined from the average potential of the cathodic and anodic current peaks in a cyclic voltammogram, is +0.23 ± 0.01 V/SCE (see Figure 8). Unless otherwise stated, all potentials are reported versus the saturated calomel electrode (SCE). A direct potential measurement in a 2 M Na_2CO_3 solution containing equal concentrations of Np(VI) and Np(V) yielded the same formal potential value as that determined by cyclic voltammetry. Oxidation of this solution at +0.4 V or reduction at 0 V at a Pt screen produced 100% Np(VI) as NpO_2^{2+} or 100% Np(V) as NpO_2^+, respectively. The absorption spectra of yellow-green Np(VI) and faint blue Np(V) are shown in Figures 9 and

TABLE VI

STABILITIES AND COLORS OF Np(VII), (VI), (V), (IV), AND (III) in 2 M Na_2CO_3 SOLUTION

Species	Stability with pH	Stability with time	Color at pH < 12	Color at pH > 13
Np(VII)	pH = ca. 14 for generation of Np(VII) chemically or electrolytically	Weeks to a month (slowly reduced by water)	-	Dark green
Np(VI)*	Precipitates at pH > 13	Stable	Yellow-green	-
Np(V)*	Stable	Np(V) precipitates over a period of hours to days	Faint blue	Faint blue (?)
Np(IV)	Precipitates at pH > 11.7	Stable	Gray	-
Np(III)	Precipitates at pH > 11.7	Very unstable (oxidized by water in seconds)	Gray-green	-

*Np(VI)/Np(V) couple in 2 M Na_2CO_3: $E^{\circ\prime}$ = +0.23 V/SCE at pH < 13

= ca. 0.0 V/SCE at pH = 14.

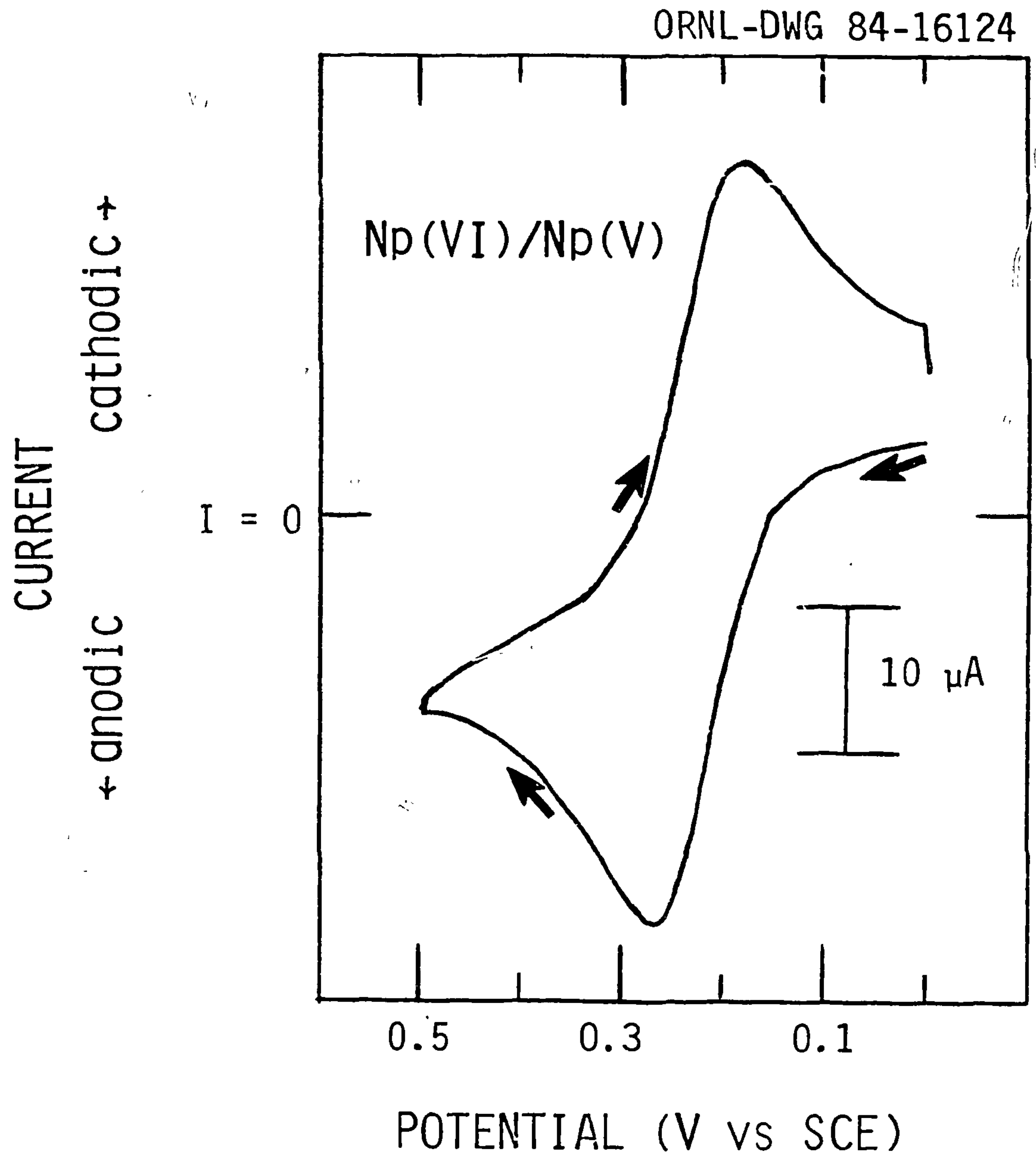

Figure 8. First scan cyclic voltammogram of Np(VI)/Np(V) in 2 M Na_2CO_3 solution, pH 12. Scan rate = 20 mV/s; Pt electrode; [Np] = 4×10^{-3} M.

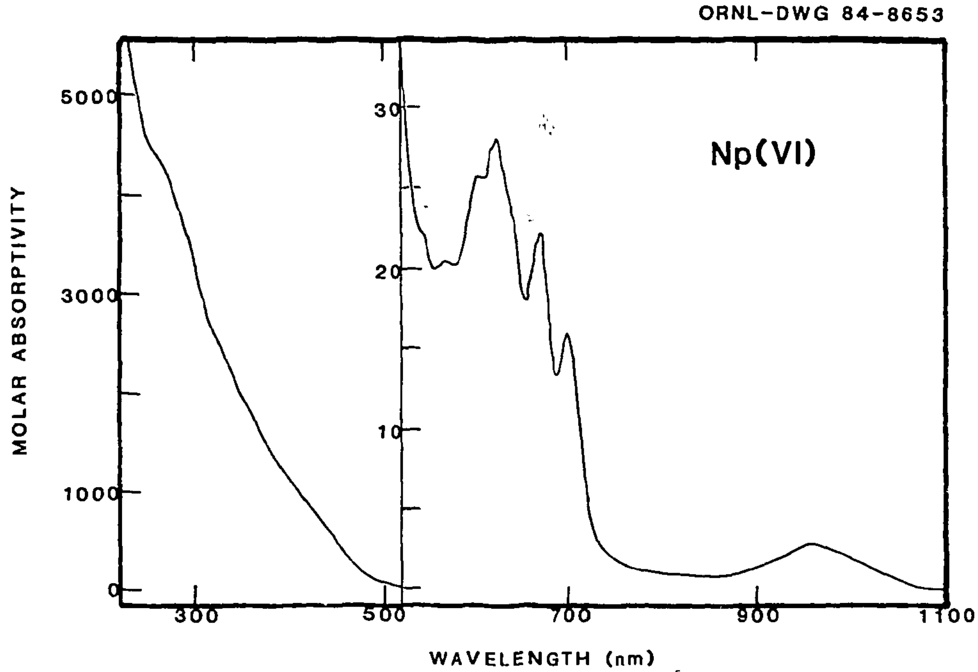

Figure 9. Absorption spectrum of Np(VI) in 2 M Na_2CO_3 solution, pH 12.9.

10, respectively. Wester and Sullivan[30] reported a constant formal potential of +0.22 V/saturated sodium calomel electrode (SSCE) for the Np(VI)/Np(V) couple in sodium carbonate and bicarbonate solutions between pH 8.3 and 11.2. In this work, no change in the formal potential of the Np(VI)/Np(V) couple in 2 M Na_2CO_3 solution in the pH range 12-13 was observed. However, in the pH range 13-14, a negative shift of over 200 mV in the formal potential of the Np(VI)/Np(V) couple was observed via cyclic voltammetry. Correlating with this negative shift in potential as the pH was increased was an increase in the molar absorptivity and a positive wavelength shift (up to +13 nm) of the 997 nm Np(V) absorption peak (see Figure 11). Wester and Sullivan[30] observed an increase in the molar absorptivity of the 997 nm peak as the carbonate to bicarbonate concentration ratio decreased (pH was reduced). The increase in the molar absorptivity of the 997-1010 nm Np(V) peak from pH 13 to about pH 14 could be attributed to the formation of hydroxo-carbonato complexes and/or mixtures of hydroxo and carbonato complexes at sufficiently high hydroxide ion concentration. Cohen and Fried[79] reported molar absorptivities from 30 to approximately 100 M^{-1} cm^{-1} for the 1010 nm absorption peak of Np(V) in 1 M tetramethylammonium hydroxide (TMAH) where the molar absorptivity was dependent on the carbonate ion concentration. By titrating Np(V) in 1 M TMAH with Np(VII), these workers showed that only part of the Np(V) in solution was responsible for the 1010 nm absorption peak and suggested that the rest of the Np(V) species was probably present in a polymeric form.[79] However, nothing unusual was

ORNL-DWG 84-8654

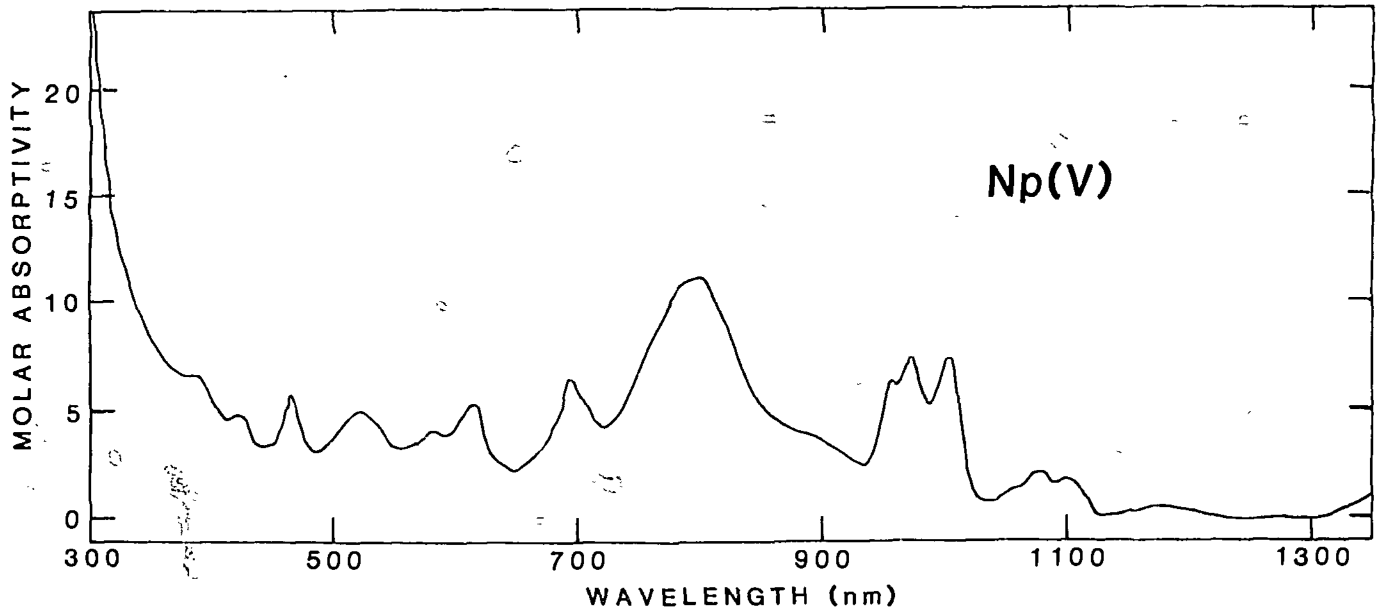

Figure 10. Absorption spectrum of Np(V) in 2 M Na_2CO_3 solution, pH 12.9.

ORNL-DWG 83-17767

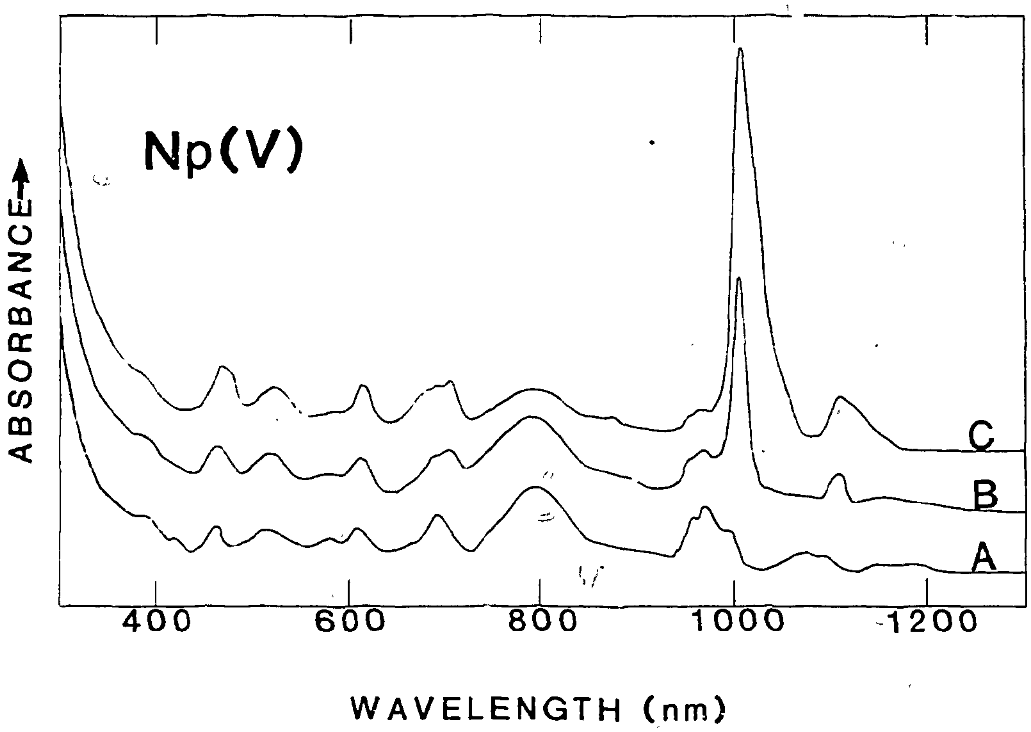

Figure 11. Absorption spectra of Np(V) in concentrated Na_2CO_3 solution as the pH is increased above 13. A: $[OH^-]$ = 0.02 M, [Np] = 1.7 x 10^{-2} M, B: $[OH^-]$ = 0.38 M, [Np] = 1.6 x 10^{-2} M; C: $[OH^-]$ = 1.3 M, [Np] = 1.3 x 10^{-2} M.

seen in the Raman spectra (of this work) of Np(V) in Na_2CO_3-NaOH solution to suggest a polymeric Np(V) component, though the concentrations and/or scattering factors may have been too small for detection of such a species.

Solutions of Np(V) in excess of ca. 10^{-2} M in 2 M Na_2CO_3 solution at varying pH were allowed to stand for a few days, and the resulting white precipitates were analyzed by Raman spectroscopy and X-ray powder diffraction. The Raman spectra obtained from the solids are identical to those obtained by Madic et al.[17] except for the appearance of a carbonate peak in our work at 1078 ± 2 cm^{-1}. This peak varied in intensity depending upon the precipitate washing procedure. In contrast, the symmetric stretch of NpO_2^+ (ν_1) at 771 ± 2 cm^{-1} and the components of the split ν_4 carbonate peak at 696 and 716 ± 2 cm^{-1} were the same for all the solids analyzed. Thus, even if different Np(V) complexes exist in Na_2CO_3 solution as the pH is increased above 13, as suggested by the potentiometric and absorption spectroscopic measurements, the same precipitates still form.

Madic et al.[17] ascribed the Np(V) carbonate precipitate to the formula $Na_3NpO_2(CO_3)_2 \cdot nH_2O$ based on X-ray diffraction data, and our X-ray data are a good match to those in the literature for this compound. Listed in Table VII are the more dominant X-ray diffraction lines we obtained, along with the corresponding data of Volkov et al.[80] for $Na_3NpO_2(CO_3)_2 \cdot nH_2O$. It should be noted that one Np(V) in Na_2CO_3-NaOH solution, where the hydroxide ion concentration was 0.87 M [the highest hydroxide ion concentration used for our Np(V) solid

TABLE VII

X-RAY POWDER DIFFRACTION DATA FOR $Na_3NpO_2(CO_3)_2 \cdot nH_2O$

	Literature (Ref. 80)[a]		Present work[b]	
h k l	d(Å)	I	d(Å)	I[c]
0 $\bar{1}$ 1	6.07	21	6.051	4
0 1 1	5.75	25	5.776	4
1 1 0	4.391	100	4.409	10
0 0 2	3.997	29	4.009	5
0 $\bar{2}$ 2	2.994	10	2.991	3
1 1 2	2.914	10	2.927	3
2 0 0	2.535	50	2.537	8
0 4 0	2.194	38	2.194	6
0 4 3	1.666	14	1.660	2
3 3 0	1.463	10	1.464	1

[a]Lines with intensities less than 10 were omitted from the table.

[b]Average values from diffraction patterns of three separate precipitates.

[c]Intensities were estimated visually on a scale from 0 to 10 with 10 being assigned to the most intense line.

work), produced a pink precipitate which may be a Na^+-Np(V)-OH^- salt, as observed by Cohen and Fried.[79]

No variation in the Np(VI) in Na_2CO_3 solution spectra from pH 11.5 to 0.1 M OH^- ion concentration was observed. Above 0.1 M OH^- ion concentration, Np(VI) is not stable in concentrated Na_2CO_3 solution. When a solution of Np(VI) having a concentration less than 10^{-2} M is made sufficiently basic, Np(V) is formed. The reductant(s) may be trace impurities, hydroxide ion, or water. If the pH of the resulting Np(V) in Na_2CO_3 solution is decreased by bubbling CO_2 through the solution, Np(VI) is produced (presumably by air oxidation). When the Np(V) in Na_2CO_3-NaOH solution is electrochemically oxidized to Np(VI), a red-brown precipitate forms. A red-brown precipitate also forms when neptunium is precipitated from the Np(V) in 2-3 M HNO_3 stock solution by the addition of concentrated NaOH. When a small aliquot of Np(V) in acid solution is introduced into Na_2CO_3 solution, a Np(VI) solution results. At concentrations above 10^{-2} M Np(VI), adding hydroxide ions to Np(VI) in Na_2CO_3 solutions to pH values in excess of 13 yields a red-brown precipitate and a Np(V) supernatant. Attempts to obtain the Raman spectrum of this solid failed. When 514.5 nm argon ion laser light struck the sample, the color of the sample faded and the sample edges were blackened. With 633 nm dye laser light illumination, the sample color remained, but small black burn spots were distributed throughout the sample. No Raman signal was observed in either case.

In concentrated aqueous carbonate solution with pH < 13, the Np(VI) and Np(V) complexes exist as $NpO_2(CO_3)_3^{4-}$ and $NpO_2(CO_3)_3^{5-}$, respectively.[17,81] In concentrated carbonate-hydroxide solution with a sufficiently high concentration of hydroxide ion, Np(VI) and Np(V) should exist as carbonato-hydroxo and/or hydroxo complexes. Dimeric and trimeric hydroxo complexes of Np(VI) such as $(NpO_2)_2(OH)_2^{+}$ and $(NpO_2)_3(OH)_5^{+}$ have been proposed.[82] Since Np(VI) is not stable to precipitation in concentrated Na_2CO_3 solution above 0.1 M OH^- ion concentration, Np(VI) only exists at very low Np concentration in carbonate-hydroxide solution.

As mentioned earlier (see pages 51 and 54), Raman spectra of Np(V) in Na_2CO_3-NaOH solution indicate that Np(V) probably does not exist as a polymeric hydroxo complex. The presence of one or more CO_3^{2-} ions in a Np(V) complex should sterically hinder the formation of polymeric Np(V) (where the bridging between NpO_2^+ ions occurs through OH^- ions). Neptunium(V) precipitates in Na_2CO_3-NaOH solutions as $Na_3NpO_2(CO_3)_2 \cdot nH_2O$ (see page 54). Precipitation of such a carbonate compound from a solution of polymeric Np(V)-hydroxo complex would be expected to be hindered (kinetically very slow). However, the precipitation of a carbonate compound of Np(V) from a solution containing a Np(V)-carbonato-hydroxo (nonpolymeric) complex should not be as hindered. Thus Np(V) probably exists in carbonate-hydroxide solution as a carbonato-hydroxo complex, in which the carbonate ions prevent (hinder) the polymerization of Np(V).

In aqueous carbonate-hydroxide solution, the redox reaction of Np(VI) and Np(V) may be described as

$$NpO_2(CO_3)_n(OH)_p{}^{(2-2n-p)+} + e^- \rightleftharpoons NpO_2(CO_3)_n(OH)_q{}^{(1-2n-q)+} + (p - q)(OH^-). \quad (8)$$

A plot of the change in half-wave potential ($\Delta E_{1/2}$) of the Np(VI)/Np(V) couple versus the log[OH^-] in concentrated Na_2CO_3 solution is shown in Figure 12. The change in half-wave potential is the difference between $E_{1/2}$ in carbonate-hydroxide solution and $E_{1/2}$ in carbonate solution, pH < 13 ($\Delta E_{1/2} = E_{1/2}([OH^-]) - 0.23$ V). The half-wave potential of the Np(VI)/Np(V) couple was estimated using cyclic voltammetry by calculating the midpoint potential between the cathodic and anodic current peaks. As mentioned earlier (see page 51), the reduction potential of the Np(VI)/Np(V) couple in 2 M Na_2CO_3 solution shifts to lower potentials when the pH > ca. 13. At [OH^-] = 0.15 M, E°' [Np(VI)/Np(V)] = +0.23 V. When [OH^-] is about 0.2–0.4 M, the Np anodic current peak is obscured by the platinum oxide formation wave. Thus, no estimates of $E_{1/2}$ were made in this [OH^-] range. When [OH^-] is ca. 0.4–0.5 M, the Np(VI)/Np(V) reduction potential has shifted sufficiently to resolve the Np anodic current peak from the platinum oxide formation wave. If Equation 8 is valid over the pH range where carbonato-hydroxo complexes form, then the slope of the line in Figure 12 should be $-(p-q)(0.059)$ as predicted by

$$\Delta E_{1/2} = (0.059)\log(K_O/K_R) - (p-q)(0.059)\log[OH^-], \quad (9)$$

where $\Delta E_{1/2}$ is in units of volts, and K_O and K_R are the hydroxo dissociation constants for the oxidized and reduced Np complexes, respectively.[83] As seen in Figure 12, the variation of $\Delta E_{1/2}$ with log[OH^-] is only approximately linear. Linear regression analysis

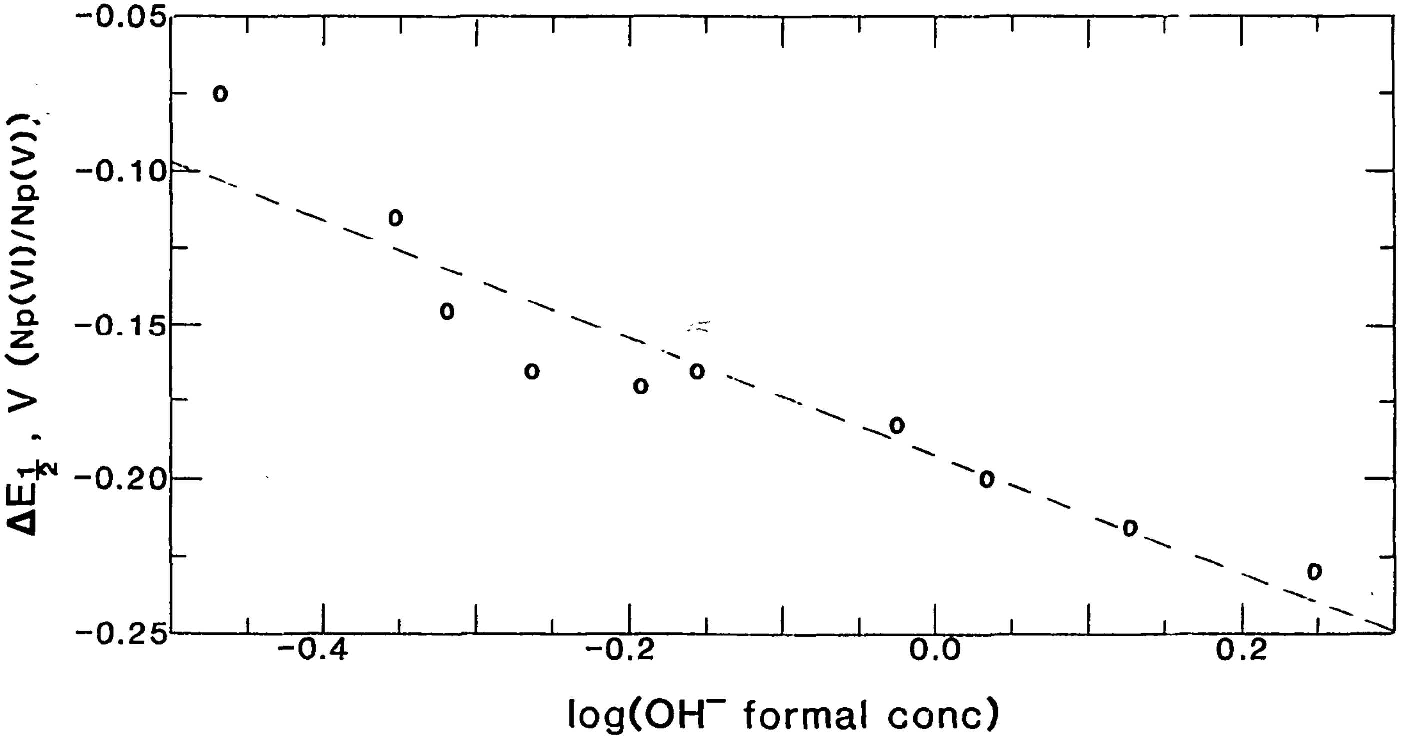

Figure 12. Change in half-wave potential ($E_{1/2}$ - 0.23 V) of the Np(VI)/Np(V) couple in concentrated carbonate-hydroxide solution as a function of log[OH^-]. The dashed line results from linear regression analysis using all the data points shown in the figure. This line does not necessarily represent the best fit to the data (e.g., a better fit may be nonlinear).

using all the data points shown in Figure 12 and data points where $[OH^-] > ca. 1 \underline{M}$ gives p-q = 2.8-3.2. This may indicate a change in hydroxo complexation number of three between Np(VI) and Np(V) complexes in carbonate-hydroxide solution. Equation 8 (see page 58) is valid only if the carbonate ion coordination number for the Np(VI) and Np(V) complexes is the same and remains constant. The nonlinearity of the data plotted in Figure 12 may indicate successive displacements of the complexed carbonate ions by hydroxide ions with increasing OH^- ion concentration. The nonlinearity may also be caused by successive addition of hydroxide ions to the complexes. The exact nature of Np(VI) and Np(V) complexes in carbonate-hydroxide solution is unknown, and further spectroscopic and electrochemical studies in carbonate, hydroxide, and carbonate-hydroxide solutions are necessary. Unfortunately, experiments with Np(VI) in carbonate-hydroxide solution are hampered by the lack of solubility of Np(VI) in this medium. In addition, in this work, the ionic strength of solutions was not maintained at a constant value. In future studies, the solution ionic strength (which could affect $E_{1/2}$) should be held constant.

2. Np(VII)

Electrolysis of Np(VI) ([Np(VI)] > 10^{-3} M) in 2 M Na_2CO_3 solution at pH 12 at potentials up to +1.1 V yielded no measurable amount of Np(VII). In order to generate Np(VII) in 2 M Na_2CO_3 solution, it was necessary to adjust the pH of the Np(V) starting solution close to 14. Neptunium(VII) was then produced by applying +0.4 V to these very basic solutions of Np(V). Simakin and

Matyashchuk[37] produced Np(VII) in solutions of 0.2–10 M NaOH and 0.25–1.5 M Na_2CO_3. In 2 M Na_2CO_3 solution, 0.2 M OH^- ion concentration is not sufficient to produce measurable amounts of Np(VII). The absorption spectrum of dark green Np(VII) in Na_2CO_3-NaOH solution is shown in Figure 13. The molar absorptivities of Np(VII) are dependent on the hydroxide ion concentration. As the hydroxide ion concentration increases, the molar absorptivities of Np(VII) decrease, but the shape of the absorption curve remains the same.

Raman spectra of Np(VII) in 1.8 M Na_2CO_3, 0.86 M NaOH solution and in 1.5 M Na_2CO_3, 2.6 M NaOH solution show the same Np(VII) peak at 734 $\pm$ 2 cm^{-1}, which agrees well with the 735 cm^{-1} Np(VII) peak in 1.25 M NaOH solution reported by Basile *et al.*[84] Rotating the plane of polarization (at the laser) by 90° produced a large reduction in the 734 cm^{-1} peak intensity, but the peak shape remained the same. The depolarization ratio I_T (obs. $\parallel$)/I_T (obs. $\perp$) for the 734 cm^{-1} Np(VII) peak is ca. 0.3 indicating that the vibration is highly symmetric. Due to the facts that only one Raman peak was seen for Np(VII) and that this vibration is highly polarized, NpO_2^{3+} is a logical Np(VII) species in Na_2CO_3-NaOH solution. Other species involving hydroxide ions, such as $NpO_2(OH)_n^{(3-n)+}$, are also possible. Whatever the true solution species may be, the linear NpO_2^{3+} unit seems to be responsible for the Np(VII) Raman peak as noted earlier by Basile *et al.*[84]

The NpO_2^{n+} frequency for Np(VII) in Na_2CO_3-NaOH solution and in NaOH solution[84] is lower than the corresponding Np(VI) frequency at

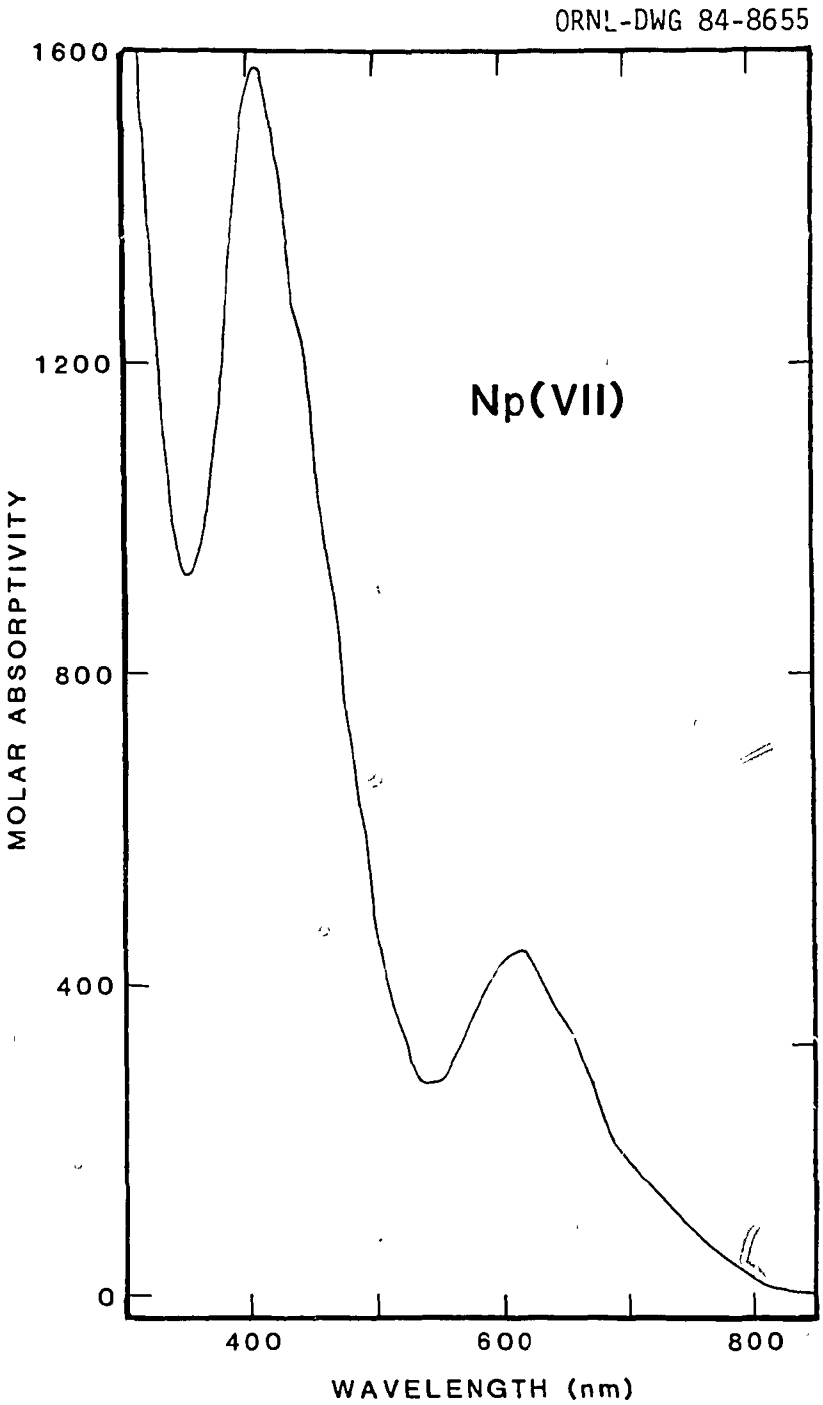

Figure 13. Absorption spectrum of Np(VII) in 1.7 M Na_2CO_3, 0.71 M NaOH solution.

802 cm^{-1} in Na_2CO_3 solution [17,32] and the Np(V) frequency at 755 cm^{-1} in Na_2CO_3 solution.[17] A solvent effect may be responsible for the lowering of the Np(VII) symmetric stretch frequency in very basic media. The Raman spectrum of Np(VII) in Na_2CO_3-NaOH solution excited with 514.5 nm argon ion laser radiation is given in Figure 14. Since (1) Np(VII) cannot be produced in Na_2CO_3 solution unless the solution is sufficiently basic and (2) no differences in the Np(VII) Raman peak in Na_2CO_3-NaOH and in NaOH solutions were observed, the Np(VII) complex in Na_2CO_3-NaOH solution probably does not involve carbonate ions. However, carbonate ion complexation cannot be entirely ruled out since changes in the ligand coordination sphere may produce only a small change in the symmetric stretch frequency of the "hard" NpO_2^{3+} cation.

Cyclic voltammograms of Np(VII) solutions at a Pt electrode revealed no anodic/cathodic waves that could be attributed to the Np(VII)/Np(VI) couple. However, the Np(VII)/Np(VI) couple may be obscured by platinum oxide formation. The electrochemically irreversible nature of a Np(VII)-hydroxo complex/Np(VI)-carbonato complex couple would also explain the lack of any anodic waves, indicating Np(VII) formation. Raman spectra of Np(VII) in Na_2CO_3-NaOH solution were also obtained using 633 nm dye laser excitation and 488.0 nm argon ion laser excitation. No direct evidence for a resonance Raman effect was observed due to the increased absorption of the laser light at both higher and lower excitation frequencies than 514.5 nm. However, based on the magnitude of the Raman peak obtained

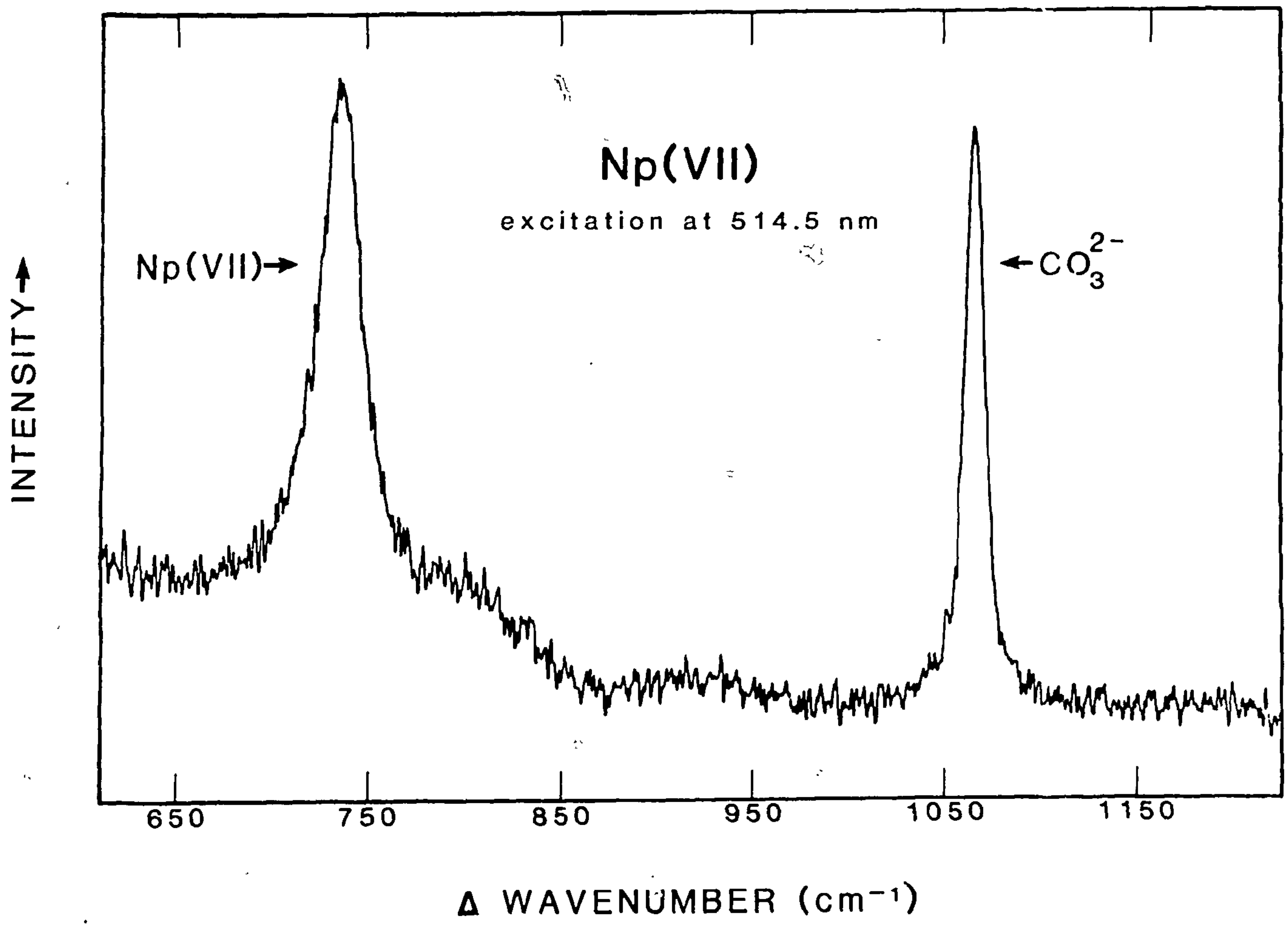

Figure 14. Raman spectrum of Np(VII) in 1.5 M Na_2CO_3, 2.6 M NaOH solution, [Np] = 3×10^{-2} M.

for Np(VII) at 10^{-2}–10^{-1} M concentration compared to that of the ν_1 carbonate peak, resonance enhancement is likely for Np(VII).

3. Np(IV) and (III)

Attempts were made to investigate Np(IV) in 2 M Na_2CO_3 solutions at pH values greater than 12. At $[OH^-]$ = 0.25 M, cyclic voltammograms of Np(V) in 2 M Na_2CO_3 solution at a HMDE exhibited a single cathodic wave at ca. −1.8 V and no anodic wave (see Figure 15B). At pH 12.9, the shape of the cathodic wave changed drastically with a sharp current peak at approximately −1.7 V and with a smaller cathodic peak preceding the main peak. At pH 10.9 this "pre-peak" at ca. −1.63 V is clearly resolved from the main cathodic peak (see Figure 15A). At higher scan rates (in excess of 100 mV/s), the two cathodic current peaks merge into a single wave.

Reduction of Np(V) in 2 M Na_2CO_3 solution at pH 10.9 at −1.60 to −1.64 V at a Hg pool produced a gray colored solution. A more intense gray-green solution was generated when the reduction occurred at −1.7 V. When the potential was removed, the gray-green color of the solution quickly faded to a gray color. The absorption spectrum of the gray solution matched the literature spectra of Np(IV) in carbonate media.[30,35] At −1.7 V the gray-green solution gradually became turbid with the formation of a gray-green precipitate. Spectra of the supernatant indicated the absence of Np(IV). With the potential removed, the gray-green precipitate would dissolve in 2 M Na_2CO_3 solution, if the pH was lower than 11.7, to give a Np(IV)

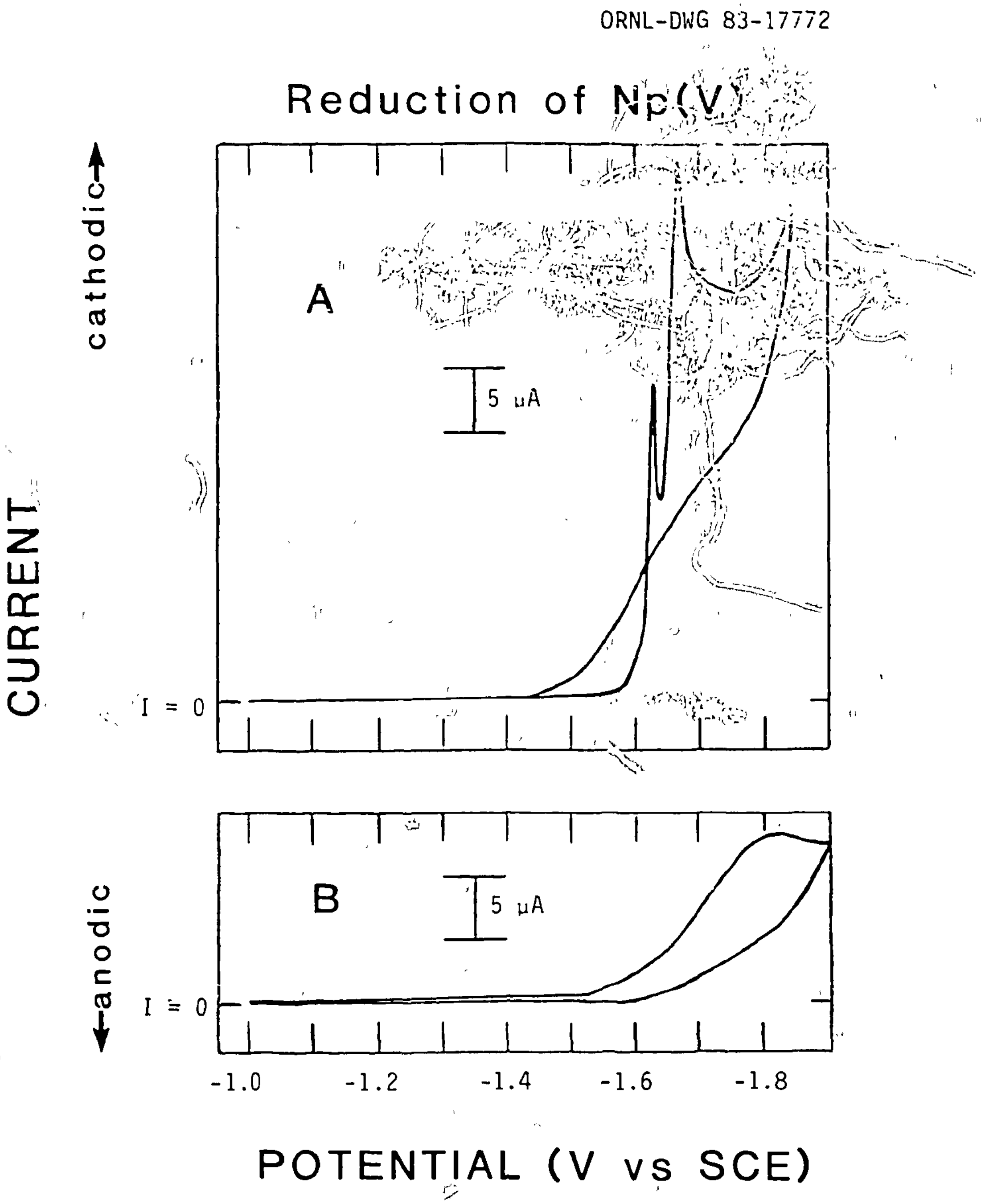

Figure 15. First scan cyclic voltammograms of Np(V) in 2 M Na_2CO_3 solution; A: pH 10.9; B: $[OH^-]$ = 0.25 M. Scan rate = 20 mV/s; HMDE; [Np] = 1.7 x 10^{-2} M. The current "crossover" in A may be an experimental artifact, such as hysteresis, of the electrochemical cell and/or supporting electrolyte rather than a feature of the neptunium oxidation/reduction itself.

solution. Increasing the pH of Np(IV) in 2 M Na_2CO_3 solutions in excess of 11.7 produced a gray precipitate. This gray precipitate could be redissolved in Na_2CO_3 solution at pH 11.7 to give a Np(IV) solution. The absorption spectrum of Np(IV) obtained (see Figure 16) is identical to that of Wester and Sullivan.[30] Reduction of Np(IV) in 1 M K_2CO_3 solution at −1.7 to −1.8 V produced the gray-green solution and no precipitate, but when the potential was removed, the color quickly faded to the gray color of a Np(IV) solution.

Cyclic voltammograms at a HMDE of Np(IV) in 2 M Na_2CO_3 (see Figure 17), 1 M Na_2CO_3, and 1 M K_2CO_3 solutions revealed an irreversible couple indicating reduction of Np(IV) to Np(III). The cathodic current to anodic current ratio did not vary noticeably with scan rate. Thus, the gray-green solution is probably highly unstable Np(III), and the gray-green precipitate is most likely a Np(III) hydroxide. The small anodic wave in the Np(IV)/Np(III) cyclic voltammogram also indicates the unstable nature of Np(III). The formal potential of the Np(IV)/Np(III) couple was estimated (from the cyclic voltammograms) to be −1.4 V in 2 M Na_2CO_3 solution and −1.5 V (−1.3 V/NHE) in 1 M K_2CO_3 solution. Fedoseev et al.[31] reported a value of −1.32 V/NHE for the Np(IV)/Np(III) couple in 1 M K_2CO_3 solution. Attempts to obtain the spectrum of Np(III) in carbonate solution failed due to the rapid oxidation of Np(III) by water. The spectrum of Np(III) in carbonate solution might be obtained by using a spectroelectrochemical cell involving a Hg pool. An amalgamated Ag, Au, or Ni screen would not have a sufficient cathodic potential range

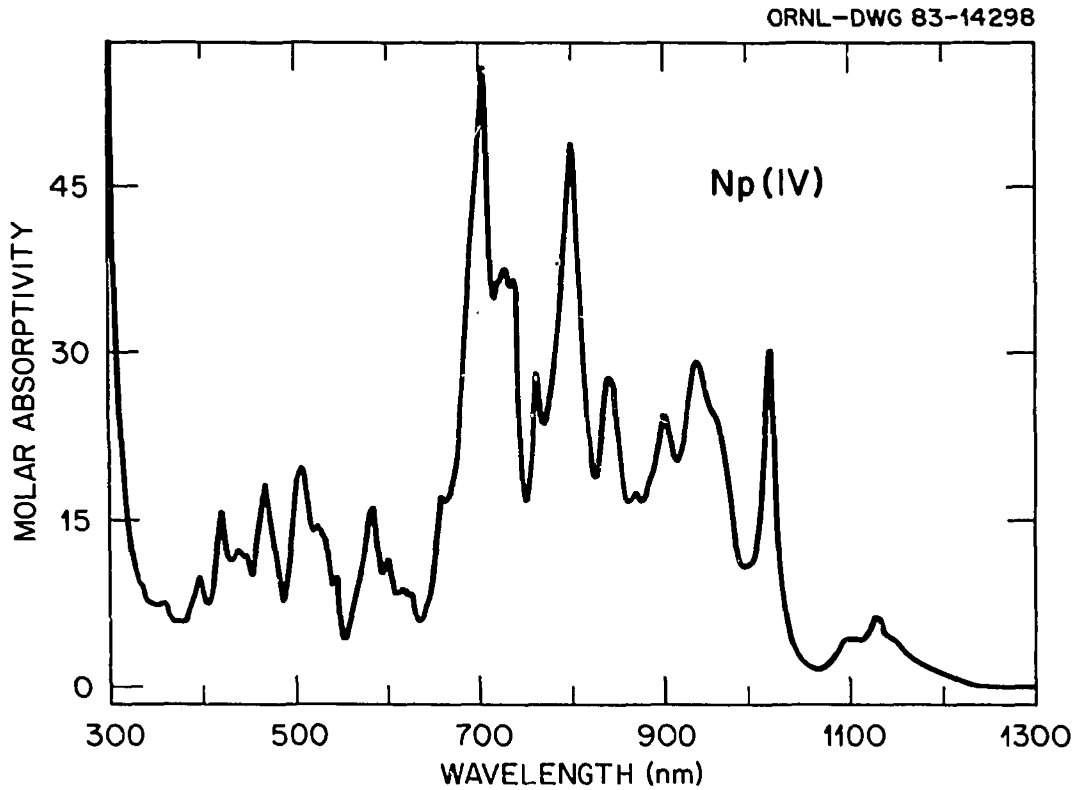

Figure 16. Absorption spectrum of Np(IV) in 2 M Na_2CO_3 solution, pH 10.9.

ORNL-DWG 83-17773

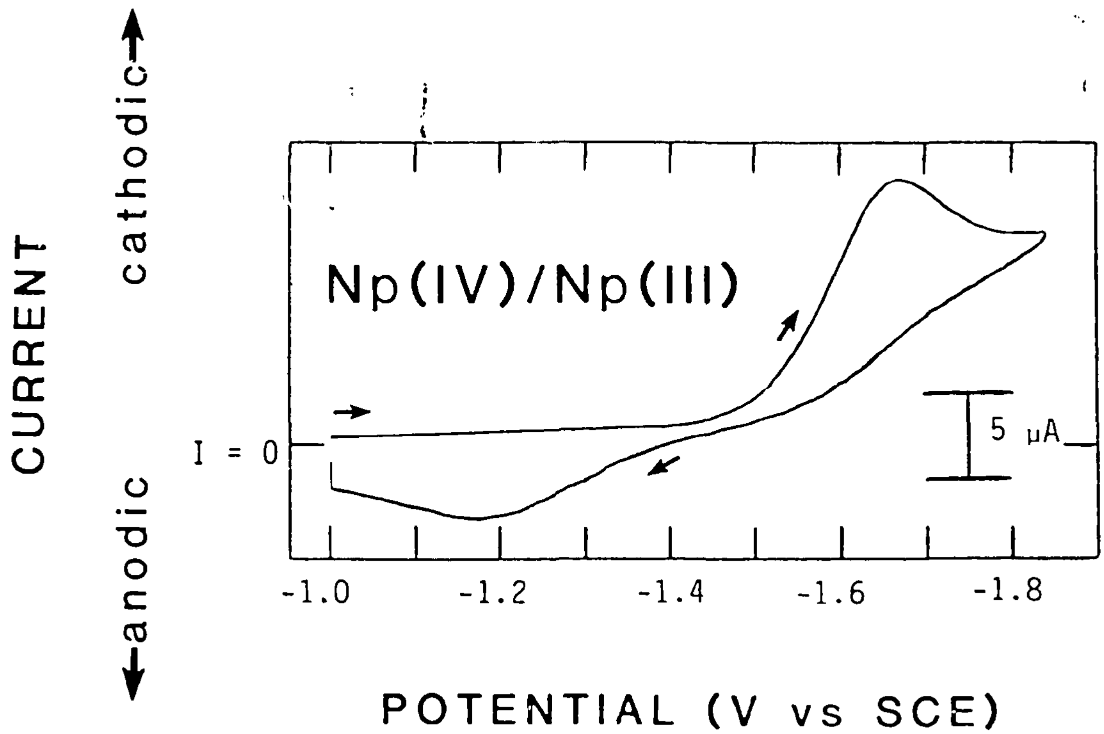

Figure 17. First scan cyclic voltammogram of Np(IV)/Np(III) in 2 M Na_2CO_3 solution, pH 10.5. Scan rate = 100 mV/s; HMDE; [Np] = 1.7 x 10^{-2} M.

for generation of Np(III). No attempt was made in the present work to obtain spectroelectrochemically the absorption spectrum of Np(III) in carbonate solution.

Cyclic voltammograms of Np(IV) solutions at potentials above -0.4 V, as shown in Figure 18, indicate oxidation of Np(IV) to Np(V), followed by oxidation of Np(V) to Np(VI). The platinum oxide formation wave almost completely obscures the Np(V) to Np(VI) anodic wave. Oxidation at 0 V at a Pt screen of Np(IV) in 2 M Na_2CO_3 solution was attempted. When the current had decayed to the background value, the electrolysis was stopped. The spectrum of the resulting solution did not exhibit any definite absorption peaks of Np(V), but it did show that there was a reduction in the Np(IV) concentration. The Np(V) peaks were probably not visible due to the spectral overlaps of Np(IV) and Np(V) and the greater molar absorptivities of Np(IV) over Np(V) in this medium. The solution was further oxidized at +0.45 V to produce a yellow-green solution of 100% Np(VI). Cyclic voltammograms of this solution were identical to those shown in Figure 8, page 49. The Np(VI) solution could then be reduced to 100% Np(V) at 0 V. Similar results were obtained for Np(IV) in 1 M Na_2CO_3-$NaHCO_3$ solution at pH 10.7. This differs from the observations of Wester and Sullivan[30] who reported no detectable amount of Np(V) or Np(VI) from controlled potential electrolysis at a Pt screen of Np(IV) in 1 M Na_2CO_3-$NaHCO_3$ solution.

Attempts were also made to determine the formal potential of the Np(V)/Np(IV) couple in concentrated Na_2CO_3 solution by direct

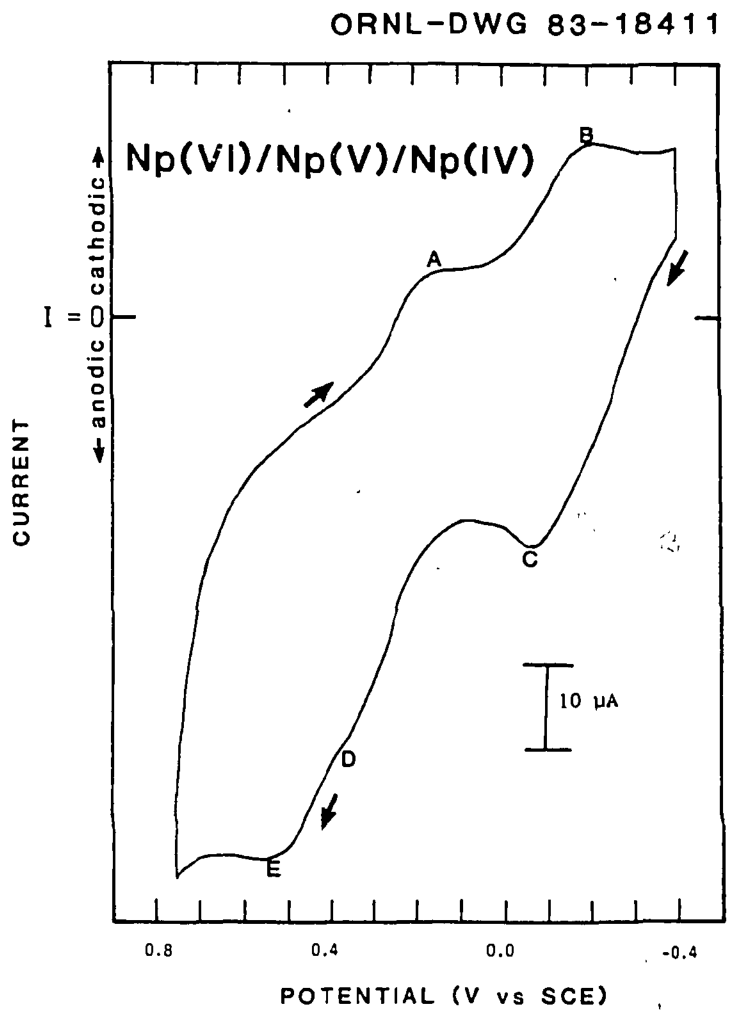

Figure 18. First scan cyclic voltammogram of Np(IV) in 2 M Na_2CO_3 solution, pH 10.8. Scan rate = 20 mV/sec; Pt electrode; [Np] = 2.4×10^{-2} M.

A: Np(VI) → Np(V) reduction wave.
B: Platinum oxide reduction wave.
C: Np(IV) → Np(V) oxidation wave.
D: Np(V) → Np(VI) oxidation wave.
E: Platinum oxide formation wave.

potential measurements of solutions prepared by mixing equal concentrations of Np(V) and Np(IV). The direct potentials measured were not stable and tended to drift toward more positive values with time. Fedoseev _et al._[31] also reported difficulty with such measurements but gave a very rough estimate of +0.1 V/NHE for the Np(V)/Np(IV) couple in 1 _M_ K_2CO_3 solution.

B. Plutonium[85]

As with neptunium, plutonium exhibits a wide range of oxidation states in aqueous carbonate media. The solution chemistry of plutonium in its various oxidation states in carbonate media depends upon the hydroxide ion concentration. The stabilities and colors of Pu(VII), (VI), (V), (IV), and (III) in 2 _M_ Na_2CO_3 solution are listed in Table VIII. These data should serve as an overview of the following detailed descriptive chemistry of plutonium in carbonate-hydroxide solution. The Pu(VI)/Pu(V) couple is discussed first, before the less stable or less accessible oxidation states of plutonium are treated.

1. Pu(VI) and (V)

The Pu(VI)/Pu(V) couple in 2 _M_ Na_2CO_3 solution is quasi-reversible at a Pt electrode, and the formal potential of the couple, as determined from the average potential of the cathodic and anodic current peaks, is +0.11 ± 0.01 V (see Figure 19). Wester and Sullivan[39] reported a formal potential of +0.11 V for the Pu(VI)/Pu(V) couple in 1 _M_ Na_2CO_3 solution, and Fedoseev _et al._[31] found a value of +0.32 V/NHE (i.e., +0.08 V/SCE) for the same couple in 1 _M_ K_2CO_3

TABLE VIII

STABILITIES AND COLORS OF Pu(VII), (VI), (V), (IV), AND (III) in 2 M Na_2CO_3 SOLUTION

Species	Stability with pH	Stability with time	Color at pH < 12	Color at pH > 13
Pu(VII)	$[OH^-]$ > 2.5 for Pu(VI) oxidation	Reduced to Pu(VI) in ca. 1 day	-	Blue-green
Pu(VI)*	Stable	Pu(V) precipitates over a period of weeks to months	Green	Green-yellow
Pu(V)*	Disproportionates at pH < 11.5	Pu(V) precipitates over a period of hours to days	Light yellow	Pink
Pu(IV)	Precipitates at pH > 11.4	Stable	Apple-green	-
Pu(III)	Insoluble in Na_2CO_3 solution (soluble in K_2CO_3 solution)	Stable (in absence of O_2)	Blue	-

*Pu(VI)/Pu(V) couple in 2 M Na_2CO_3: $E^{\circ\prime}$ = +0.11 V/SCE at pH < 13

= +0.09 V/SCE at $[OH^-]$ = 1 M

= +0.06 V/SCE at $[OH^-]$ = 2 M

ORNL-DWG 83-19002

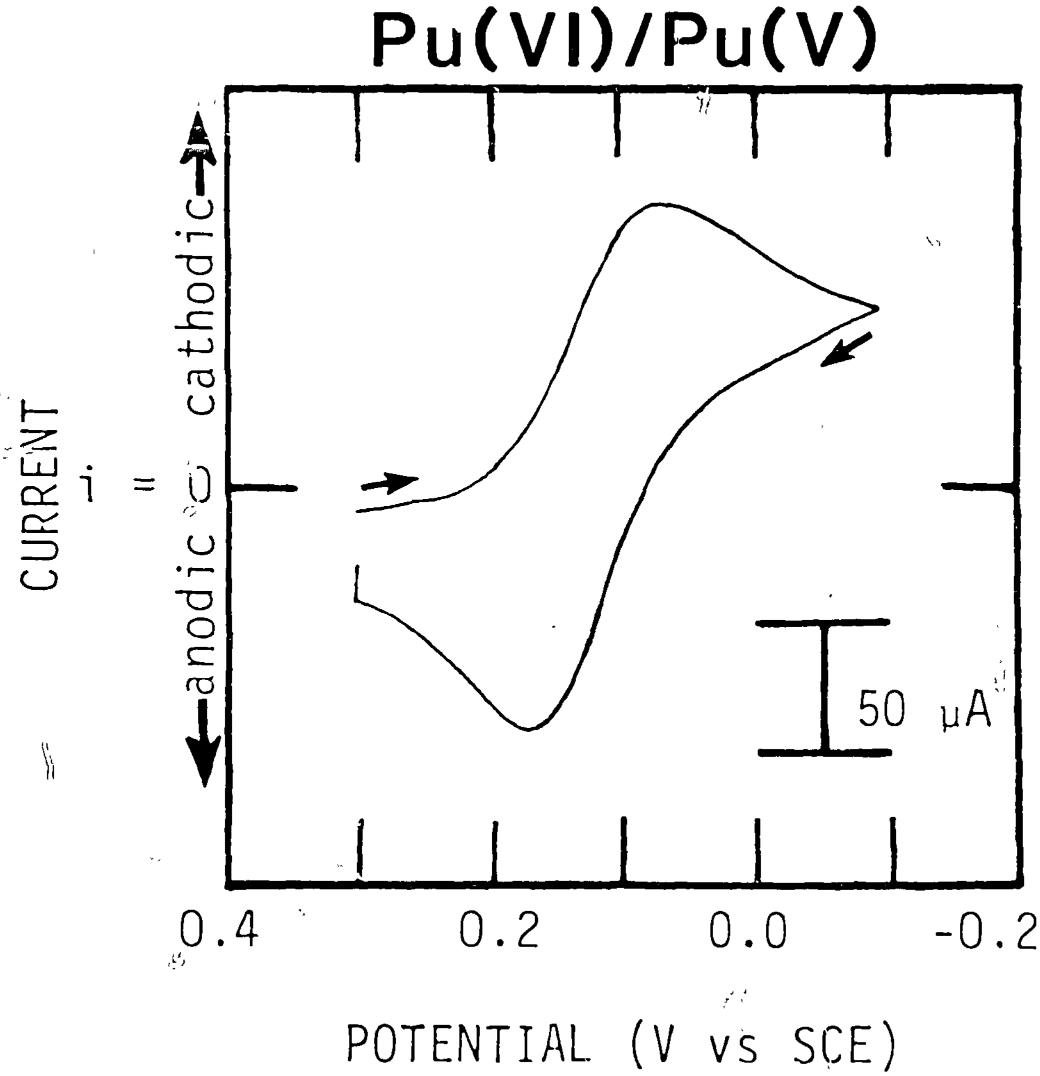

Figure 19. First scan cyclic voltammogram of Pu(VI)/Pu(V) in 2 M Na_2CO_3 solution, pH 12. Scan rate 20 mV/s; Pt electrode; [Pu] = 1.9 x 10^{-2} M.

solution. Oxidation of mixed Pu(VI)/Pu(V) in 2 M Na_2CO_3 solution at +0.35 V or reduction at −0.10 V at a Pt screen produced 100% Pu(VI) as PuO_2^{2+} and 100% Pu(V) as PuO_2^{2+}, respectively. The absorption spectra of green Pu(VI) and light yellow Pu(V) in 2 M Na_2CO_3 solutions are shown in Figures 20 and 21, respectively. In the pH range 12–13, the formal potential of the Pu(VI)/Pu(V) couple remains constant. However, in the pH range 13–14, a small negative shift in the formal potential of the Pu(VI)/Pu(V) couple was observed via cyclic voltammetry. At 1 M hydroxide ion concentration, $E^{\circ'}$ = +0.09 V, and at 2 M hydroxide ion concentration, $E^{\circ'}$ = +0.06 V for the Pu(IV)/Pu(V) couple in 2 M Na_2CO_3 solution. This negative shift in $E^{\circ'}$ is much smaller than the over 200 mV shift observed for the Np(VI)/Np(V) couple in 2 M Na_2CO_3 solution over the pH range 13–14 (see page 51). This indicates that the hydroxo (and/or mixed hydroxo-carbonato) complexation constant ratio of actinide(VI) to actinide(V) is higher for neptunium than for plutonium in sodium carbonate medium.

Correlating with the negative shift in the formal potential of the Pu(VI)/Pu(V) couple in 2 M Na_2CO_3 solution, as the hydroxide ion concentration was increased, were changes in the absorption spectra of Pu(VI) and (V) as shown in Figures 22 and 23, respectively. The colors of green Pu(VI) and light yellow Pu(V) in Na_2CO_3 solution changed to green-yellow and pink, respectively, as the hydroxide ion concentration was increased. The changes in the spectrum of Pu(V) are much more subtle than the dramatic changes in the spectrum of Pu(VI). The major absorption peak in the visible light region (at ca. 850 nm)

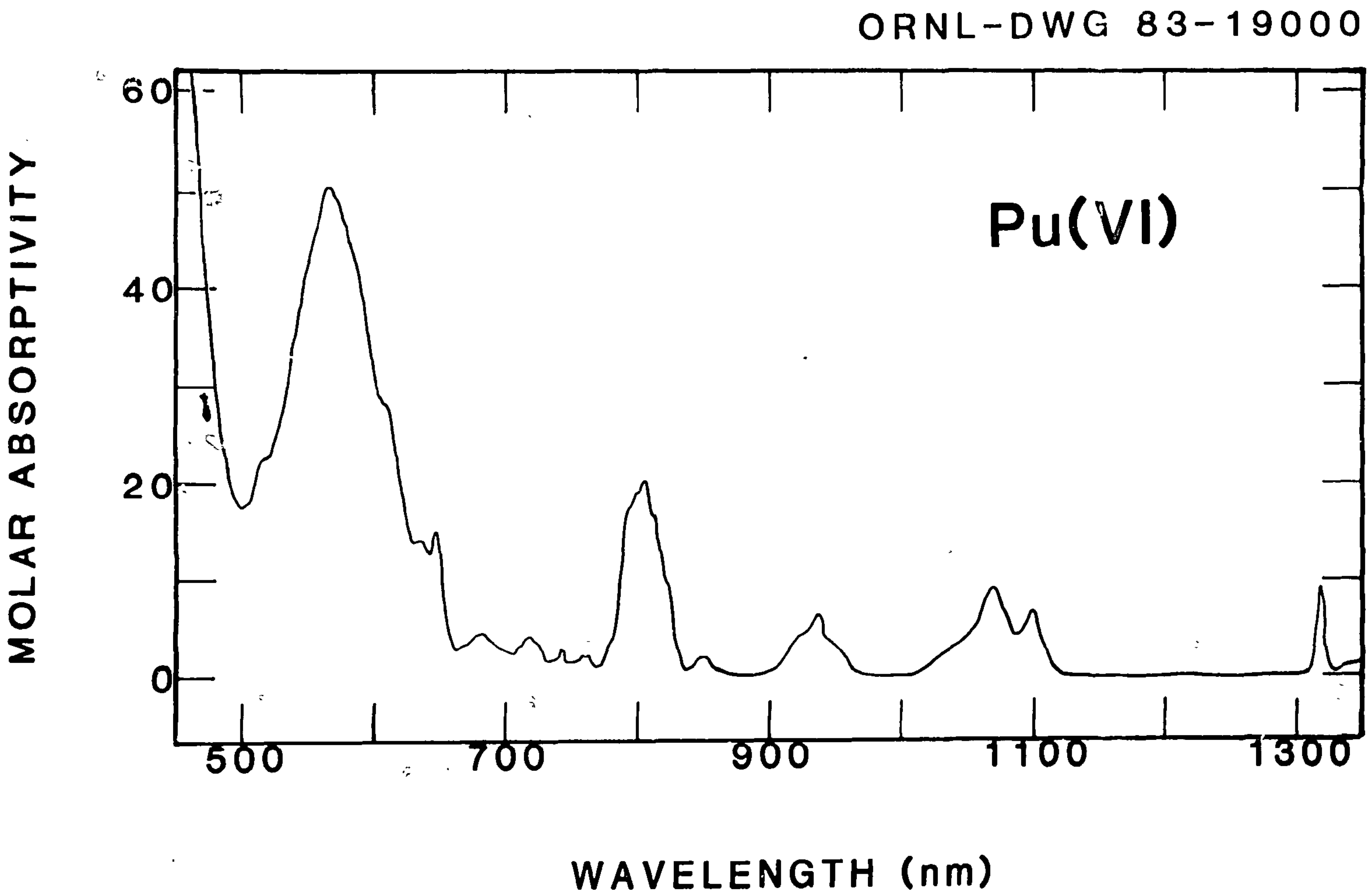

Figure 20. Absorption spectrum of Pu(VI) in 2 M Na_2CO_3 solution, pH 12.6.

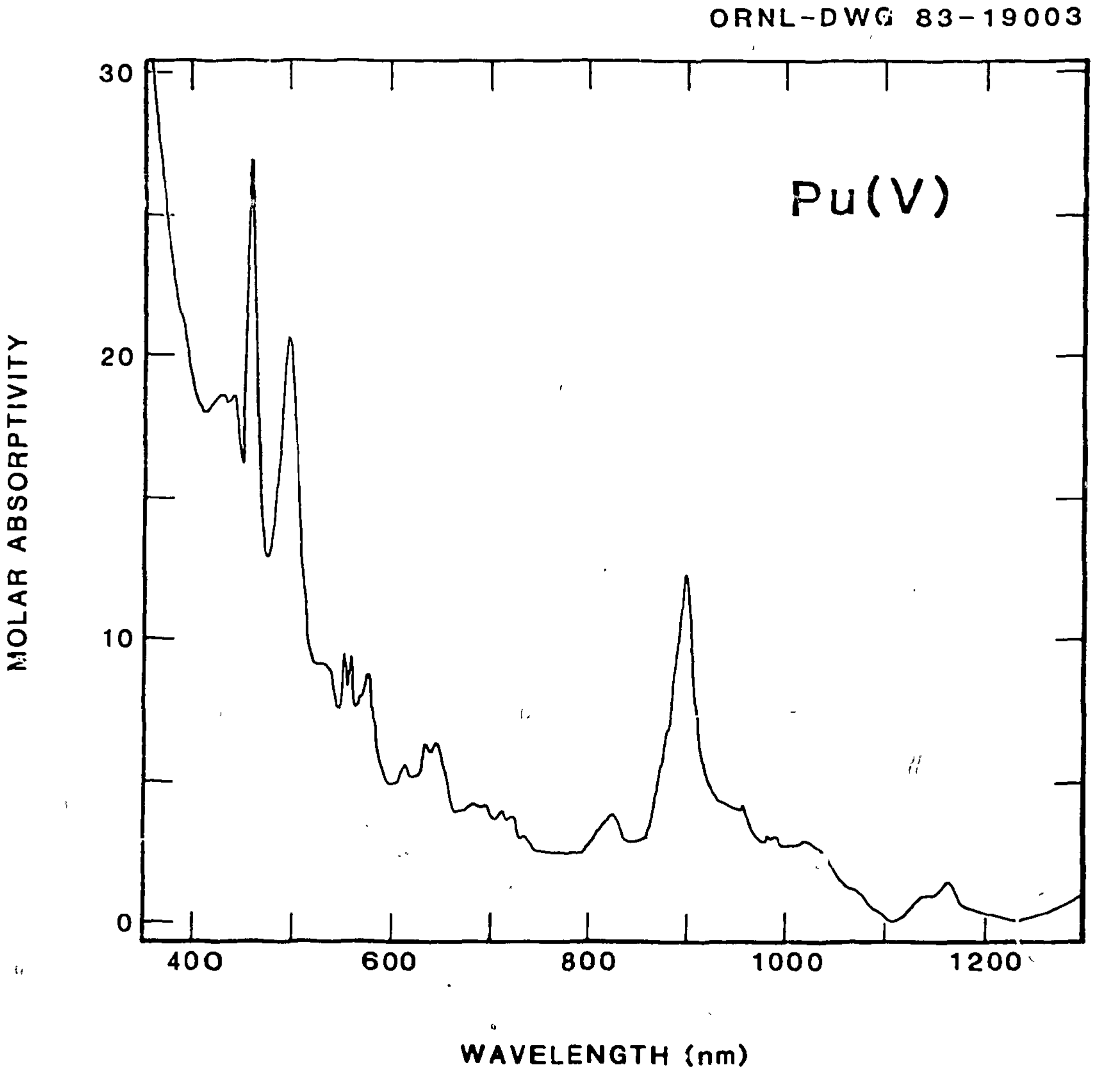

Figure 21. Absorption spectrum of Pu(V) in 2 M Na_2CO_3 solution, pH 12.6.

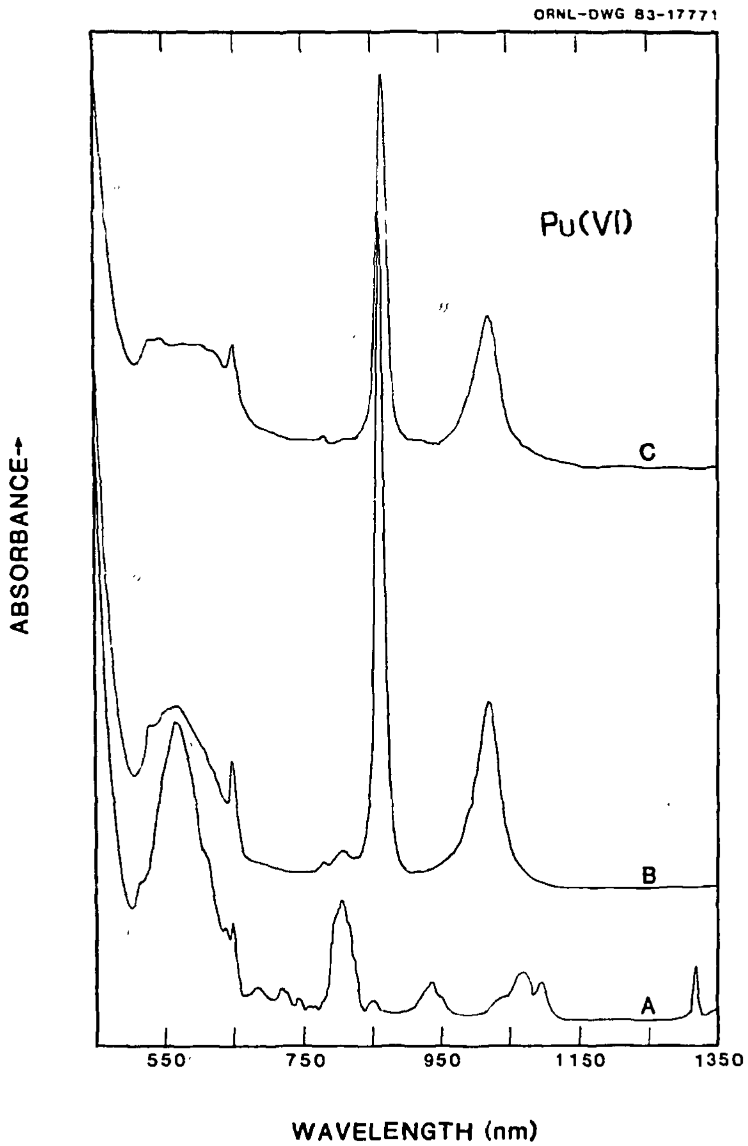

Figure 22. Absorption spectra of Pu(VI) in concentrated Na_2CO_3 solution at various hydroxide ion concentrations. A: $[OH^-]$ = 0.06 M, [Pu] = 1.7 x 10^{-2} M; B: $[OH^-]$ = 0.60 M, [Pu] = 1.6 x 10^{-2} M; C: $[OH^-]$ = 1.44 M, [Pu] = 1.3 x 10^{-2} M.

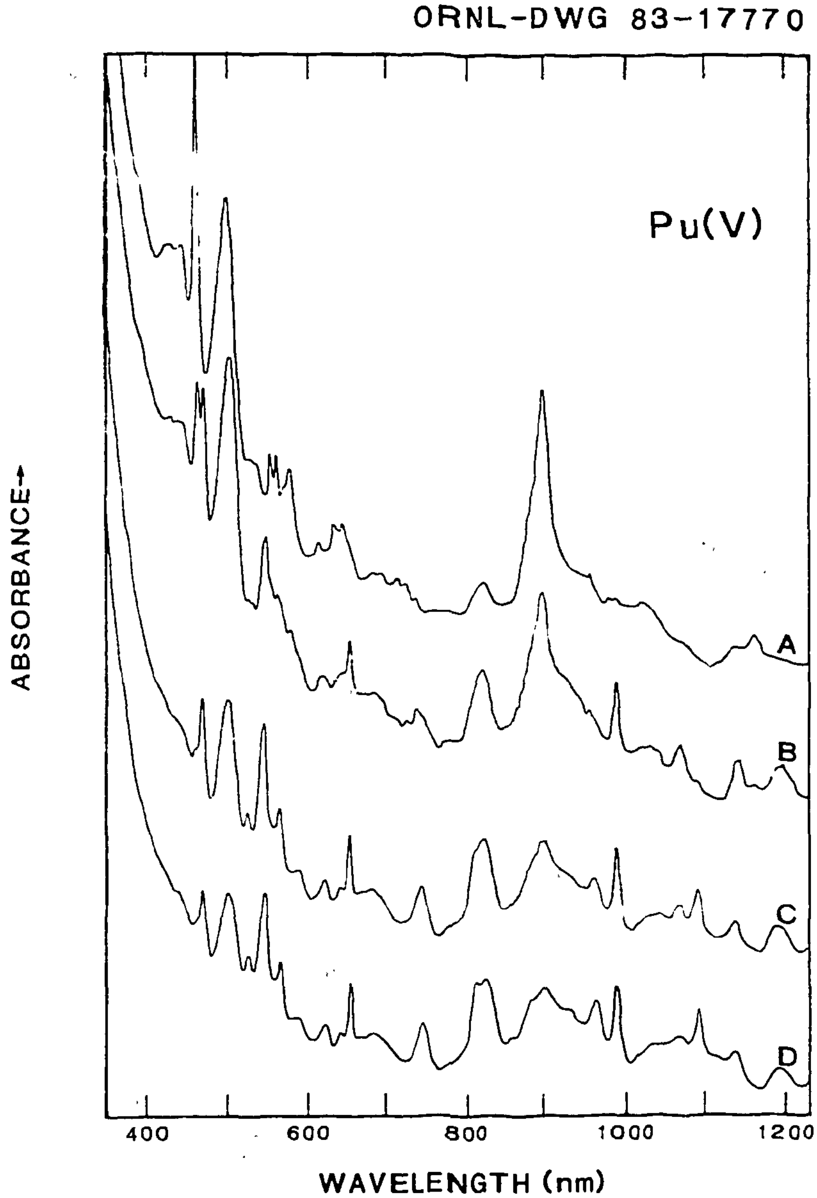

Figure 23. Absorption spectra of Pu(V) in concentrated Na_2CO_3 solution at various hydroxide ion concentrations. A: $[OH^-]$ = 0.04 M, [Pu] = 1.5 x 10^{-2} M; B: $[OH^-]$ = 1.04 M, [Pu] = 1.3 x 10^{-2} M; C: $[OH^-]$ = 1.75 M, [Pu] = 1.0 x 10^{-2} M; D: $[OH^-]$ = 2.29 M, [Pu] = 0.91 x 10^{-2} M.

of Pu(VI) in Na_2CO_3-NaOH solution shifts slightly to higher wavelengths as the hydroxide ion concentration is increased (see Figure 22). The molar absorptivity of this peak increases initially as the hydroxide ion concentration is increased, but then it decreases at even higher hydroxide ion concentrations (compare Figure 22B and 22C).

In concentrated aqueous carbonate solution with pH < 13, the Pu(VI) and Pu(V) complexes exist as $PuO_2(CO_3)_3^{4-}$ and $PuO_2(CO_3)_3^{5-}$, respectively.[17,40] In concentrated carbonate-hydroxide solution with a sufficiently high concentration of OH^- ion, Pu(VI) and Pu(V) should exist as carbonato-hydroxo and/or hydroxo complexes. Polymeric hydroxo complexes of Pu(VI) such as $(PuO_2)_2(OH)_2^{2+}$ and $(PuO_2)_4(OH)_7^+$ have been proposed.[82,86] Madic et al.[82] observed Raman spectral bands in aqueous solutions of Pu(VI) indicating the existence of such polymeric Pu(VI) complexes. Raman spectra (in this work) of Pu(VI) in concentrated carbonate-hydroxide solution did not exhibit these bands. Tetravalent Pu is known to form polymers in aqueous solution.[87] However, no evidence in this work was seen for soluble polymeric Pu(IV) in carbonate-hydroxide solution. Thus, Pu(VI) and Pu(V) are proposed to exist in carbonate-hydroxide solution as nonpolymeric carbonato-hydroxo complexes rather than as polymeric hydroxo complexes [see page 57 for a similar discussion concerning Np(VI) and Np(V) complexation].

If the redox reaction of Pu(VI) and Pu(V) in carbonate-hydroxide solution can be described as

$$PuO_2(CO_3)_n(OH)_p^{(2-2n-p)+} + e^- \rightleftarrows PuO_2(CO_3)_n(OH)_q^{(1-2n-q)+} + (p-q)(OH^-), \quad (10)$$

then a plot of the change in $\Delta E_{1/2}$ ($\Delta E_{1/2} = E_{1/2}([OH^-]) - 0.11$ V, where 0.11 V is $E_{1/2}$ in carbonate solution, pH < 13) versus the log$[OH^-]$ in concentrated carbonate solution (see Figure 24) should yield a linear slope proportional to -(p-q) (see Equation 9, page 58) in the pH range where carbonato-hydroxo complexes form. The half-wave potentials of the Pu(VI)/Pu(V) couple were estimated from carbonate-hydroxide solutions of Pu(V) using cyclic voltammetry. The ionic strength of the carbonate-hydroxide solutions was not maintained at a constant value. While Figure 24 does reveal an approximately linear relationship between $\Delta E_{1/2}$ and log$[OH^-]$, a non-integral value of p-q was obtained. Linear regression analysis using all the data points shown in Figure 24 and data points where $[OH^-]$ > ca. 1.1 <u>M</u> gives p-q = 1.6-1.7. While this result may indicate a change in hydroxo complexation number of one or two between Pu(VI) and Pu(V) complexes in carbonate-hydroxide solution, certain assumptions implicit in Equations 9 (see page 58) and 10 may not be valid. These assumptions are that the carbonate ion coordination number for the Pu(VI) and Pu(V) complexes is the same and remains constant. A more complete mapping of $\Delta E_{1/2}$ versus log$[OH^-]$ in solutions with constant ionic strength is necessary to see if a truly linear relationship between $\Delta E_{1/2}$ and log$[OH^-]$ at pH > 13 exists and if Equation 10 is valid in carbonate-hydroxide solution.

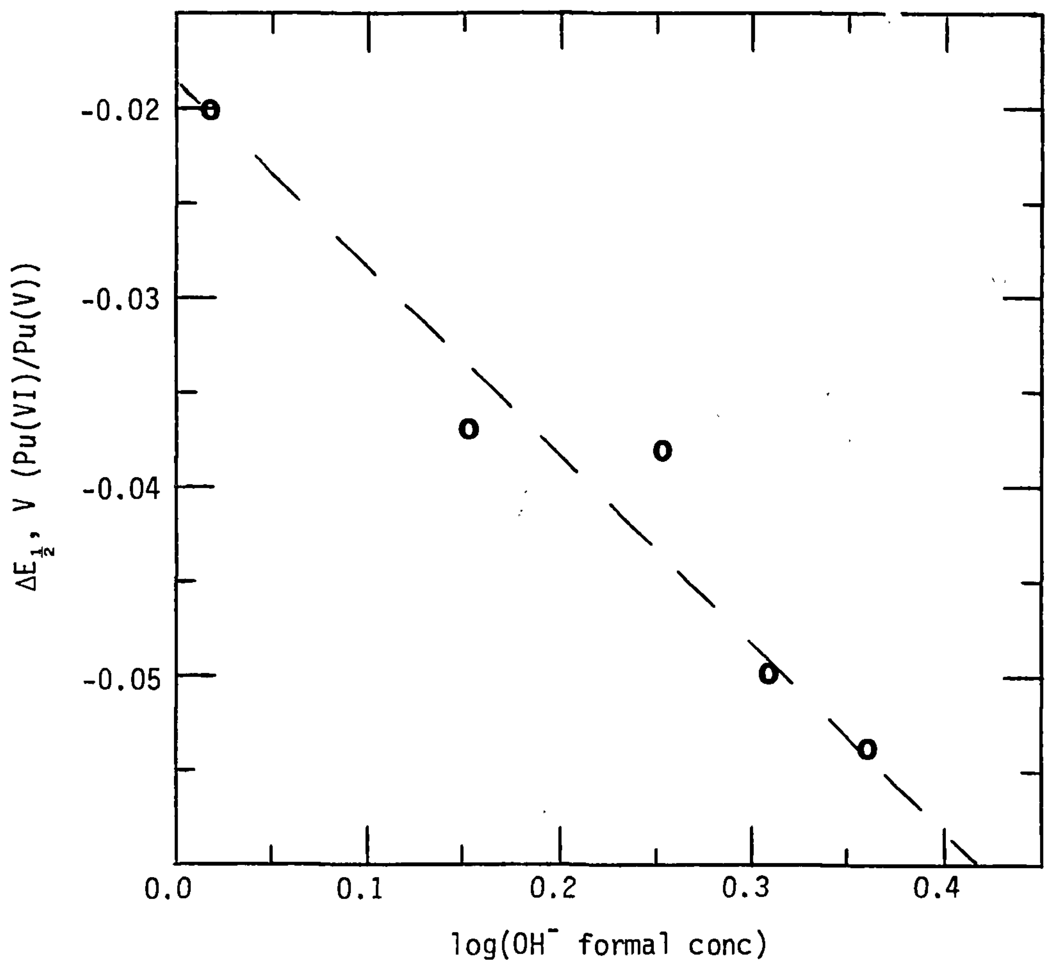

Figure 24. Change in half-wave potential ($E_{1/2}$-0.11 V) of the Pu(VI)/Pu(V) couple in concentrated carbonate-hydroxide solution as a function of log[OH^-]. The dashed line results from linear regression analysis and does not necessarily represent the best fit to the data (e.g., a better fit may be nonlinear).

Wester and Sullivan[39] reported a Pu(V) spectrum in 1 M Na_2CO_3 solution exhibiting an absorption peak at about 485 nm. In this work varying the pH from 10 to 14 of 1 M and 2 M Na_2CO_3 solutions of Pu(V) produced no absorption peak at this wavelength. The 485 nm peak in Wester and Sullivan's spectrum of Pu(V) may be actually due to Pu(IV), whose strongest absorption in the visible wavelength region occurs at ca. 485 nm. The lack of a Pu(VI) peak at ca. 850 nm in Wester and Sullivan's spectrum[39] is attributed to a difference in pH from that in the present work, where a small peak at about 850 nm was observed in the Pu(VI) spectrum (see Figure 20, page 76). This 850-870 nm Pu(VI) absorption peak in Na_2CO_3-NaOH solution (see Figure 22, page 78) corresponds to a similar peak observed by others in NaOH solution.[88]

When the hydroxide precipitate produced by adding NaOH solution to the Pu(VI) stock solution was introduced into 2 M Na_2CO_3 solution, a Pu(VI) solution plus a white precipitate resulted. This white precipitate dissolved in 1 M HCl with fizzing (CO_2 gas evolution), and the absorption spectrum of the resulting solution matched that known for Pu(V) in acid solution.[89] The Raman spectrum of this same white precipitate was rather nondescript. A broad peak at 1085 ± 10 cm^{-1}, assigned to carbonate ion vibrations, and a small signal at 759 ± 2 cm^{-1} suggested the solid might be a Pu(V) dioxy cation carbonate. The Pu(V) carbonate precipitate may have resulted for a variety of reasons. The hydroxide precipitate [from the Pu(VI) stock solution] may have been a mixture of primarily Pu(VI) hydroxide and a small amount of Pu(V) hydroxide. Due to the low formal potential of the

Pu(VI)/Pu(V) couple in Na_2CO_3 solution, some Pu(VI) may have been reduced by trace impurities, hydroxide ion, or water. In addition, 10^{-2}–10^{-1} M Pu(VI) in Na_2CO_3 solution slowly precipitates Pu(V) carbonate over a period of weeks to months.

Although the Raman spectrum of the white Pu(V) carbonate solid did not match very well that of $Na_3PuO_2(CO_3)_2 \cdot nH_2O$ given by Madic et al.[17] in quality or appearance, the vibration frequencies observed in this work at 693 ± 2 cm^{-1}, 710 ± 5 cm^{-1}, and 759 ± 2 cm^{-1} do match those they report for this compound. The Pu(V) carbonate solid may have been somewhat amorphous resulting in the rather indefinite Raman spectrum of the solid. A similar white solid, precipitated from a Na_2CO_3 solution containing Pu(V), was also analyzed by Raman spectroscopy. Its spectrum was identical to that given by Madic et al.[17] for $Na_3PuO_2(CO_3)_2 \cdot nH_2O$.

A difference in the stabilities of Pu(VI) in 2 M and in 5 M K_2CO_3 solutions was noted. Hexavalent plutonium is stable in 2 M Na_2CO_3 and 2 M K_2CO_3 solutions. When the plutonium hydroxide precipitate formed by adding NaOH to the Pu(VI) stock solution was mixed with 5 M K_2CO_3 solution, an apple-green precipitate of Pu(IV) (as discussed later) and a supernatant containing Pu(VI) resulted. In a matter of days, the Pu(VI) present in the solution precipitated. In contrast, when the plutonium hydroxide was dissolved in 2 M K_2CO_3 or 2 M Na_2CO_3 solution, a stable Pu(VI) solution resulted along with some white Pu(V) carbonate salt (as identified by its acid solution absorption spectrum).

2. Pu(VII)

Electrolysis of Pu(VI) in 2 M Na_2CO_3 solution at pH 12 to pH 14 at potentials up to +1.1 V yielded no observable Pu(VII) as determined by absorption spectrophotometric analysis. Ozonolysis also failed to produce Pu(VII) in this pH range. In 2 M Na_2CO_3 solution the hydroxide ion concentration needed to be in excess of ca. 2.5 M in order to generate blue-green Pu(VII) by the oxidation of Pu(VI) with ozone. Due to excessive water oxidation at a Pt screen, no measurable amount of Pu(VII) could be produced by electrolysis of the same Pu(VI) solution in a three electrode electrolysis cell. Bhattacharyya et al.[90] oxidized Pu(VI) to (VII) at +2.8 V in carbonate-free sodium hydroxide solution using a two electrode electrolysis cell and Pt coil electrodes. Komkov et al.[91] oxidized Pu(VI) to (VII) in KOH solution both by electrolysis and by reaction with persulfate and hypobromite ions. Oxidation of Pu(VI) in NaOH solution using ozone has also been reported.[88,92] The absorption spectrum of Pu(VII) in Na_2CO_3-NaOH solution (see Figure 25) is very similar to that in hydroxide media.[88,92] Plutonium(VII) is reduced by water to Pu(VI). A 10^{-2} M Pu(VII) in Na_2CO_3-NaOH solution is reduced completely to Pu(VI) in approximately one day.

The rate of oxidation of Pu(VI) in Na_2CO_3-NaOH solution with ozone was slower than that in just NaOH solution. In addition lower concentrations of NaOH could be used alone than in combined Na_2CO_3-NaOH solutions to produce Pu(VII) by ozonolysis of Pu(VI). Thus, carbonate ion seems to hinder the oxidation of Pu(VI) to

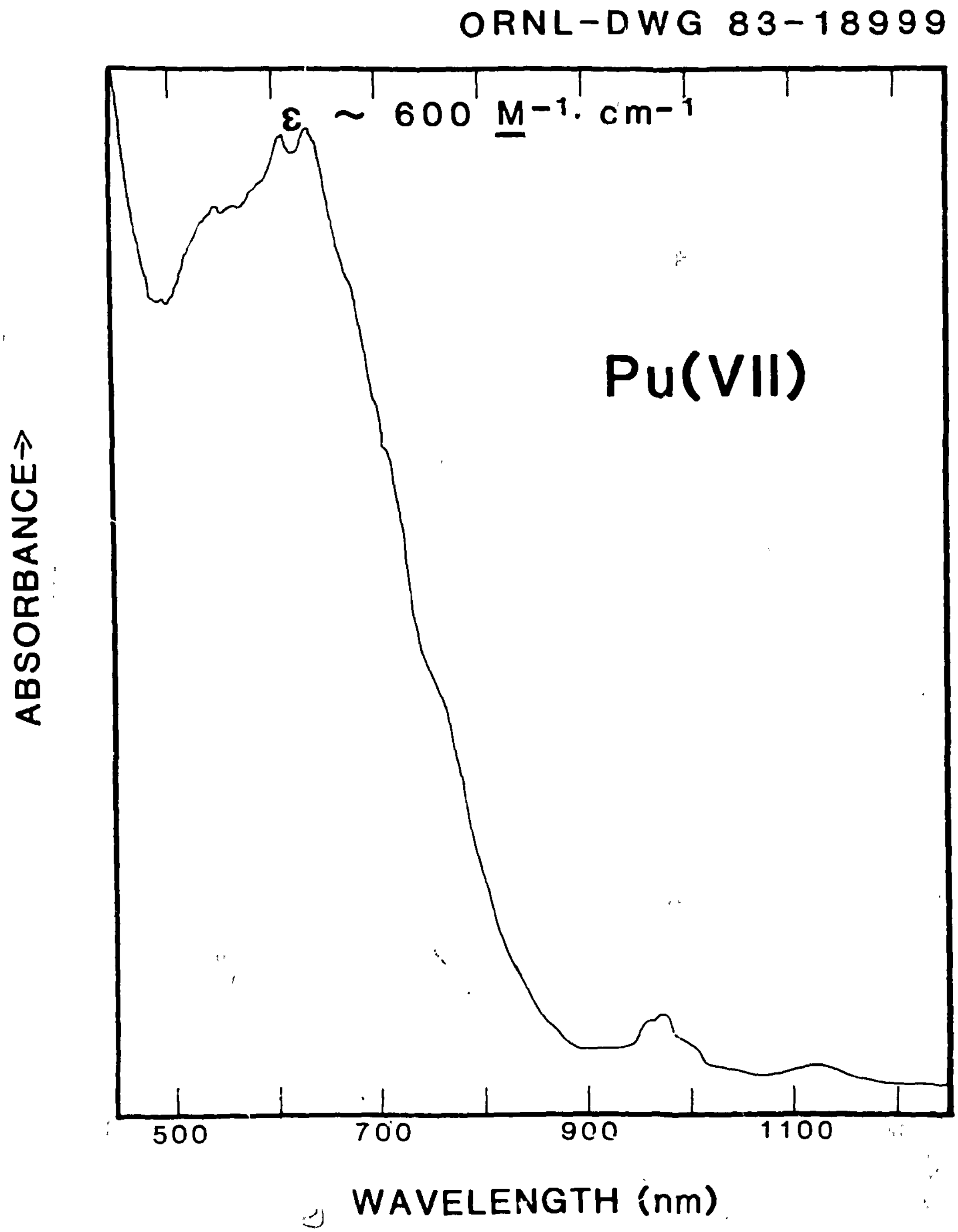

Figure 25. Absorption spectrum of Pu(VII) in 1.1 M Na_2CO_3, 2.7 M NaOH solution.

Pu(VII). These results suggest the following: (1) a greater negative shift in the E°' of the Pu(VII)/Pu(VI) couple is provided by hydroxide ions than by carbonate ions, (2) as the carbonate ion concentration is increased, carbonate ions compete more effectively with hydroxide ions for complexation of Pu(VI), and (3) the complexation of Pu(VII) in carbonate-hydroxide media seems to be due principally, if not completely, to hydroxide ions. The formation of mixed hydroxo-carbonato complexes of Pu(VII) cannot be completely discounted. However, their formation is deemed unlikely because, for instance, absorption spectra of Pu(VII) in both NaOH and Na_2CO_3-NaOH solutions are essentially identical and the oxidation of Pu(VI) to Pu(VII) proceeds in NaOH or Na_2CO_3-NaOH solution but not in Na_2CO_3 solution alone, as already discussed.

The Raman spectrum of Pu(VII) in Na_2CO_3-NaOH solution exhibits a single, small, Pu peak at 703 ± 6 cm^{-1} (see Figure 26). Increasing the concentration of Pu(VII) above 3×10^{-2} M does not appreciably increase the Pu(VII) Raman signal due to increased absorption of the 514.5 nm laser light. Laser generated heating of the dark solutions created convection currents therein which resulted in noisy Raman spectra. The Pu(VII) peak was judged to be only moderately polarized at most (see Figure 26). The depolarization ratio ρ $[I_T(\text{obs.} \parallel)/I_T(\text{obs.} \perp)]$ of the 703 cm^{-1} peak is 0.6 ± 0.2 (only a rough estimate could be made due to the poor signal/noise ratio of the peak). This is in contrast to the larger reduction seen for the Raman peak of Np(VII) in Na_2CO_3-NaOH solution (ρ = 0.3, see page 61) when the plane of

ORNL-DWG 83-17589

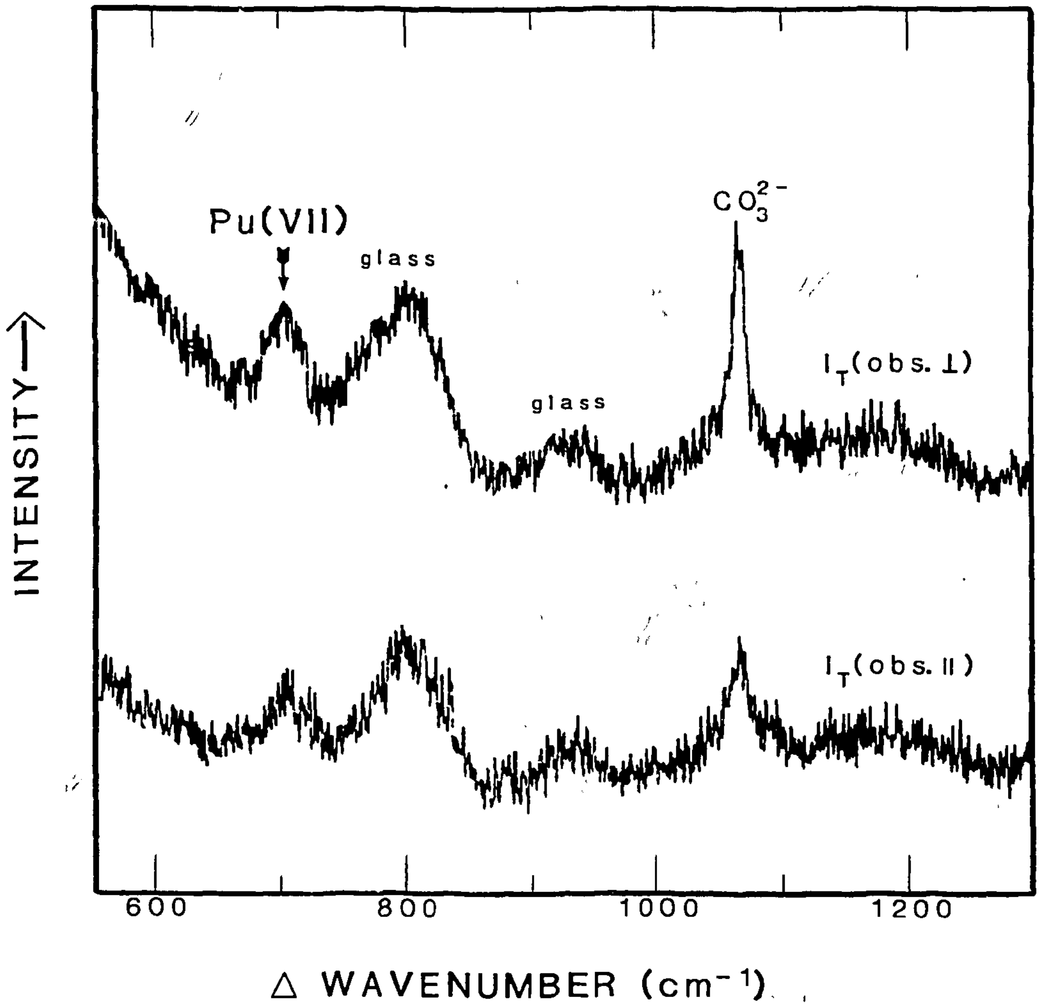

Figure 26. Raman spectra of Pu(VII) in 0.9 M Na_2CO_3, 4.7 M NaOH solution, [Pu] = 3.7 x 10^{-2} M. Excitation at 514.5 nm.

polarization of the laser beam was rotated by 90°. This suggests that Pu(VII) may not be in the linear form PuO_2^{3+} or $PuO_2(OH)_n^{(3-n)+}$ in solution, as was suggested in the case of Np(VII) (see page 61). Unfortunately, the weakness of the Pu(VII) Raman scattering signal precluded detection of any other Pu(VII) vibrations which might aid the elucidation of its structure.

The Pu(VII) Raman vibration at 703 cm^{-1} in Na_2CO_3-NaOH solution is lower than those of the symmetric stretches at 788 cm^{-1} for Pu(VI) and 760 cm^{-1} for Pu(V) in 2 M Na_2CO_3 solutions.[17] If the structure of Pu(VII) is similar to the PuO_2^{n+} structure of Pu(VI) and (V), then one would expect the Pu(VII) Raman vibration to occur at a frequency higher than those of Pu(VI) and (V). Differences in complexation may be responsible for lowering the Pu(VII) vibration frequency in Na_2CO_3-NaOH solution below those of Pu(VI) and (V) in Na_2CO_3 solution. Raman spectra of Pu(VI) in 3.3 M NaOH, 0.8 M Na_2CO_3 solution and in 4.1 M NaOH, 0.38 M Na_2CO_3 solution were obtained. The PuO_2^{2+} symmetric stretch frequency (ν_1) was measured in both cases at 772 ± 2 cm^{-1}. This is lower than the 788 cm^{-1} value for ν_1 in 2 M Na_2CO_3 solution[17] and the 794 cm^{-1} value in a solution which was 0.26 M ClO_4^- ion concentration, $\mu = 1.0$, and pH = 13.3.[82] Thus, the value of ν_1 for Pu(VI) depends on the solution environment.

3. Pu(IV) and (III)

Disproportionation of Pu(V) in bicarbonate media has been reported.[39] At pH 9.3 in 1 M $NaHCO_3$-Na_2CO_3 solution, reduction of

Pu(VI) at −0.1 V at a Pt screen electrode produces 100% apple-green Pu(IV) based on absorption spectral analysis. At pH 11.0 in the same medium, reduction of Pu(VI) at −0.1 V at a Pt screen electrode produces a solution of ca. 80% Pu(IV) and 20% Pu(V). This indicates that Pu(V) only partially disproportionates at this pH. At pH 11.0, in approximately one day, the disproportionation of Pu(V) into a mixture of Pu(VI), (V), and (IV) comes to equilibrium. Even at pH 11.4, where Pu(IV) begins to precipitate from Na_2CO_3 solution,[41] Pu(V) is still unstable to disproportionation. Thus, direct potential measurements of mixtures of Pu(IV) and (V) solutions are not suitable for determining $E°'$ of the Pu(V)/Pu(IV) couple. Due to the irreversible nature of the Pu(V)/Pu(IV) couple in Na_2CO_3 solution, as discussed later, cyclic voltammetry does not permit the determination of the formal potential of the Pu(V)/Pu(IV) couple. A suitable method for the direct determination of $E°'$ of the Pu(V)/Pu(IV) couple in Na_2CO_3 solution has not yet been found.

Bulk reduction of Pu(V) in Na_2CO_3 solution led to precipitates of either Pu(IV) or Pu(III) depending upon the solution pH. Reduction of Pu(V) to a soluble Pu(IV) species in Na_2CO_3 solution was not possible because of the overpotential associated with the reduction of the PuO_2^+-carbonato complex. Cyclic voltammograms of Pu(V) in 2 M Na_2CO_3 solution at various pH values were recorded. At pH 11 to 12.5, a sharp cathodic wave at about −1.05 V and a small, broad, anodic wave were seen (see Figure 27). At pH 13 to 14, the reduction wave at ca. −1.1 V still was sharp, but somewhat broader than that

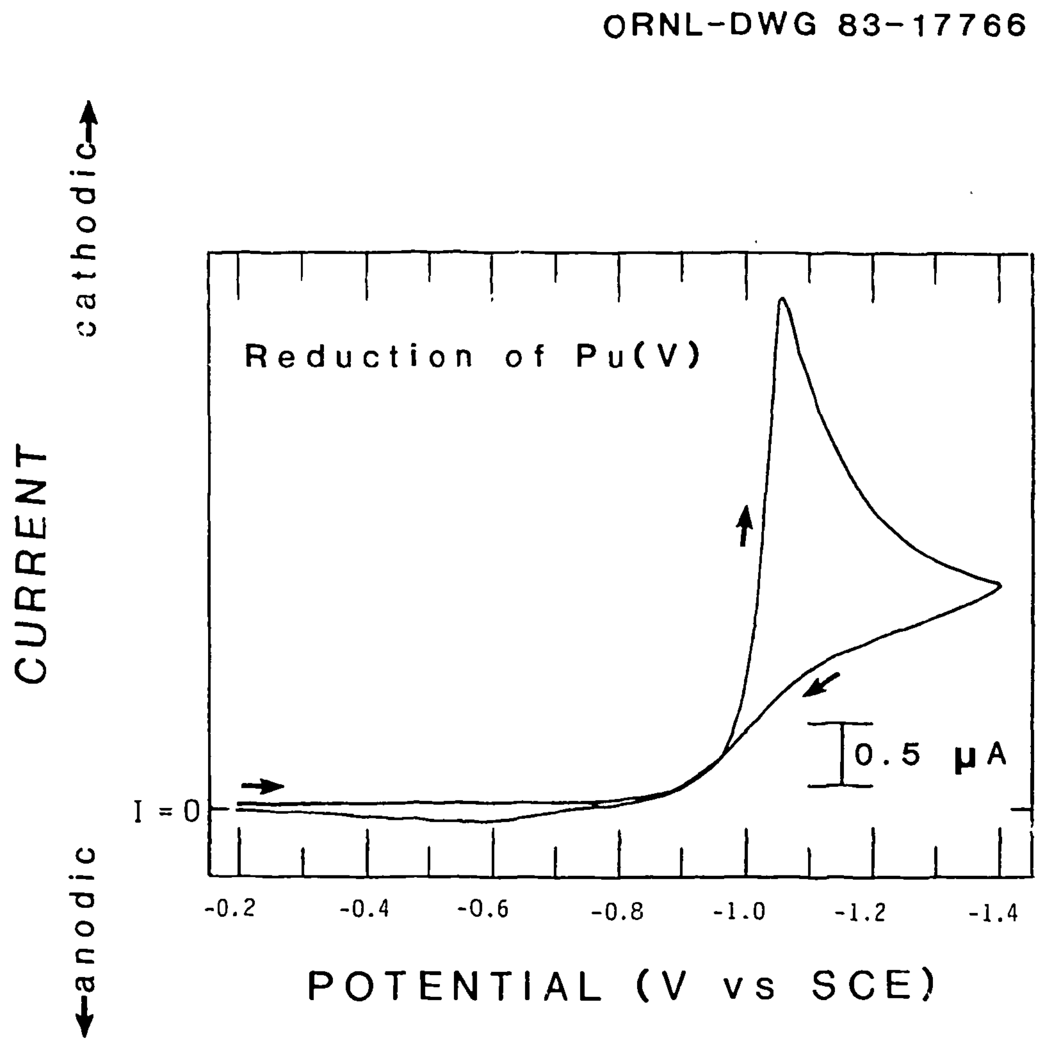

Figure 27. First scan cyclic voltammogram of Pu(V) in 2 M Na_2CO_3 solution, pH 12.3. Scan rate = 20 mV/s; HMDE; [Pu] = 3.3 x 10^{-3} M.

shown in Figure 27, and a small anodic wave at approximately -0.75 V was seen. In 1 M Na_2CO_3 solution at pH 12 to 14, a smoother cathodic reduction wave and an anodic wave at about -0.9 V were seen (see Figure 28). At pH 11, the cyclic voltammograms of Pu(V) in 1 M Na_2CO_3 solution appear identical to those of Pu(V) in 2 M Na_2CO_3 solution at pH 11 to 12.5. Thus, the shapes of the cyclic voltamm rams are dependent upon the carbonate ion concentration and pH. The behavior of the cathodic wave is indicative of the reduction of Pu(V) to (IV) followed immediately by the reduction of Pu(IV) to (III). As the pH is increased, Pu(IV) tends to precipitate out thus preventing an overall two electron reduction. Higher carbonate ion concentrations help to solubilize the Pu(IV) around the HMDE (small electrode area compared to solution volume) and thus aid in the reduction of Pu(V) to (III) in Na_2CO_3 solution. These conclusions are supported by the bulk electrolytic reduction work (large electrode area compared to solution volume) discussed next.

Reduction of Pu(V) in Na_2CO_3 solutions at pH > 11.4 using a Hg pool at -1.4 V produced apple-green Pu(IV) solid. This solid was insoluble in 1 M and 2 M Na_2CO_3 solutions, pH < 11.4, and in water, but it did dissolve in 1 M HCl. This behavior differs from that of a similarly obtained Np(IV) hydroxide precipitate (see page 67) which could be redissolved in Na_2CO_3 solution of sufficiently low pH. If the Pu(IV) solid was allowed to remain in contact with the Na_2CO_3 solution overnight, the resulting apple-green precipitate would not

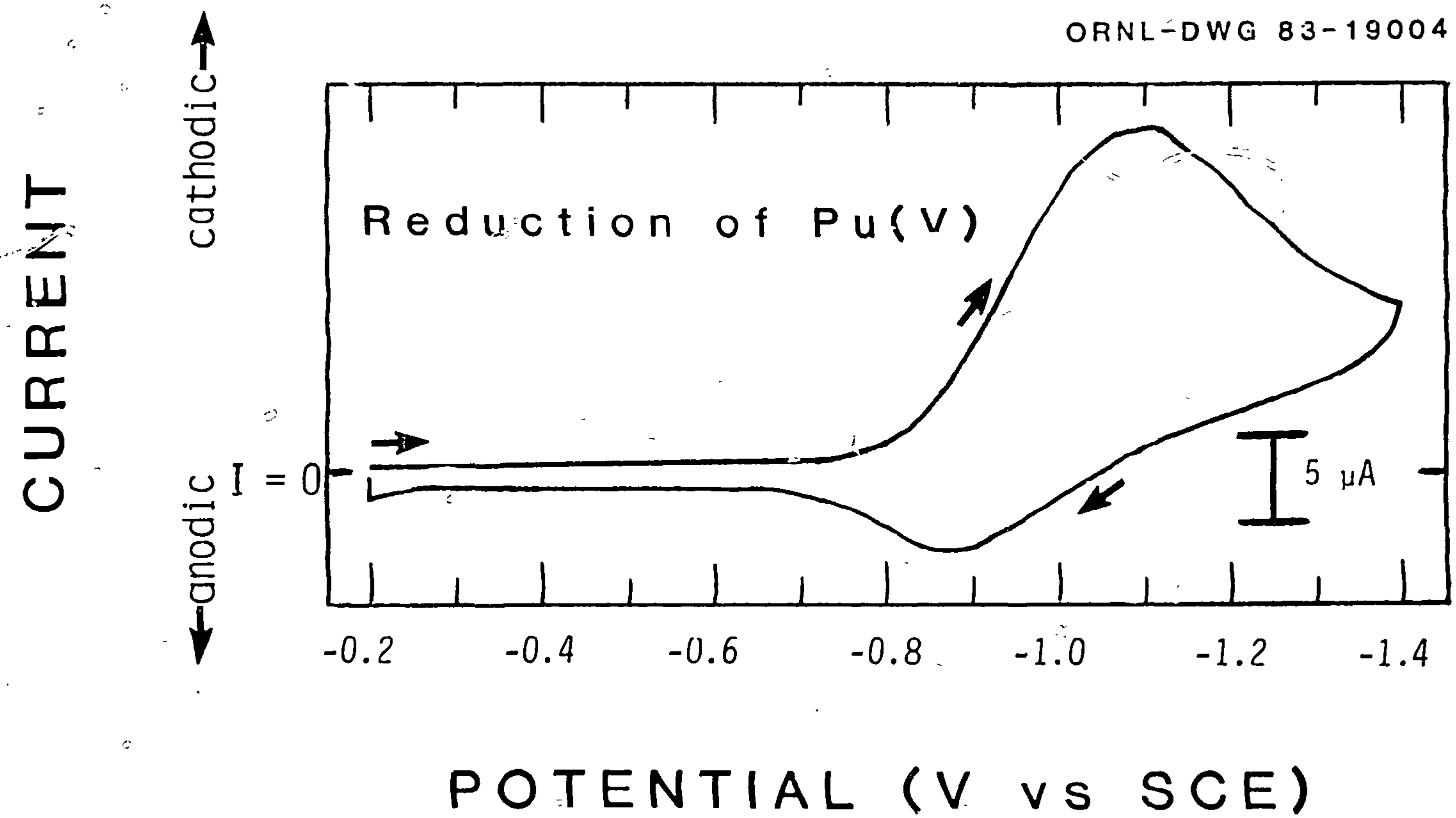

Figure 28. First scan cyclic voltammogram of Pu(V) in 1 M Na_2CO_3 solution, $[OH^-]$ = 0.25 M. Scan rate = 20 mV/s; HMDE; [Pu] = 1.7×10^{-2} M.

dissolve even in 1 M HCl, indicating that the Pu(IV) solid had probably polymerized.

At pH < 11.4, reduction of Pu(V) in 1 M or 2 M Na_2CO_3 solution produced a blue precipitate of Pu(III) as noted earlier.[39] Thus the cathodic wave seen in the HMDE cyclic voltammograms of Pu(V) represents the reduction of Pu(V) to (IV) and Pu(IV) to (III) [and possibly Pu(V) to (III)]. If the pH is above 11.4, Pu(IV) precipitates out of Na_2CO_3 solution leaving a supernatant void of plutonium. In K_2CO_3 solution, however, Pu(IV) is soluble up to pH 12 or pH 13. The absorption spectrum of Pu(IV) in 3.4 M K_2CO_3 is shown in Figure 29. It matches that given by Wester and Sullivan[39] in 1 M $NaHCO_3$ solution.

Cyclic voltammograms of Pu(IV) in 1 M and 2 M Na_2CO_3 solutions at −0.4 V to +1.1 V at a Pt electrode exhibited no anodic waves corresponding to the oxidation of Pu(IV). Bulk electrolysis of Pu(IV) in 1 M $NaHCO_3$, 1 M Na_2CO_3, and 2 M Na_2CO_3 solutions at a Pt screen electrode at potentials up to +1.1 V yielded no measurable amounts of Pu(V) or (VI) based on absorption spectral analysis. This is in contrast to what was observed in the case of neptunium, where oxidation of Np(IV) to (VI) was possible (see page 70).

The Pu(IV)/Pu(III) couple was observed via cyclic voltammetry at a HMDE in Na_2CO_3 and K_2CO_3 solutions. The couple is highly irreversible.[28,39,41] In 1 M $NaHCO_3$-Na_2CO_3 solution at pH 9.3, the anodic wave was seen at ca. −0.3 V and the cathodic wave at about −1.05 V. At pH 10.0, the anodic wave appeared at −0.4 V and the cathodic wave was at ca. −1.1 V. As the pH was raised from 9.3 to

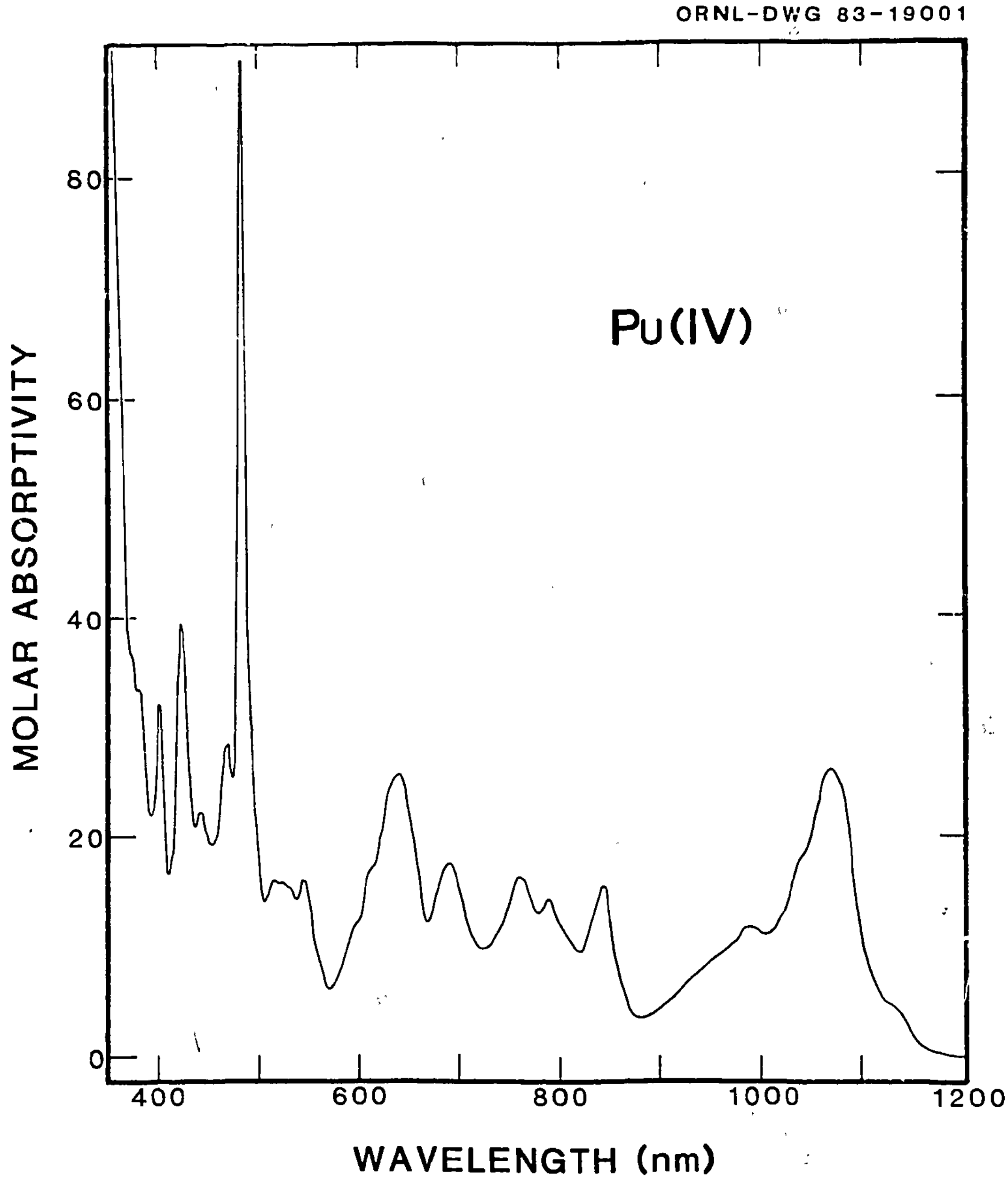

Figure 29. Absorption spectrum of Pu(IV) in 3.4 M K_2CO_3 solution, pH 11.9.

10.0, the anodic peak current to cathodic peak current ratio decreased by a factor of about three. The cyclic voltammogram of Pu(IV) in 1 M K_2CO_3 solution at pH 11.6 is shown in Figure 30.

Reduction of Pu(IV) in Na_2CO_3 solution at a Hg pool yielded a blue precipitate of Pu(III). In K_2CO_3 solution, reduction of Pu(IV) at -1.3 V produced a blue solution of Pu(III). Due to the sensitivity of Pu(III) to air oxidation, the absorption spectrum of Pu(III) was obtained spectroelectrochemically. Using an amalgamated nickel porous metal foam optically transparent electrode [Ni(Hg)-PMF-OTE], the spectrum of Pu(III) in 1 M K_2CO_3 solution was recorded (see Figure 31). Due to the evolution of hydrogen gas at the Ni(Hg)-PMF electrode, the electrode was raised out of the path of the spectrophotometer light beam (PMF still in contact with the solution) while recording the spectrum. The Pu(III) spectrum could also be recorded by removing the PMF electrode (with no jarring of the OTE cell to avoid stirring) and scanning over the VIS-near-IR range in a few minutes. After ca. ten minutes, with no movement of the OTE cell, oxidation of the Pu(III) to (IV) was evident. Agitating the OTE cell increased the rate of air absorption by the solution and hence, increased the rate of oxidation of the Pu(III). At -1.3 V at a Ni(Hg)-PMF electrode, noticeable reduction of water producing hydrogen gas and hydroxide ions was observed. The hydroxide ions reacted with the Pu(III) solution to form $Pu(OH)_3$ solid which caused the rising background toward the UV wavelength region in the spectrum of Pu(III) shown in Figure 31. Raising the electrode out of the path of the light beam, but still

ORNL-DWG 83-17768

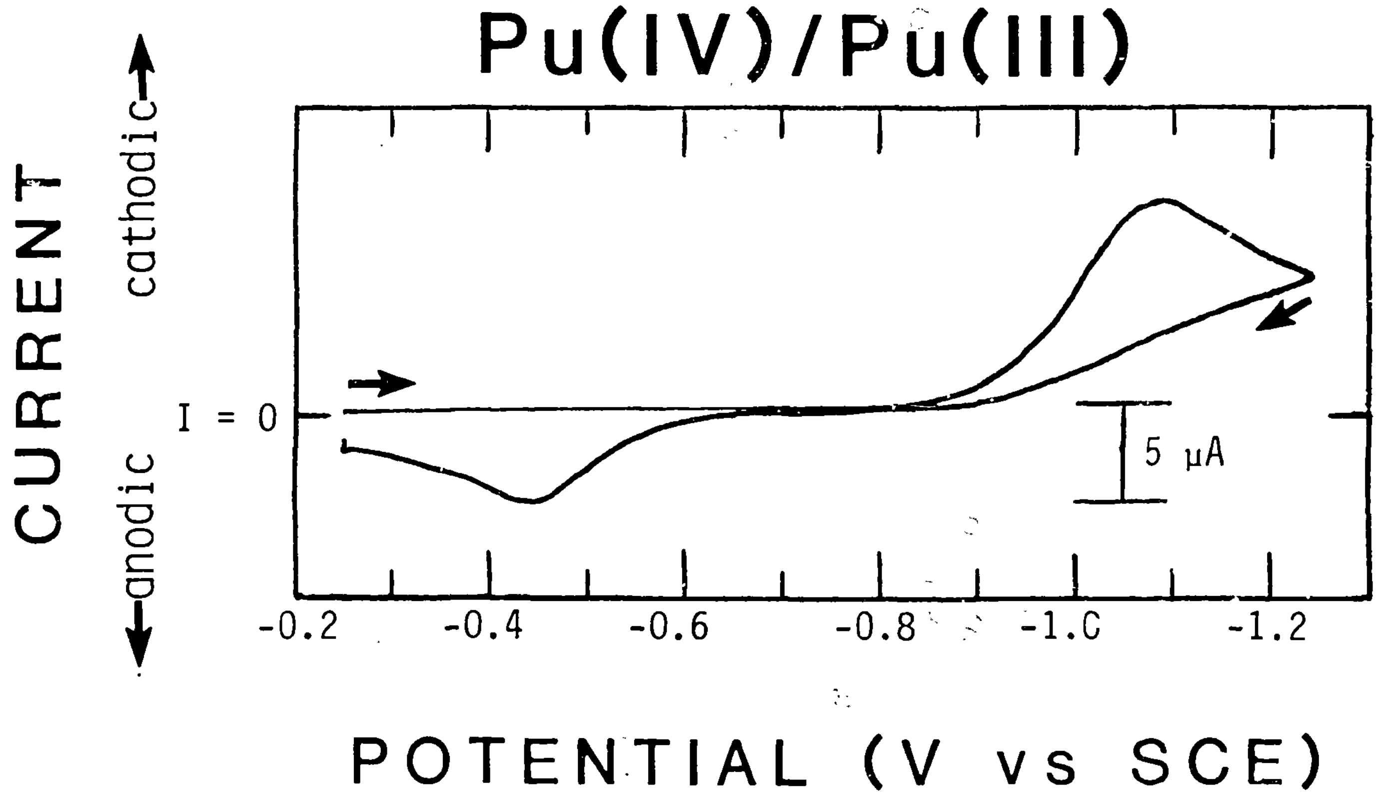

Figure 30. First scan cyclic voltammogram of Pu(IV)/Pu(III) in 1 M K_2CO_3 solution, pH 11.6. Scan rate = 50 mV/s; HMDE; [Pu] = 2.0 x 10^{-2} M.

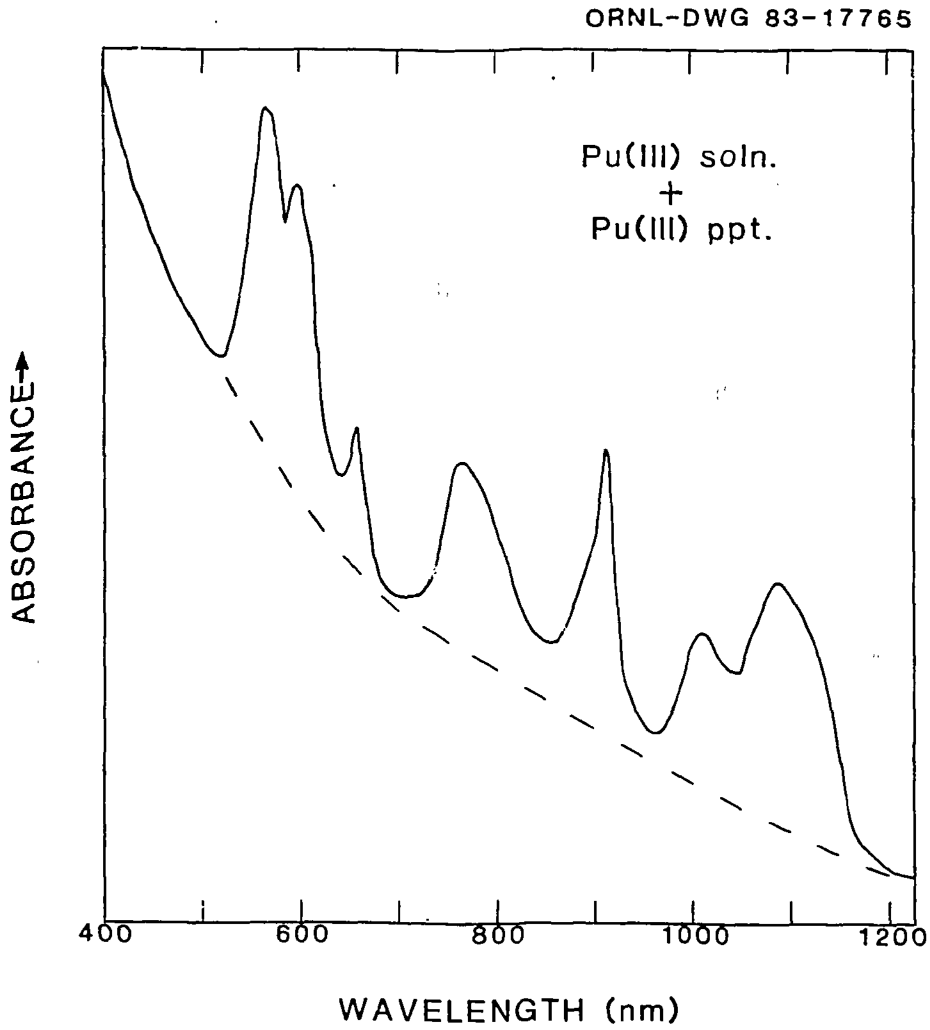

Figure 31. Absorption spectrum of Pu(III) in 1 M K_2CO_3 solution, pH 11.0. The dashed line indicates approximately the light scattering background due to the $Pu(OH)_3$ precipitate.

maintaining its contact with the solution, did not reduce the high light scattering background due to $Pu(OH)_3$. Solid $Pu(OH)_3$, formed at the top of the solution where the PMF was in contact with the solution, passed through the spectrophotometer light path as it slowly settled to the bottom of the OTE cell. Extensive electrolysis of Pu(IV) solutions to insure reduction to 100% Pu(III) was not possible since Pu(III) in solution would precipitate out with time. Thus, in the reported spectrum of Pu(III) (see Figure 31), some residual Pu(IV) may still be present even though the major Pu(IV) visible absorption peak at ca. 485 nm is absent. An OTE cell utilizing a Hg pool electrode would substantially reduce the amount of hydrogen gas and hydroxide ions formed at −1.3 V, but liquid mercury is not a convenient electrode for OTE cells.

The Pu(III) VIS-near-IR absorption spectrum in basic carbonate solution is very similar to that in perchloric acid solution.[89] The molar absorptivity of the 560 nm Pu(III) peak was estimated from the corresponding Pu(IV) spectrum to be about 20-30 $\underline{M}^{-1}$ cm^{-1}. The absorption spectra of Pu(IV) in bicarbonate[39] and K_2CO_3 solutions are also very similar to the spectrum of Pu(IV) in perchloric acid solution.[89] The spectrum of Pu(III) in carbonate solution appears to match the associated acid solution spectrum somewhat more closely in frequencies and molar absorptivities than does the Pu(IV) in carbonate solution spectrum match that of Pu(IV) in acid solution. This is apparently the result of greater complexation of Pu(IV) by carbonate ion in comparison to that of Pu(III).

C. Americium

^{243}Americium(III) in 2 M Na_2CO_3 solution was oxidized with ozone to Am(VI) as identified by its solution spectrum.[44,47] Hexavalent Am (AmO_2^{2+}) is orange-brown or dark red (at higher Am concentrations) in Na_2CO_3 solution. In 2 M Na_2CO_3 solution, Am(VI) is unstable to reduction by water. A 10^{-4} M Am(VI) in 2 M Na_2CO_3 solution is reduced completely to Am(V) in ca. 15 min. A 10^{-2} M Am(VI) in 2 M Na_2CO_3 solution is reduced to 100% Am(V) in approximately 1-2 days. Coleman *et al.*[47] observed that Am(VI) was stable in dilute Na_2CO_3 solution, but the stability of Am(VI) decreased with increasing carbonate ion concentration and increasing temperature. Pentavalent Am (AmO_2^{+}) in Na_2CO_3 solution has a featureless spectrum in the range 360-1300 nm[44] and exhibits only a general rise in absorbance into the UV wavelength region. Am(V) in Na_2CO_3 solution has a very faint (almost colorless) yellow color.

Addition of NaOH solution to Am(VI) in Na_2CO_3 solution causes immediate reduction of orange-brown Am(VI) to the almost colorless Am(V).[45] Oxidation of this Na_2CO_3-NaOH solution produced orange-brown Am(VI) or yellow-brown Am(VI) depending on the OH^- ion concentration. Up to ca. 0.3 M NaOH, Am(VI) in Na_2CO_3 solution is orange-brown and gives identical spectra to the literature spectra of Am(VI) in Na_2CO_3 solution.[44,47] Above approximately 0.3 M NaOH, Am(VI) is yellow-brown in color. The spectrum of this Am(VI) solution differs from that of Am(VI) at lower hydroxide ion concentration.

Hexavalent Am in Na_2CO_3 solution has an intense charge-transfer band with a peak maximum at about 369 nm (ε = 2812 $\underline{M}^{-1}$ cm^{-1}).[44] Above about 0.3 $\underline{M}$ OH^- ion concentration no absorbance peak at 369 nm was detected for Am(VI) in Na_2CO_3-NaOH solution. Only a general rise in absorbance is seen (see Figure 32). The molar absorptivities of Am(VI) in Na_2CO_3-NaOH solution are similar in magnitude to those of Am(VI) in just Na_2CO_3 solution. With increasing hydroxide ion concentration, Am(VI) becomes more unstable to reduction by water. Thus in the spectrum of Am(VI) in Na_2CO_3-NaOH solution, some Am(V) must be present. The spectrum of 100% Am(VI) in Na_2CO_3-NaOH solution could be obtained spectroelectrochemically using a Pt screen optically transparent electrode. Unfortunately the quality of such a spectrum would be degraded by bubbles from oxygen evolution due to the high applied potential needed for Am(VI) production.[17] Cohen has reported the Am(VI) spectrum in CsOH solution.[93]

Americium(V) in Na_2CO_3 solution up to pH 12 is faintly yellow colored. At pH 13 and above, Am(V) is light pink in color [somewhat reminescent of Am(III)]. The absorption spectrum of Am(V) in Na_2CO_3-NaOH solution is noticeably different from the corresponding spectrum in Na_2CO_3 solution. The former spectrum exhibits numerous absorption peaks. Above 0.1 $\underline{M}$ OH^- ion concentration, no further major changes in the Am(V) spectrum were observed in Na_2CO_3 solution. This differs somewhat from the results obtained for Np(V) (see page 53) and Pu(V) (see page 79) in Na_2CO_3 solutions where more gradual changes in the An(V) absorption spectra were seen with increasing OH^- ion concentration. The molar absorptivity of the 750 nm Am(V) peak in 1.9

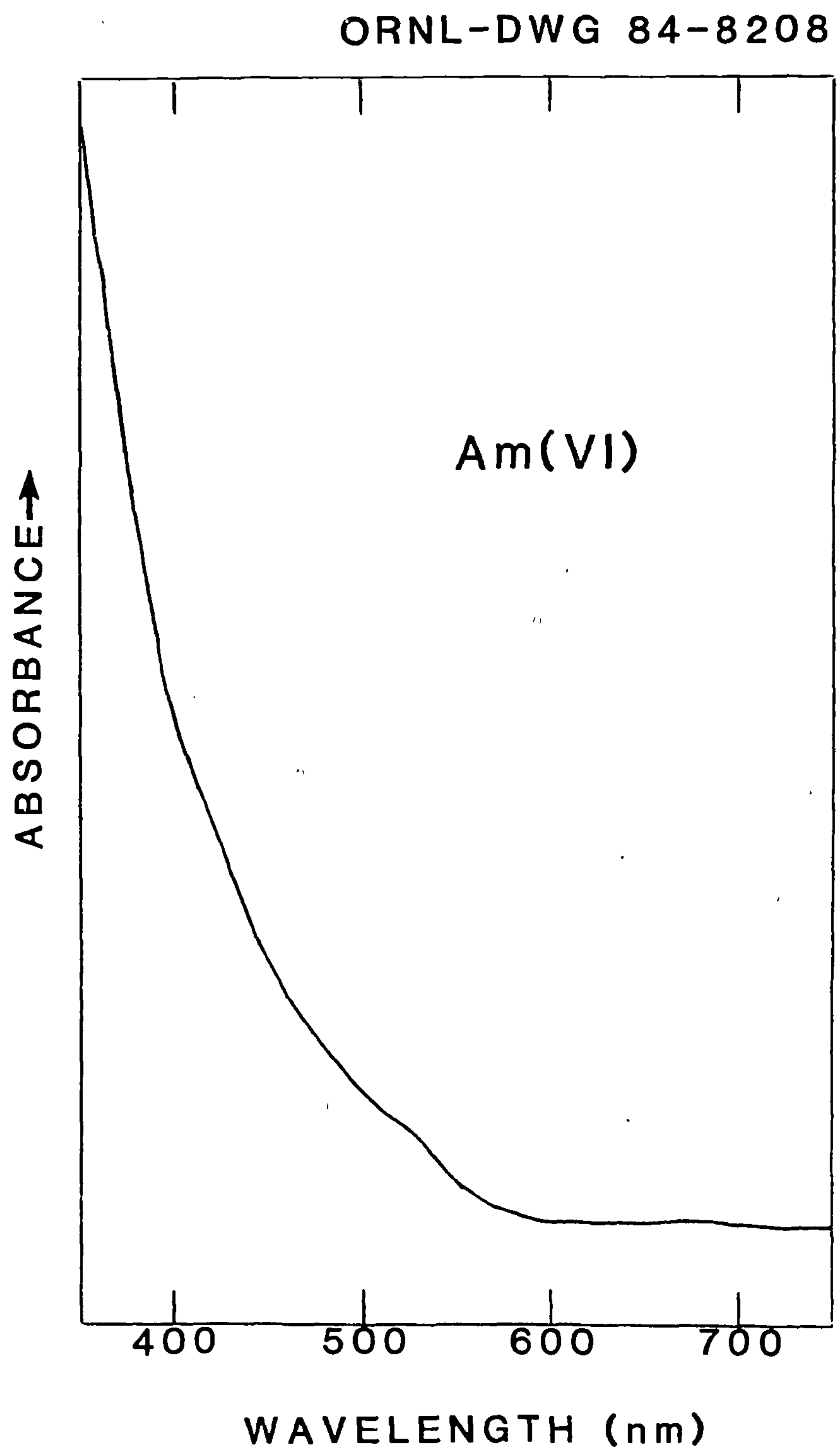

Figure 32. Absorption spectrum of Am(VI) in 1.6 M Na_2CO_3, 1.0 M NaOH solution.

M Na_2CO_3, 0.38 M NaOH solution is ca. 10-15 M^{-1} cm^{-1} (see Figure 33). Thus, at 0.1 M hydroxide ion concentration or greater in 2 M Na_2CO_3 solution, Am(V) exists primarily, if not completely, as a hydroxo (and/or carbonato-hydroxo) complex(es).

D. Californium[94]

The absorption spectrum of light green ^{249}Cf(III) in 2 M Na_2CO_3 solution is shown in Figure 34. This spectrum is similar to that of Cf(III) in 1 M $DClO_4$.[95] The absorption bands of Cf(III) in Na_2CO_3 solution are somewhat red-shifted in comparison to the associated Cf(III) absorption bands in $DClO_4$ solution. The differences between the spectra of Cf(III) in carbonate and acid media are greater than the differences seen for the corresponding carbonate and acid solution spectra of Am(III)[45,96] and Cm(III).[94,97] This indicates that Cf(III) is more strongly complexed by carbonate ions than is Am(III) or Cm(III). The absorption spectrum of Cf(III) in K_2CO_3 solution was practically identical to that obtained in Na_2CO_3 solution.

The estimated standard potential of the Cf(IV)/Cf(III) couple in noncomplexing solution is +3.2 V/NHE.[5] The 1.7 V negative shift in $E^{\circ\prime}$ for the Am(IV)/Am(III) and Ce(IV)/Ce(III) couples in carbonate solution[4,45] indicated that it might be possible to oxidize Cf(III) in aqueous carbonate solution. The estimated standard potentials of the Tb(IV)/Tb(III) and Pr(IV)/Pr(III) couples in noncomplexing solutions are +3.1 V/NHE and +3.2 V/NHE, respectively.[5] Hobart *et al.*[4] oxidized Tb(III) and Pr(III) to their tetravalent states in carbonate solution.

ORNL-DWG 84-8206

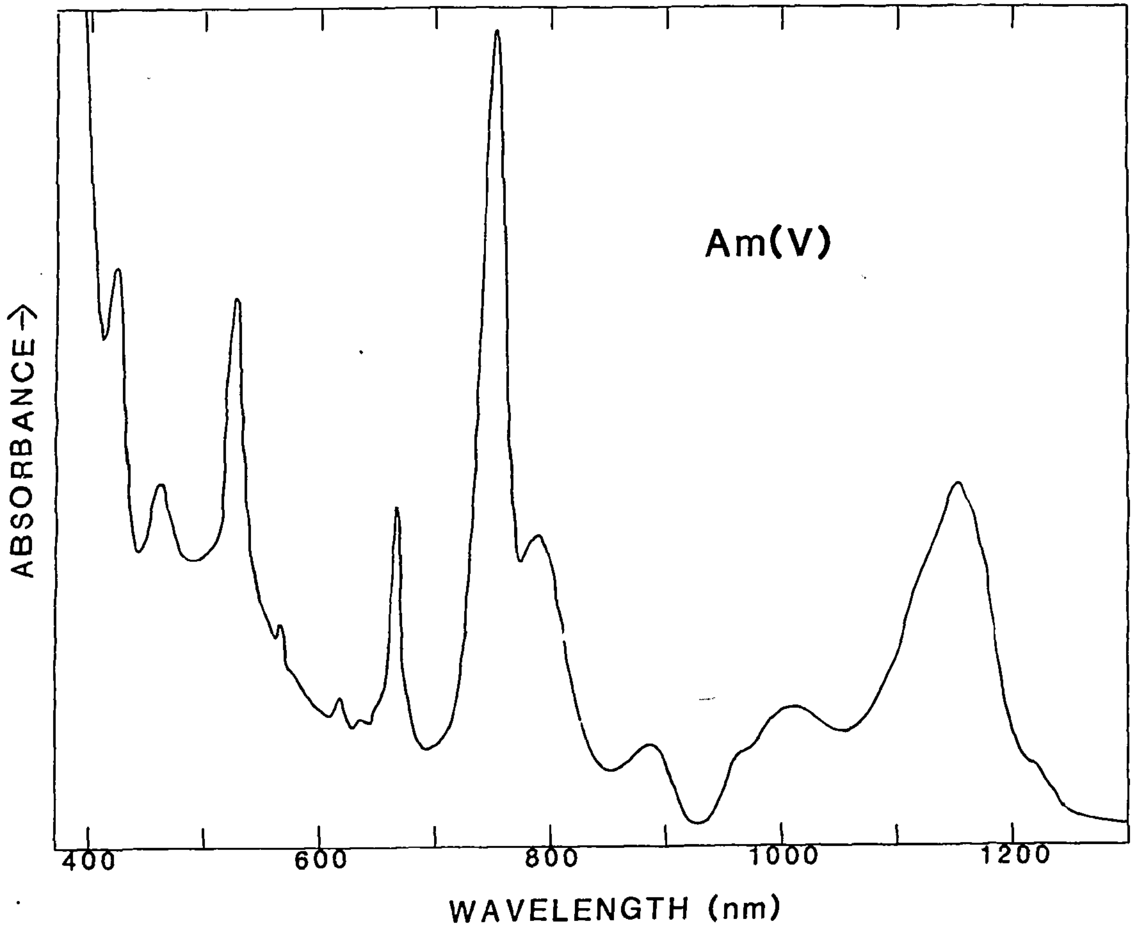

Figure 33. Absorption spectrum of Am(V) in 1.9 $\underline{M}$ Na_2CO_3, 0.38 $\underline{M}$ NaOH solution.

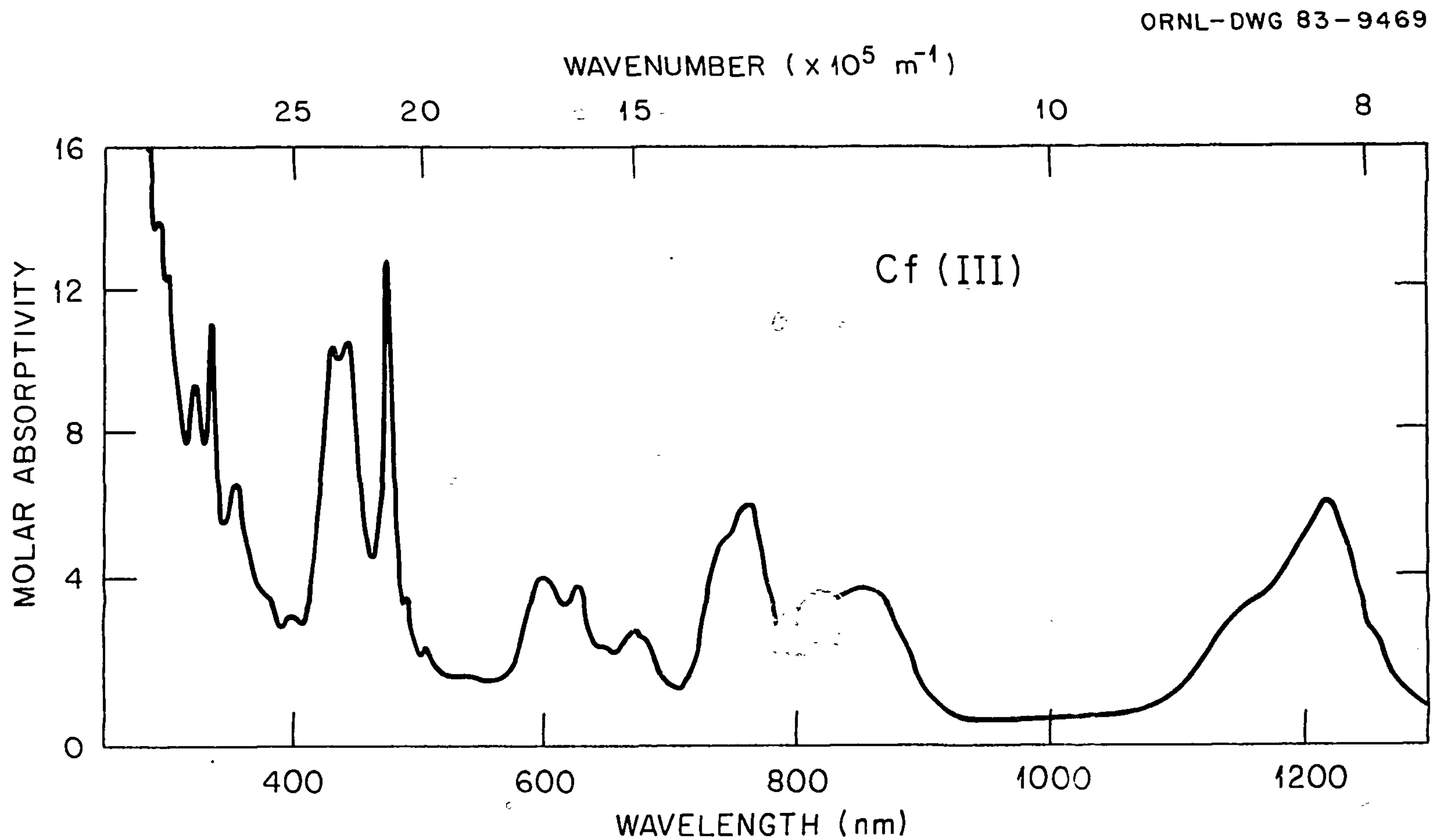

Figure 34. Absorption spectrum of Cf(III) in 2 M Na_2CO_3 solution, pH 12.

This was further indication that Cf(IV) might be stabilized in aqueous carbonate solution.

Spectroelectrochemical and bulk electrolysis experiments up to applied potentials of +1.1 V at Pt electrodes produced no evidence of Cf(III) oxidation in carbonate and bicarbonate solutions. Chemical oxidation using ozone and Ag(I)-peroxydisulfate also failed. Since Tb(III) and Pr(III) were oxidized in carbonate solution in the presence of hydroxide ions,[4] the effect of hydroxide ion concentration on Cf(III) oxidation in carbonate solution was studied. Up to OH^- ion concentrations where $Cf(OH)_3$ would precipitate from carbonate solution, Cf(III) was not oxidized using chemical oxidants or electrochemistry. Cyclic voltammograms of Cf(III) in carbonate solution at RVC and Pt electrodes at various pH values between 9 and 14 showed no anodic waves indicating Cf(III) oxidation. Thus carbonate and hydroxide ions do not provide sufficient negative shift in $E^{\circ\prime}$ of the Cf(IV)/Cf(III) couple to stabilize Cf(IV) in solution. Similar attempts to oxidize Cm(III) in carbonate-hydroxide and carbonate-bicarbonate solutions[94] were also unsuccessful.

E. Terbium[98]

Studies of terbium in aqueous carbonate-hydroxide solution were performed to understand better the nature of the Tb(IV) species in this medium and the failure to oxidize Cm(III) and Cf(III) in carbonate-hydroxide solution.[94]

1. Preparation and Stability of Tb(IV) Solutions

In order to oxidize Tb(III) in aqueous carbonate solution, attention must be paid to the concentrations of carbonate ion, hydroxide ion, and Tb(III). Two methods were used to oxidize Tb(III): chemical oxidation with ozone, and electrochemical oxidation at a Pt screen.

Using Pt wire and RVC strand as working electrodes, cyclic voltammograms of Tb(III) in K_2CO_3 solutions having hydroxide ion concentrations from 0.1 to 1 M exhibited no anodic waves indicating oxidation of Tb(III). Terbium(III) in 5 M K_2CO_3 solution was then electrolyzed at a Pt screen. When the potential applied to the screen was increased above +0.96 V, a brown coloration at the electrode surface could be seen. At +1.06 V the solution was a definite chocolate-brown color. When the potential was removed, however, the color faded in a matter of seconds. When aliquots of concentrated KOH solution were added to the electrolysis solution while greater than +1 V was applied to the Pt screen, the chocolate-brown color changed to a yellow color. This yellow color remained after removal of the applied potential. With increasing electrolysis time, the solution became a darker red-brown color. The absorption spectrum of this solution revealed an intense, broad, charge transfer band with a peak maximum at about 360-365 nm and a UV "cut-off" near 250 nm. The spectrum matched that of Tb(IV) in carbonate-hydroxide solution reported previously.[4] Attempts were made to obtain the absorption spectrum of the transient chocolate-brown solution (in 5 M K_2CO_3) using a Pt-optically transparent electrode (OTE). Unfortunately, interference from O_2 gas evolution at the high positive potentials needed to generate Tb(IV) prevented our obtaining a suitable spectrum.

of the chocolate-brown species. The noisy spectrum obtained did, however, reveal absorbance in the same wavelength region as that of the stable red-brown Tb(IV) solutions, but the quality of the spectrum was too poor to warrant any detailed comparison. The change in the color of the solution with the addition of hydroxide ions may be an indication of the formation of different Tb species in solution. The chocolate-brown-colored solution could not be produced in K_2CO_3 solutions less concentrated than ca. 4 M.

After the electrolysis of Tb(III) in carbonate-hydroxide solution, a brown (tea-colored) film was observed on the Pt screen. This film was insoluble in water but was soluble in acid. No such film was formed on the Pt screen if hydroxide ions were not added to the solution prior to electrolysis. This result is additional evidence suggesting that the chocolate-brown and red-brown solution colors are due to different Tb complexes. Films were produced electrolytically on both Pt screens and wire electrodes. Using an Ar ion laser (excitation at 514.5 nm), no Raman signal was obtained when the laser light was reflected from the electrode surface.

The brown film which formed on the Pt electrodes resulted in a slow rate of oxidation of Tb(III). Even with electrolysis times greater than 8 hours, Tb(III) solutions were only partially oxidized. The rate of oxidation of water (based on the observed anodic current) was not substantially reduced by the presence of the brown film. With the very long electrolysis times, the hydroxide ion concentration was lowered sufficiently such that Tb(IV) was no longer stable, and the characteristic red-brown color faded. If hydroxide ions were added before electrolysis, the amount of film formation was too great to allow complete oxidation in reasonable times. A more effective oxidation method found in this work was to apply greater than +1 V to the Tb(III) in carbonate solution until the solution was uniformly colored chocolate-brown. Then with the potential still applied, aliquots of KOH solution were injected into the terbium solution at some distance away from the Pt screen (to keep film formation to a minimum).

Oxidation of Tb(III) solutions with ozone was faster than electrolytic oxidation and also more convenient (especially for large volumes of solution). An additional advantage is that water is oxidized by ozone in carbonate-hydroxide solution at a much slower rate than it is oxidized at a Pt electrode at +1 V.

As stated earlier, hydroxide ions must be added to stabilize Tb(IV) in carbonate solution. In 1-3 $\underline{M}$ K_2CO_3 solution, ca. 0.1 $\underline{M}$ KOH is needed to oxidize Tb(III) with ozone. To oxidize Tb(III) in 4 $\underline{M}$ K_2CO_3 solution requires a slightly higher OH^- ion concentration. In 5 $\underline{M}$ K_2CO_3 solution approximately 0.2 $\underline{M}$ hydroxide ion is required to oxidize Tb(III) with ozone. As the hydroxide ion concentration increases, the stability of Tb(IV) (with respect to reduction by water) increases. On the other hand, with increasing OH^- ion concentration, Tb(IV) tends to precipitate as a flocculent red-brown solid. Increasing the carbonate ion concentration tends to increase the solubility of Tb(IV), but it slows down the rate of oxidation of Tb(III) with ozone and by bulk electrolysis.

As seen in Table IX, increasing the KOH concentration tends to promote the precipitation of Tb(IV), whereas higher carbonate ion concentrations help solubilize Tb(IV). In 5 M K_2CO_3 solutions, with KOH concentration $\geq$ 0.6 M, the Tb(IV) precipitate is orange-brown in color and centrifuges (settles) much slower than the previously described red-brown solid. After vacuum drying, the orange-brown solid has the same appearance as the dried red-brown solid. The color difference may be due to different particle sizes rather than to different compounds. If the Tb(IV) solid is left in contact with the solution for a sufficiently long period of time (over two weeks), the orange-brown color of the solid slowly fades to white. Thus these solids are not stable in the presence of K_2CO_3-KOH solution.

Terbium(III) solutions at sufficiently elevated temperature are not oxidized by ozone. When heated, Tb(IV) solutions are quickly reduced by water, or they form red-brown precipitates. Cooling a Tb(III) solution to ice bath temperature does not have a dramatic effect on the rate of oxidation of Tb(III) with ozone. Thus, proper conditions must be carefully controlled to oxidize Tb(III) completely, to stabilize Tb(IV), and to promote or avoid the precipitation of Tb(IV) from carbonate-hydroxide solution.

The concentration of Tb(III) in carbonate-hydroxide solution is also critical in oxidizing Tb(III). For example, in 5 M K_2CO_3 solution, a 4.8×10^{-2} M Tb(III) solution cannot be oxidized electrochemically at a Pt screen. However, increasing the Tb(III) concentration to 6.0×10^{-2} M allows for its oxidation to Tb(IV). At

TABLE IX

EFFECTS OF [K_2CO_3] AND [KOH] ON Tb(III) OXIDATION (WITH OZONE)

[K_2CO_3]	[KOH]	Stability of Tb(IV)
1 M	0.15 M	Tb(IV) precipitation; no Tb(IV) solution.
2 M	0.15 M	Tb(IV) solution stable for a few hours; reduced by water to Tb(III).
2 M	0.3 M	Tb(IV) precipitates from solution in ca. 1 hour.
5 M	0.5 M	Stable for weeks to precipitation or reduction by water.
5 M	0.6 M	Solution slowly precipitates over a period of days to weeks.

1.0 x 10^{-3} M Tb(III) in 1-4 M K_2CO_3 solution, Tb(III) can be oxidized with ozone. In 5 M K_2CO_3 solution, 1 x 10^{-3} M Tb(III) is not sufficient for oxidation to tetravalent terbium. As the carbonate ion concentration increases, the minimum concentration of Tb(III) needed to oxidize Tb(III) electrochemically or with ozone increases. One explanation of this effect is that at higher carbonate ion concentrations, the Tb(III) ions are complexed so strongly by carbonate ions that their oxidation to a Tb(IV)-carbonato-hydroxo complex is not possible. Since hydroxide ions are needed to produce Tb(IV), the tetravalent Tb complex is probably not a simple carbonato species. Thus, a change in the oxidation state of Tb is accompanied by a significant change in its complexation (irreversible couple). By increasing the Tb concentration sufficiently, the $[CO_3^{2-}]/[Tb(III)]$ ratio is lowered to the point where Tb(III) can be oxidized to Tb(IV) having a different complexation environment. Another possible explanation is given later.

2. Reduction of Tb(IV) Solutions

Cyclic voltammograms of Tb(IV) solutions at Pt wire and Hg drop electrodes to −2 V revealed no cathodic wave that could be attributed to the reduction of Tb(IV). Bulk electrolysis at Hg pools to potentials sufficiently negative to reduce water failed to reduce Tb(IV). This indicates that Tb(IV) can be very stable and that the Tb(IV)/Tb(III) couple is irreversible. The existence of a thermodynamically stable clustered (possibly polymeric) Tb(IV) species would explain this inability to reduce Tb(IV). Ions such as Cl^-, Br^-, and I^- did not react with the Tb(IV) species. However, tetravalent Tb was reduced with lead or amalgamated zinc in a matter of minutes. Terbium(IV) solutions that were otherwise stable for weeks to months were reduced in a day in the presence of a Pt screen (no potential applied). The Pt surface apparently acts as a catalyst for the reduction of Tb(IV) by water.

Cerium(III) in K_2CO_3 solution reduces Tb(IV) to Tb(III) and produces Ce(IV). In the presence of hydroxide ions, Ce(IV) is reduced to Ce(III) in K_2CO_3 solution. Thus, only small concentrations of Ce(III) in comparison to those of Tb(IV) are needed ([Ce(III)]/[Tb(IV)] < ca. 0.1) to reduce completely Tb(IV) in K_2CO_3 solution.

A search was made for a suitable analytical titrant to reduce Tb(IV) quantitatively in carbonate-hydroxide solution. No such titrant was found. However, ferrocyanide [$Fe(CN)_6^{4-}$] ions did react with Tb(IV) in a manner to give some useful information. At conditions where Tb(IV) was stable to precipitation and to reduction by water, Tb(IV) did not react with $Fe(CN)_6^{4-}$ ion at room temperature. At conditions where Tb(IV) was unstable to reduction by water, the reaction of Tb(IV) with $Fe(CN)_6^{4-}$ ion was rapid. A compromise between these two extremes was made, i.e., Tb(IV) in 3 $\underline{M}$ K_2CO_3, 0.25 $\underline{M}$ KOH solution. Titrations monitored spectrophotometrically at 500 nm [for Tb(IV)] indicated that it takes less than one-half mole of $Fe(CN)_6^{4-}$ ion to reduce a mole of Tb(IV). More quantitative results were not obtained for the following reasons. First, in 3 M K_2CO_3, 0.25 M KOH solution, Tb(IV) slowly precipitates. During the titration of Tb(IV) with $Fe(CN)_6^{4-}$ ion, the original Tb(IV) concentration was monitored spectrophotometrically at 360 nm (absorption peak maximum). Due to difficulty in stabilizing Tb(IV) with respect to precipitation and in oxidizing Tb(III) quantitatively in this solution, only a rough estimate, ca. 1000 M^{-1} cm^{-1} could be made of the molar absorptivity of Tb(IV). Hobart *et al.*[45] estimated the molar absorptivity of the 360 nm absorption peak to be greater than 1000 M^{-1} cm^{-1}. Second, as the Tb(IV) titration neared the equivalence point, the rate of the reaction of Tb(IV) with $Fe(CN)_6^{4-}$ ion decreased. Adding excess $Fe(CN)_6^{4-}$ solution did not reduce all of the Tb(IV). Even at the beginning of the titration, when the reaction rate was the fastest, unreacted $Fe(CN)_6^{4-}$ ion in the presence of Tb(IV) could be seen spectrophotometrically. The Tb(IV) titrations with $Fe(CN)_6^{4-}$ ion did indicate, however, that the redox reaction was not a simple one-electron exchange between Fe(II) and Tb(IV). This can be accounted for by the presence of a clustered Tb(IV) species and/or by a mixed valence Tb(IV,III) species. As a Tb(IV) cluster is reduced, the cluster may be destroyed and the remaining Tb(IV) ions quickly reduced by water. The oxidized Tb complex may involve both Tb(IV) and Tb(III) ions (mixed-valence species). Analysis of the red-brown Tb(IV) solid (as discussed later) lends support to the existence of a clustered Tb(IV) or Tb(IV,III) species.

The Raman spectrum of Tb(IV), in 5 M K_2CO_3, 0.48 M KOH solution is shown in Figure 35. At ca. 580 cm^{-1}, a weak, broad peak is seen. Raman spectra of carbonate-hydroxide solutions void of terbium and Tb(III) in carbonate-hydroxide solution revealed no such Raman peak. A Raman signal from the glass container partially obscures the low frequency side of this peak. The peak signal is very weak and could only be seen after multiple scans were made. For comparison, notice the ν_1 CO_3^{2-} ion peak ($[CO_3^{2-}]$ = 5 M) at 1065 cm^{-1} shown in Figure 35. No other Raman peaks which could be attributed to Tb(IV) were seen in the region from 100 to 3800 cm^{-1}.

3. Co-precipitation of Tb(IV)

The precipitation of trivalent lanthanides and Ce(IV) with the $[Co(NH_3)_6]^{3+}$ cation in carbonate solution has been studied.[99,100] Precipitation occurs within minutes to hours. Upon mixing a solution of $Co(NH_3)_6^{3+}$ in 5 M K_2CO_3, 0.6 M KOH with a solution of Tb(IV) in 5 M K_2CO_3, 0.6 M KOH, a flocculent dark green precipitate formed over a period of days to a week. This green solid, as well as the red-brown Tb(IV) solid, was soluble in 1 M HCl. Hexamminecolbalt(III) is not stable in K_2CO_3-KOH solution. In the absence of Tb(IV), the colbalt precipitated as a dark green-brown or red-brown solid that was only slightly soluble in 1 M HNO_3 and insoluble in 1 M HCl. This solid is presumably an oxide of cobalt (CoO, Co_2O_3, or Co_3O_4). The absorption spectrum of the green Co-Tb solid dissolved in acid was different from that of $Co(NH_3)_6^{3+}$ ion in acid solution. Thus, the $Co(NH_3)_6^{3+}$ unit

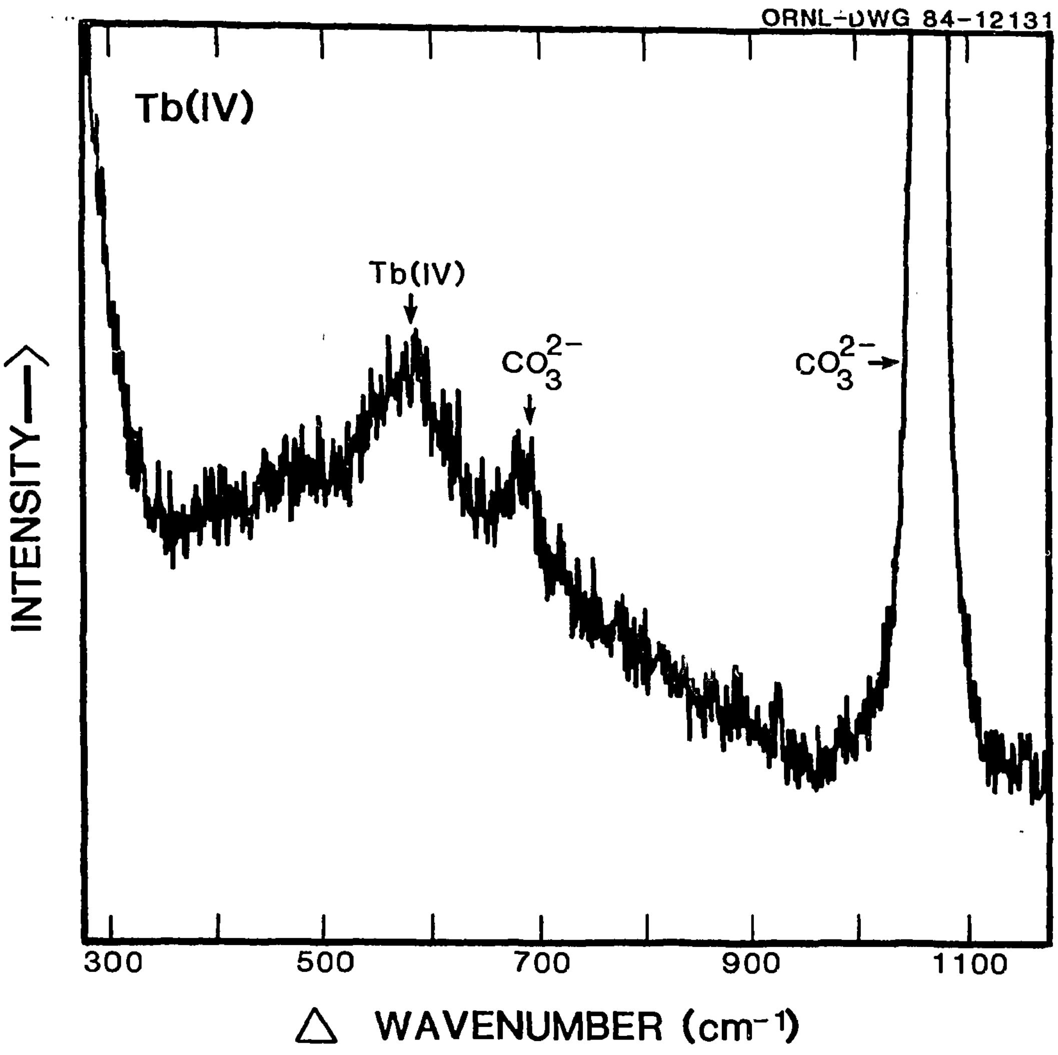

Figure 35. Raman spectrum of Tb(IV) in 5 M K_2CO_3, 0.48 M KOH solution. Original concentration of Tb(III) before oxidation by ozonolysis was 0.095 M. Laser excitation was achieved at 514.4 nm (Ar ion laser).

probably did not remain intact during its co-precipitation with Tb(IV).

The infrared spectra of mineral oil mulls of the green Co-Tb and the red-brown Tb(IV) solids are shown in Figure 36. Infrared spectra of water dispersed in mineral oil and mulls of $TbCl_3$ hexahydrate were recorded also to aid in the identification of water in the unknown solids. The small band at 1700-1600 cm^{-1} indicates the presence of water. The intensity of the broad band centered at ca. 3300 cm^{-1} in comparison to that of the 1700-1600 cm^{-1} band is too large to be attributed to water. The band at 3300 cm^{-1} is therefore attributed to hydroxide ions. Bubbling argon through separate acid solutions of both solids into limewater indicated the presence of carbonate ions. The IR peak at 850-800 cm^{-1} in both solids is attributed to the ν_2 vibration of CO_3^{2-} ion. The peak at 1050 cm^{-1} in the spectrum of the green Co-Tb compound (Figure 36A) could be assigned to the ν_1 vibration of CO_3^{2-} ion. No such peak is seen in the IR spectrum of the red-brown Tb(IV) solid (Figure 36B). The 1050 cm^{-1} peak might also result from a vibration of NH_3 in the Co-Tb compound. Both solids exhibit a broad absorption band centered at about 1500-1400 cm^{-1}, and these bands could be due to vibrations of Tb-O bonds or to ν_3 vibrations of CO_3^{2-} ions. The broadness of this band is another indication of a clustered Tb(IV) species where the energy of various vibrations is transferred throughout the cluster. Due to the dark color of these solids, attempts to obtain their Raman spectra using Ar ion (514.5 nm) and Kr ion (647.1 nm) laser excitations were unsuccessful.

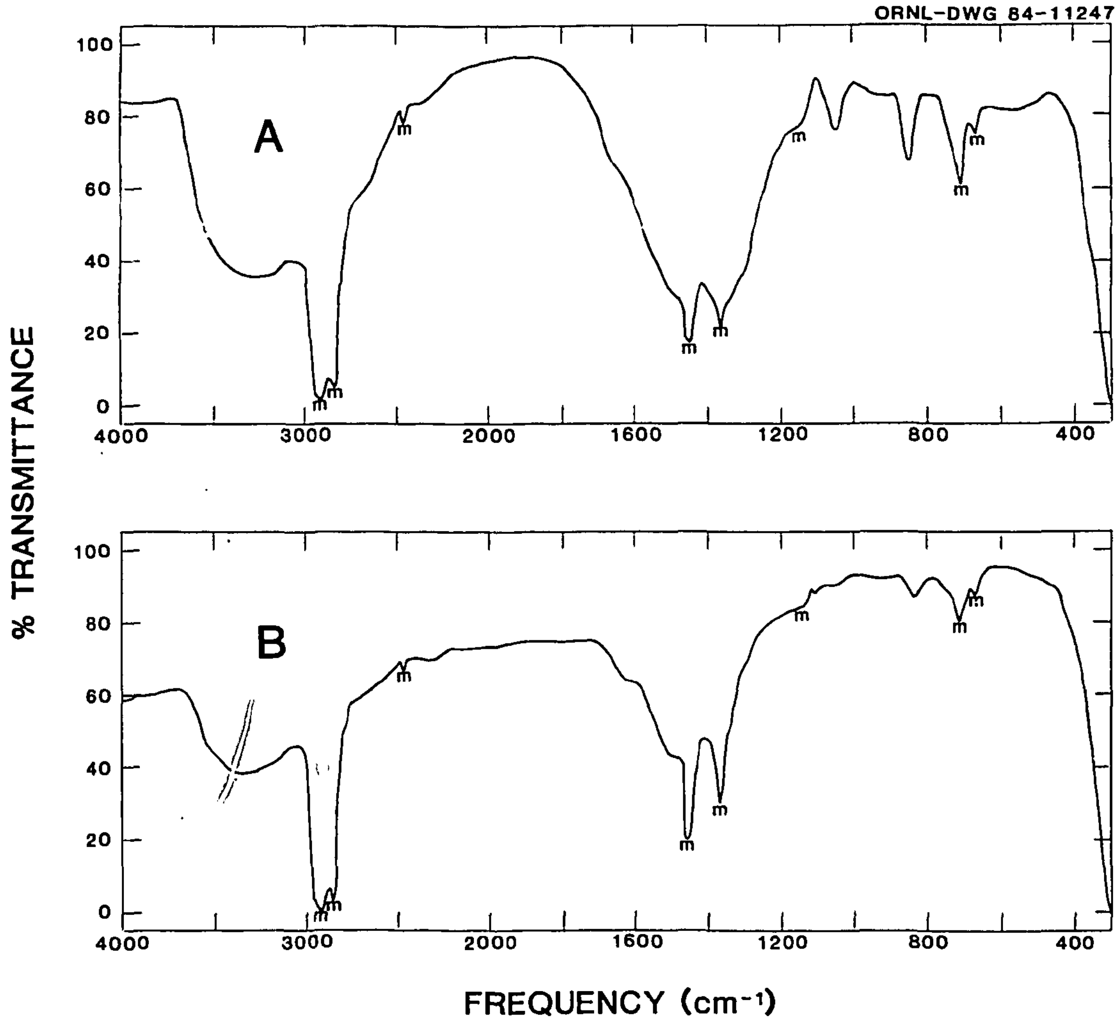

Figure 36. IR transmission spectra (using AgCl windows) of mineral oil mulls of (A) Co-Tb solid and (B) Tb(IV) solid. The absorbances due to mineral oil are marked "m." Note the frequency scale change at 2000 cm^{-1}.

4. Analysis of the Tb(IV) Solids

Since the $Co(NH_3)_6^{3+}$ ion did not appear to remain intact in the green Co-Tb solids, no further studies were performed on these compounds. The red-brown Tb(IV) solid was analyzed for Tb and CO_3^{2-} ion in order to aid in understanding the composition of the Tb(IV) species in solution.

The percentage by weight of Tb in the red-brown solid was not constant and varied from ca. 61-68%. Samples dried in vacuum over a week showed the same variation in percent Tb as samples dried for only a day. Thus, the weight variation is probably not due to adsorbed water. The variation may, however, be due to different degrees of hydration or complexation by water. Water molecules trapped within the solid may not be removed by vacuum treatment at room temperature. The variation in the percentage of Tb may also be due to the formation of a variety of related compounds or nonstoichiometric Tb compounds. The ratio of moles of Tb to moles of CO_3^{2-} ion was determined from a number of samples precipitated from solutions of varying carbonate and hydroxide ion concentrations and was equal to 1.5 ± 0.1. The ratio being greater than one is another indication of a clustered (or polymeric) form of Tb(IV). Flame tests of solutions of KCl and K_2CO_3 gave brilliant purple-colored flames. No purple color indicating the presence of potassium ion was seen in flame tests of acid solutions of the red-brown Tb(IV) solids. Possible stoichiometric structures for the Tb(IV) solids (that do not involve oxide ions) are listed below:

(1) $Tb(IV)_{3m}(CO_3^{2-})_{2m}(OH^-)_{8m} \cdot nH_2O$

(2) $Tb(IV)_{2m}Tb(III)_m(CO_3^{2-})_{2m}(OH^-)_{7m} \cdot nH_2O$

(3) $Tb(III)_{2m}Tb(IV)_{2m}(CO_3^{2-})_{2m}(OH^-)_{6m} \cdot nH_2O$.

If the Tb(IV) solution complex(es) has (have) a similar formula(s) to those listed above, this would explain the irreversible nature of the Tb(IV)/Tb(III) couple. The solids and the oxidized Tb complex(es) may contain a mixture of Tb(IV) and Tb(III) ions. The Tb(IV) complex(es) may be a stoichiometric or nonstoichiometric oxide(s) of Tb(IV) with an ionic shell of Tb(III), CO_3^{2-}, and OH^- ions. The Tb(IV) solutions may actually be suspensions of ultra-fine solid Tb(IV) particles. Terbium(IV) solutions that were stable to precipitation were ultra-centrifuged. No precipitates were collected. Based on the centrifugation time and the centrifugal force applied (but neglecting coulombic interactions between Tb(IV) and K^+ and CO_3^{2-} ions) the particle(s) size(s) is (are) probably less than 20 nm. If the Tb(IV) species is not actually dissolved in the K_2CO_3-KOH solution, mass transport of Tb(IV) to a metal cathode would be strongly hindered, making it difficult (if not impossible) to reduce Tb(IV) electrochemically.

Hobart[101] prepared a red-brown solid by oxidizing at a RVC electrode Tb(III) in a carbonate-hydroxide solution. X-ray data indicated that the solid was a somewhat noncrystalline mixed-valence compound. Thermogravimetric-mass spectroscopy (TGA-MS) indicated the presence of at least two carbonate molecules per terbium atom. This differs from the Tb/CO_3^{2-} ion ratio of 3/2 determined for the Tb(IV) solid produced in the present work. The reflectance spectrum of the present red-brown Tb(IV) solid was compared to that of the solid produced by Hobart.[101] The reflectance spectrum of the present Tb(IV) solid exhibited absorbance over a broad wavelength region from ca. 1300 nm down into the UV with a UV-VIS peak maximum at about 350-355 nm. Hobart's reflectance spectrum[101] is very similar but with a UV-VIS peak maximum at approximately 380 cm.

The existence of clustered or polymeric Tb(IV) or Tb(IV,III) species in K_2CO_3-KOH solution is also supported by earlier work of Propst.[102] He prepared solid Tb(IV) by electrolytic deposition on a conducting glass electrode from Tb(III) in K_2CO_3-KOH solution. A polymeric Tb(IV) deposit was produced with deposition times greater than 6 min.

As mentioned previously, decreasing the concentration of Tb(III) or increasing the concentration of CO_3^{2-} ion in K_2CO_3-KOH solution makes it more difficult to oxidize Tb(III). If a clustered form of Tb(IV) exists, the formation of such a species may require a sufficiently high concentration of Tb(III) to decrease the mean distance between Tb(III) complex ions in solution, thus promoting cluster formation. Increasing the K^+ and CO_3^{2-} ion concentrations might serve to disperse the Tb(III) complex ions making it more difficult to form the cluster.

CHAPTER IV

RESULTS AND DISCUSSION: DIMETHYL SULFONE STUDIES

A. Lanthanides[103]

Molten dimethyl sulfone ($DMSO_2$) has been used as a solvent for voltammetric studies of various inorganic species.[50,104-108] Polarography and direct potential measurements have been performed in $DMSO_2$. To the knowledge of this author, bulk electrolysis experiments have not been reported in $DMSO_2$. Preliminary electrolysis experiments with Fe(III), Fe(II), and Cu(II) were carried out in $DMSO_2$. The supporting electrolytes used were $LiClO_4$, TEAP, and TBAP. Solutions of Fe(III) ($Fe(NO_3)_3 \cdot 9H_2O$) in $DMSO_2$ were reduced to Fe(II) and then oxidized back to Fe(III) at a Pt screen electrode. Divalent Cu ($CuCl_2 \cdot 2H_2O$) in $DMSO_2$ was reduced to Cu(0) at Ni-PMF, Ni(Hg)-PMF, and Hg pool electrodes. Both Pt wire and AgCl-coated Ag wire in fritted glass or asbestos fiber junction tubes were found suitable as reference electrodes for such bulk electrolysis experiments. Based on these experiments, it was hoped that electrochemical reductions of Eu(III), Yb(III), and Sm(III) could be performed in $DMSO_2$.

1. Lanthanide(III)/Lanthanide(II) Couples

a. Spectroscopy. The absorption spectra of hydrated trichloride salts of Sm, Eu, and Yb in 1 M $HClO_4$ and in molten dimethyl sulfone solutions are shown in Figures 37-42, respectively. The aqueous solution absorption spectra of Sm(III), Eu(III), and Yb(III) are adapted from those of Carnall.[12] All $DMSO_2$ solution

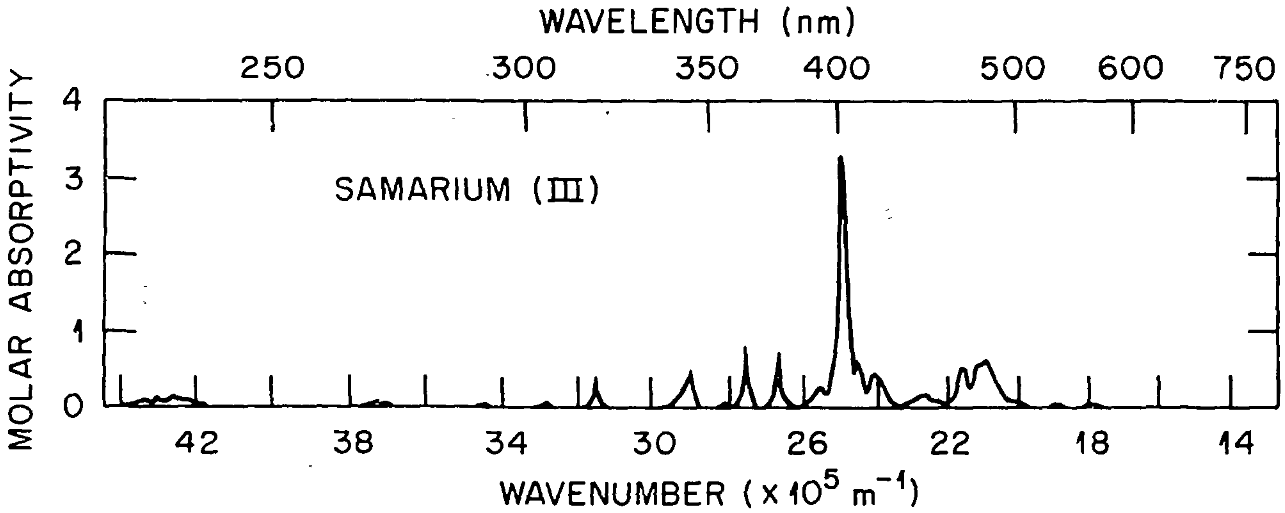

Figure 37. Absorption spectrum of $SmCl_3 \cdot 6H_2O$ in 1 M $HClO_4$ solution.

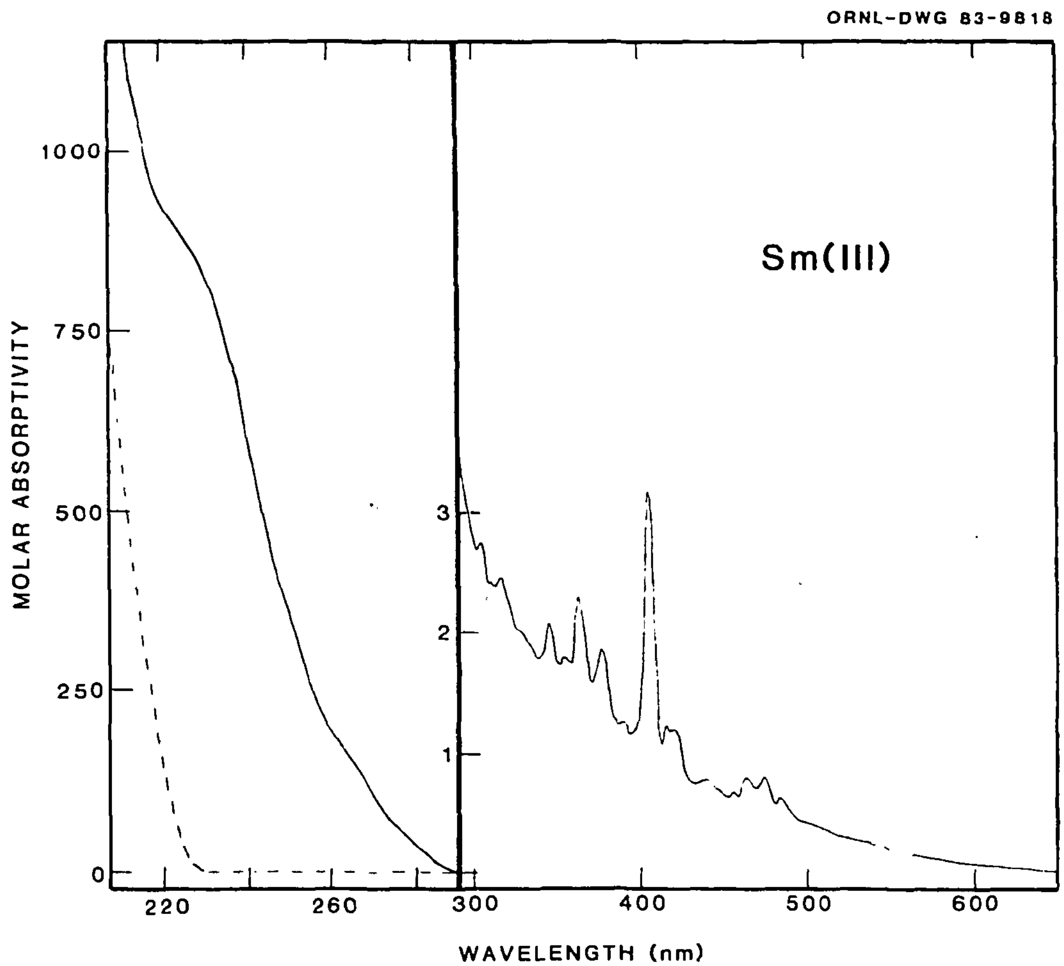

Figure 38. Absorption spectrum of $SmCl_3 \cdot 6H_2O$ in molten $DMSO_2$. The dashed line indicates absorption due to $DMSO_2$.

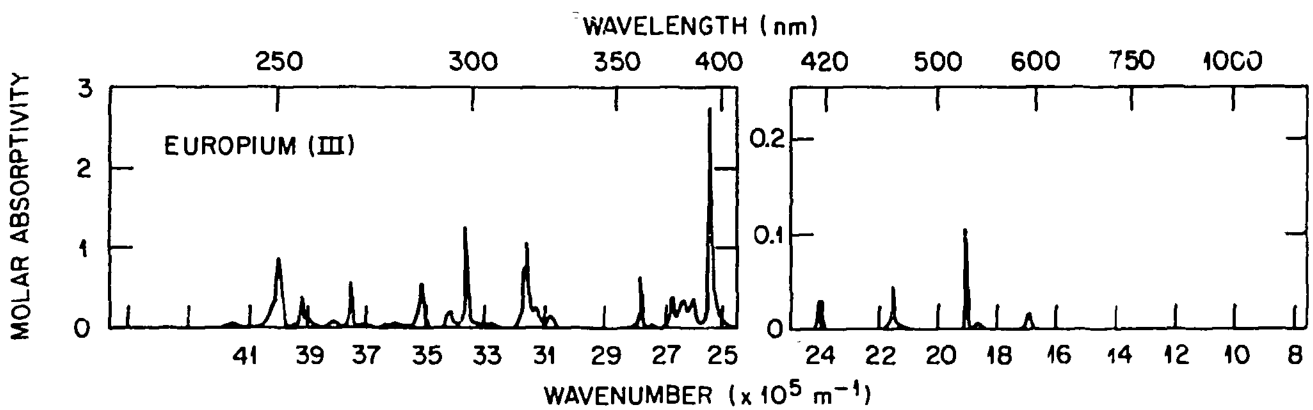

Figure 39. Absorption spectrum of $EuCl_3 \cdot 6H_2O$ in 1 $\underline{M}$ $HClO_4$ solution.

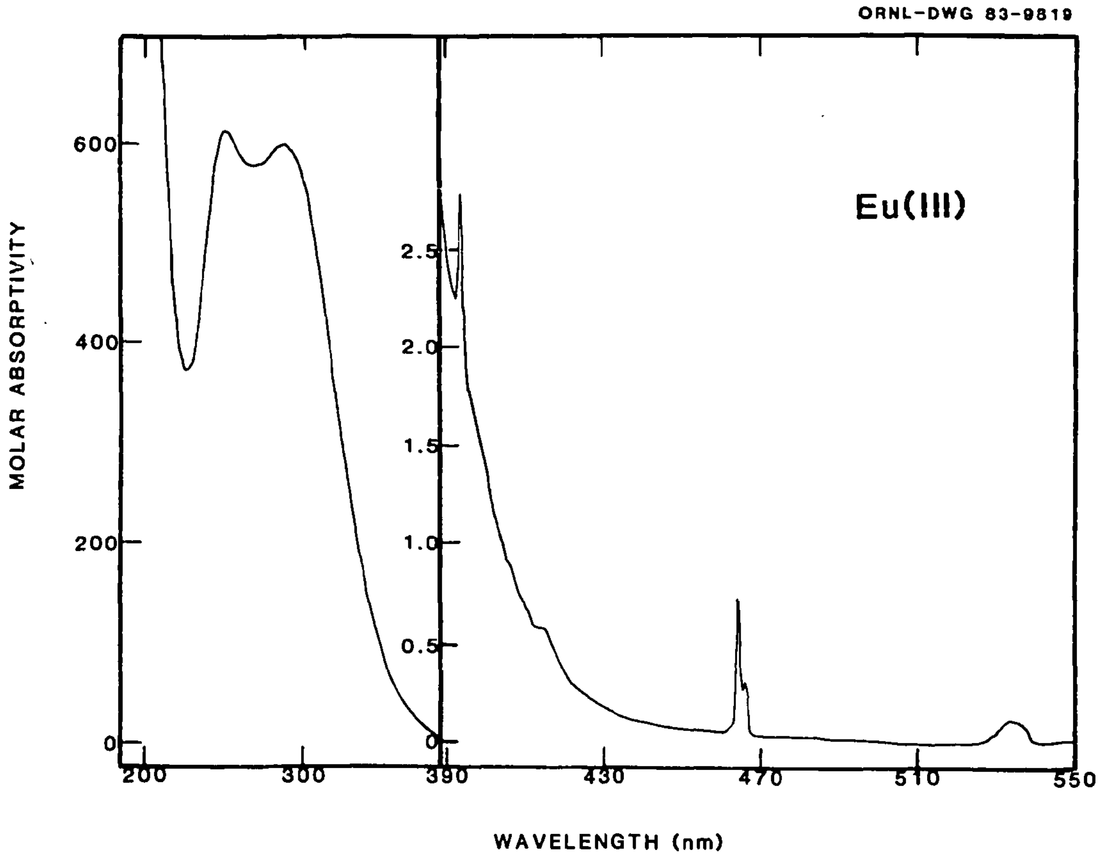

Figure 40. Absorption spectrum of $EuCl_3 \cdot 6H_2O$ in molten $DMSO_2$.

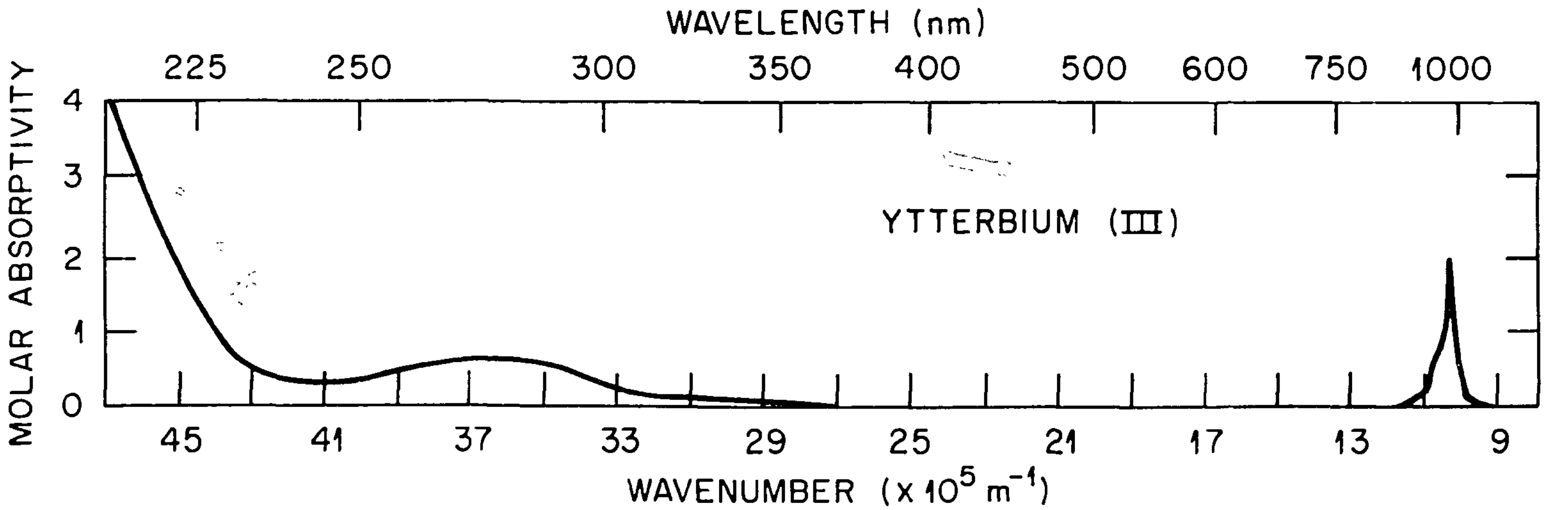

Figure 41. Absorption spectrum of $YbCl_3 \cdot 6H_2O$ in 1 M $HClO_4$ solution.

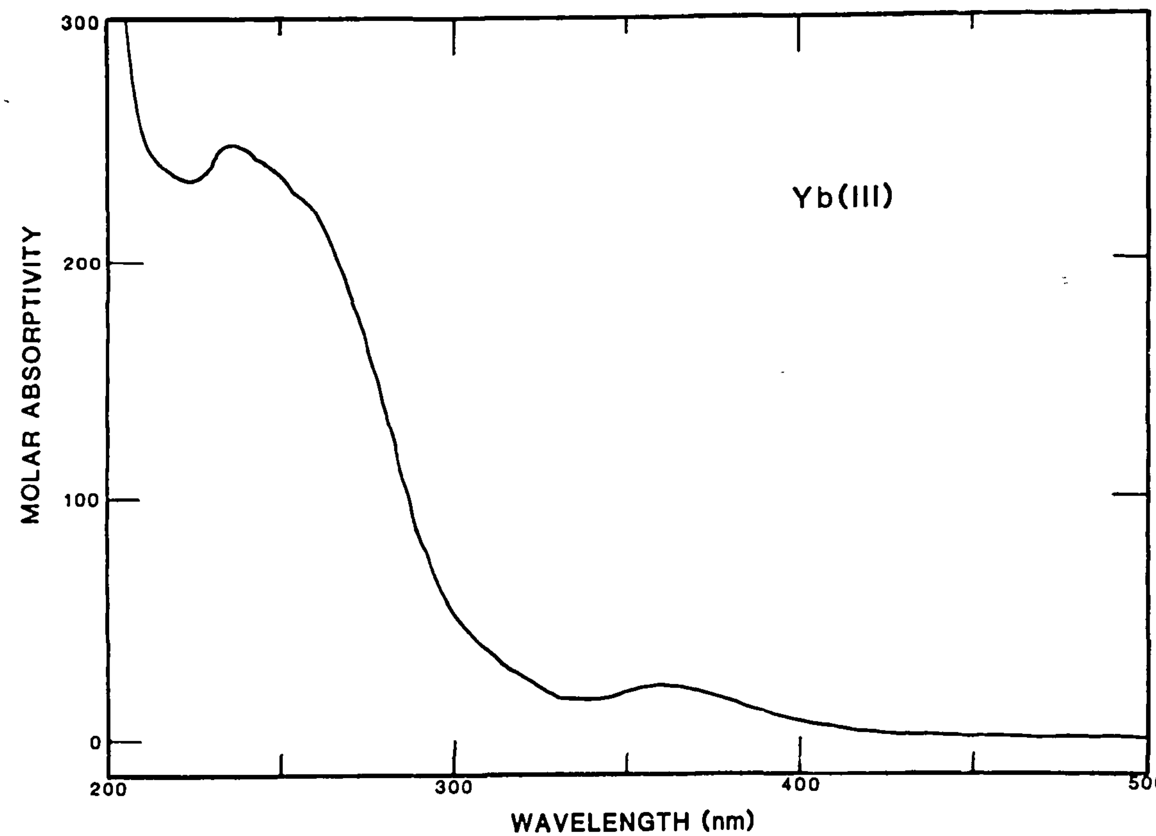

Figure 42. Absorption spectrum of $YbCl_3 \cdot 6H_2O$ in molten $DMSO_2$.

absorption spectra were recorded at 400 K (127°C). The f-f transitions in Eu(III) and Sm(III) in 1 M $HClO_4$ solutions occur at wavelengths similar to those exhibited by the same species in $DMSO_2$ solutions. They differ to some extent, however, in molar absorptivities. Greater similarities exist between the Sm(III) spectra in $DMSO_2$ solution and in 1 M $HClO_4$ solution than between the corresponding two spectra of Eu(III).

The striking differences between the aqueous and $DMSO_2$ spectra of Sm(III), Eu(III), and Yb(III) lie in the UV region. In aqueous solutions Eu(III) and Sm(III) show only weak f-f bands in the UV, and Yb(III) exhibits a weak, broad band absorbance in the UV. In $DMSO_2$ Eu(III) has two, intense, UV absorption bands centered at 250 and 288 nm (see Figure 40, page 126). Both Sm(III) and Yb(III) exhibit strong absorbances with a UV "cut-off" around 210 nm for Sm(III) (see Figure 38, page 124), and a UV absorbance peak at ca. 236 nm for Yb(III) (see Figure 42, page 128). The UV absorption spectrum of Sm(III)-in-$DMSO_2$ solution actually exhibits an absorption peak maximum at ca. 224 nm. This peak is partially obscured by the background absorption (see Figure 38, page 124) and is only observable at absorbances above 1.5. The bands seen in the spectra of Eu(III), Yb(III), and Sm(III) are ascribed to a charge-transfer mechanism. The absorption peak positions are shifted to lower energies (frequencies) in $DMSO_2$ compared to those seen in H_2O because $DMSO_2$ is a poorer coordinating ligand than H_2O, thus making chloride ion complexation more favorable in $DMSO_2$. Similar charge-transfer bands are seen for lanthanide(III) tribromides in anhydrous ethanol,[109] and octahedral lanthanide hexahydrates[110] and lanthanide hexahalides[5] in nitriles (e.g., acetonitrile).

The absorption spectra of Eu(II) in 1 M $HClO_4$ and in molten dimethyl sulfone solutions are shown in Figures 43 and 44, respectively. Europium(II) in aqueous solution has two f-d bands centered at 240 and 320 nm which do not appear in the spectrum of Eu(II) in $DMSO_2$. In water Eu(III) is colorless and Eu(II) is pale yellow, but in $DMSO_2$ the reverse is true (see the next section for the preparation of Eu(II) in $DMSO_2$ solution).

b. Electrochemistry. Cyclic voltammograms of Ln(III)/Ln(II) couples in $DMSO_2$ for Eu, Yb, and Sm are shown in Figure 45. The working electrode was a hanging mercury drop, and the reference electrode was a platinum wire in a fritted glass tube filled with the supporting electrolyte. The formal potential of a Ln(III)/Ln(II) couple can be estimated by taking the average of the cathodic and anodic current peak potentials. Thus the formal potentials of the Ln(III)/Ln(II) couples in $DMSO_2$ were determined to be -0.36 ± 0.05 V, -1.07 ± 0.01 V, and -1.61 ± 0.05 V versus the Pt reference electrode for Eu, Yb, and Sm, respectively. The larger errors in the Eu and Sm potentials result from the poorly defined anodic waves in these voltammograms. The poor nature of the anodic peak in the Sm(III)/Sm(II) voltammogram is probably due to the background cathodic current of the reduction of the water of hydration. The anodic and cathodic voltammetric peak positions were better identified by working at low current scale attenuations where only the anodic or cathodic waves (but not both simultaneously) could be kept on scale (at the recorder).

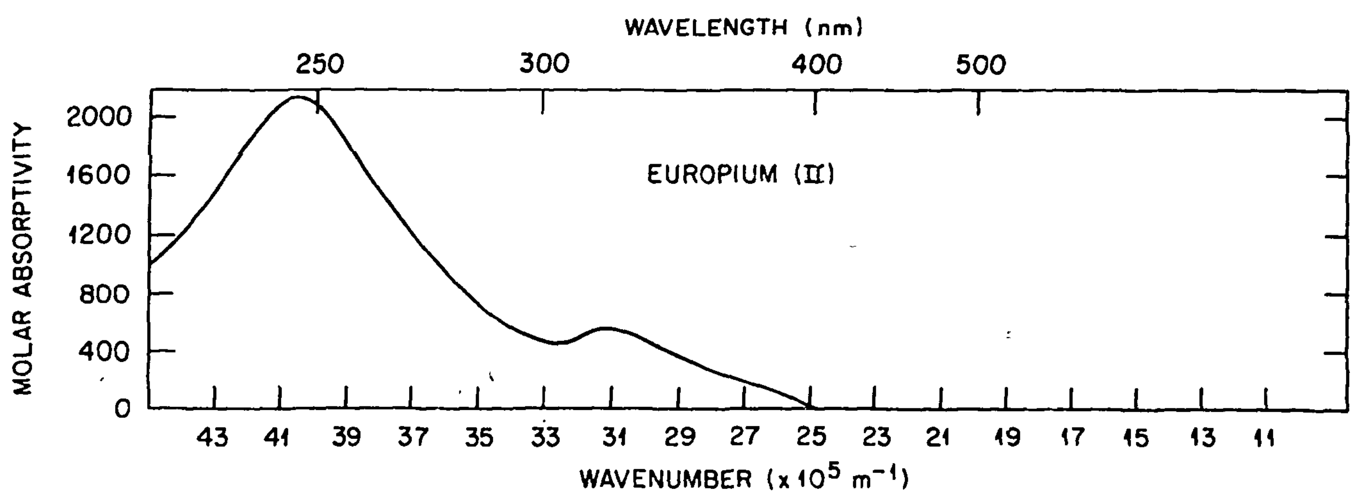

Figure 43. Absorption spectrum of Eu(II) in 1 M $HClO_4$ solution.

ORNL-DWG 83-9822

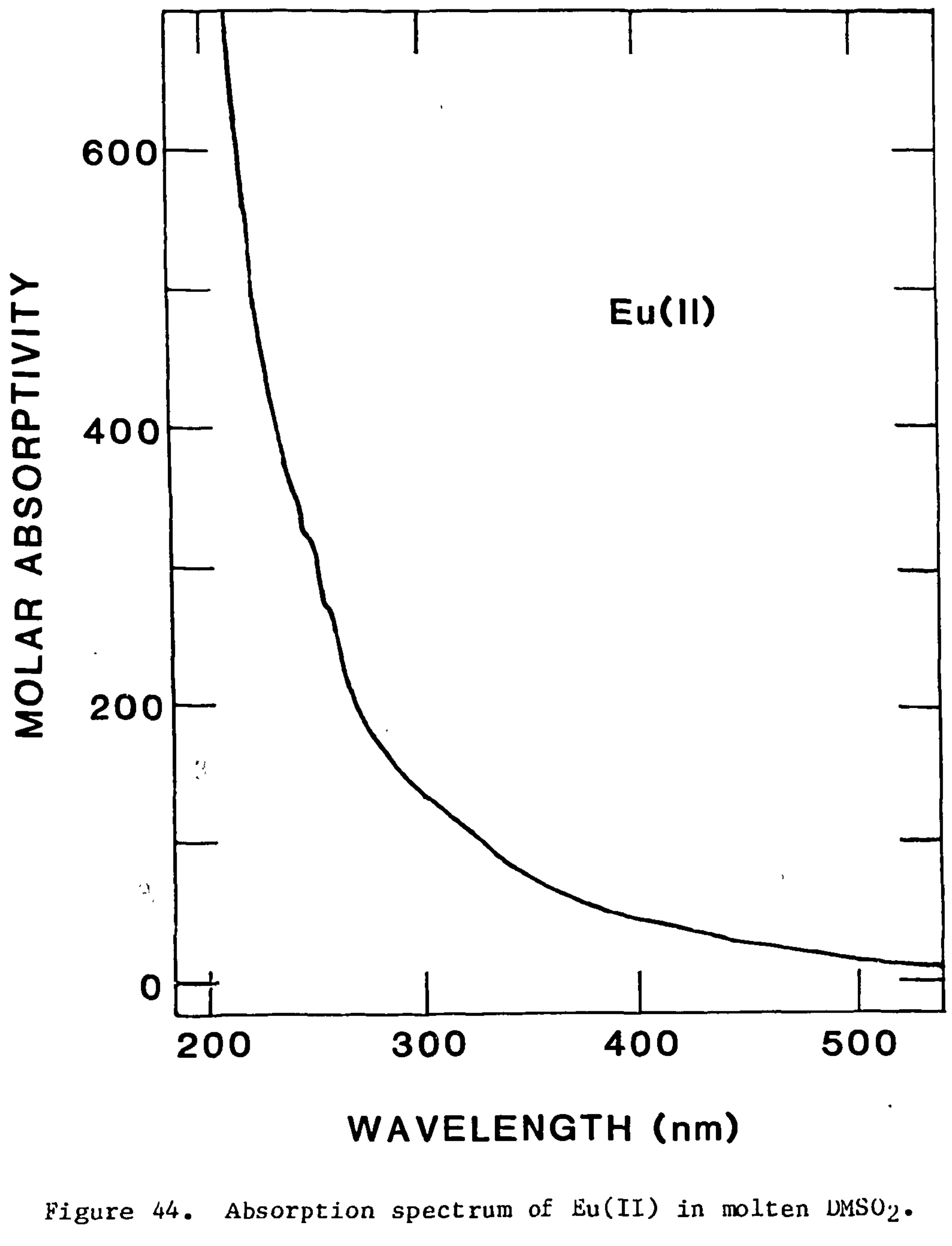

Figure 44. Absorption spectrum of Eu(II) in molten $DMSO_2$.

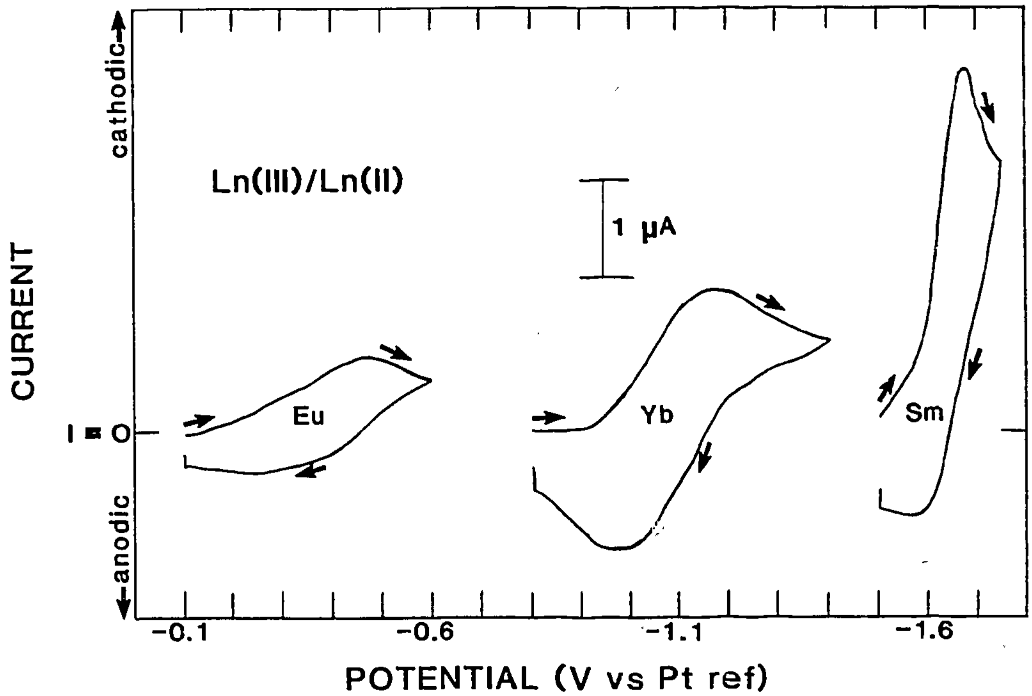

Figure 45. First scan cyclic voltammograms of $EuCl_3 \cdot 6H_2O$, $YbCl_3 \cdot 6H_2O$, and $SmCl_3 \cdot 6H_2O$ in molten $DMSO_2$. Scan rate = 50 mV/s; HMDE; [lanthanide(III)] = 2-5 x 10^{-3} M.

For bulk electrolysis, Yb(III) and Sm(III) were introduced into $DMSO_2$ as DMSO adducts of $YbCl_3$ and $SmCl_3$ for the following reason. When $SmCl_3 \cdot 6H_2O$ was used at potentials more negative than approximately -1.5 V vs. a Pt reference electrode, bubbles at the Ni(Hg)-PMF or Hg pool working electrode were seen (with sufficiently high concentrations of $SmCl_3 \cdot 6H_2O$) and were attributed to the reduction of the water of hydration to hydrogen gas. No bubbles were observed in a blank solution containing only the supporting electrolyte and the solvent. The $YbCl_3 \cdot n(DMSO)$ and $SmCl_3 \cdot n(DMSO)$ solutions did not yield any observable bubbles at the working electrodes when electrolyzed at potentials more negative than -1.5 V vs. a Pt reference electrode.

Bulk electrolysis of Eu(III) at -0.8 to -1 V vs. a Pt reference electrode in $DMSO_2$ using a Pt screen, Ni(Hg)-PMF, or a Hg pool as a working electrode produced Eu(II). The resulting solution could be reoxidized to Eu(III) at -0.1 V vs. a Pt reference electrode at a Pt screen working electrode (mercury and nickel electrodes were not used to avoid the oxidation of Hg and Ni). Divalent Eu in $DMSO_2$ solution could also be obtained by shaking a Eu(III)-in-$DMSO_2$ solution with amalgamated zinc.

Efforts to generate Yb(II) and Sm(II) by electrolytic reduction of bulk solutions of $YbCl_3 \cdot 6H_2O$ or $YbCl_3 \cdot n(DMSO)$ and $SmCl_3 \cdot n(DMSO)$ in molten $DMSO_2$ have not been successful. At potentials more negative than -1.1 V vs. a Pt reference electrode, bulk reduction in molten $DMSO_2$ of any species whose reduction potential is more negative than approximately -1 V has not been possible. However, when a potential of −1.4 V vs. a Pt reference electrode is applied to a solution of Eu(III), Eu(II) if formed. Thus the problem is not a simple surface passivation effect on the working electrode by the solvent. Various reference electrodes and working electrodes were tested in an effort to overcome this problem but without success. Electrochemical arrangements (including the supporting electrolyte) identical with those used in $DMSO_2$ were tested in DMSO at room temperature and found to work satisfactorily. However, at ca. 90°C and above, reduction of Yb(III) to yellow Yb(II) in DMSO was not possible. With prolonged electrolysis time, Yb(III) would precipitate from solution. This white precipitate was assumed to be the product of the reaction of Yb(III) with residual H_2O molecules and/or hydroxide ions at elevated temperatures. No such white precipitates were seen in reductions of $YbCl_3 \cdot n(DMSO)$ and $SmCl_3 \cdot n(DMSO)$ in molten dimethyl sulfone. The low electrolysis currents obtained in comparison with the background electrolysis current of $DMSO_2$ solutions void in Yb(III) or Sm(III) indicated that little water as well as Yb(III) and Sm(III) were being reduced. Thus, the reduction of Yb(III) and Sm(III) at large electrodes does not correspond (agree) with the reduction of these species at a HMDE (microelectrode) (see Figure 45, page 133).

In order to eliminate water contamination, bulk reduction of anhydrous $YbCl_3$ and $SmCl_3$ in 0.5 M TBAP in $DMSO_2$ solutions at a Ni(Hg)-PMF working electrode in an inert atmosphere (He) gloved box was attempted. Unfortunately, $YbCl_3$ and $SmCl_3$ were insoluble in $DMSO_2$. Using chloride containing supporting electrolytes such as tetramethylammonium chloride or lithium chloride did not increase the solubility of the lanthanide trichlorides. Formation of adducts with water or DMSO seems to aid in the solubility of $YbCl_3$ and $SmCl_3$ in $DMSO_2$. Bulk reduction of slurries of $YbCl_3$ and $SmCl_3$ in $DMSO_2$ (in case these species had a slight solubility in $DMSO_2$) produced no observable Yb(II) and Sm(II). Anhydrous $Yb(ClO_4)_3$ and $Sm(ClO_4)_3$ (produced by heating solutions of Yb(III) and Sm(III) in 1 M $HClO_4$ to dryness) also were insoluble in $DMSO_2$.

Since the goal was to see if Yb(II) and Sm(II) [and possible actinides such as Cf(II)] could be stabilized in $DMSO_2$ solution, attempts were made to dissolve directly divalent compounds of Yb and Sm in $DMSO_2$. The dichlorides of ytterium and samarium were not soluble in $DMSO_2$. Unfortunately, due to difficulties with the preparation/vacuum system used,[111] the dibromides of Yb and Sm were not available for dissolution experiments (at the time this thesis was written).

2. Lanthanide(IV)/Lanthanide(III) Couples

Owing to the poor coordinating ability of $DMSO_2$, ligands which are weak complexing agents in water may be strong complexing agents in $DMSO_2$. For instance, Ce(IV) can be produced in $DMSO_2$ solution containing Ce(III) trichloride simply by bubbling air through the solution. This indicates that there has been a substantial negative shift in the Ce(IV)/Ce(III) reduction potential in $DMSO_2$ solution compared with that in aqueous solution. The spectra of Ce(III) and Ce(IV) in molten $DMSO_2$ are shown in Figures 46 and 47, respectively.

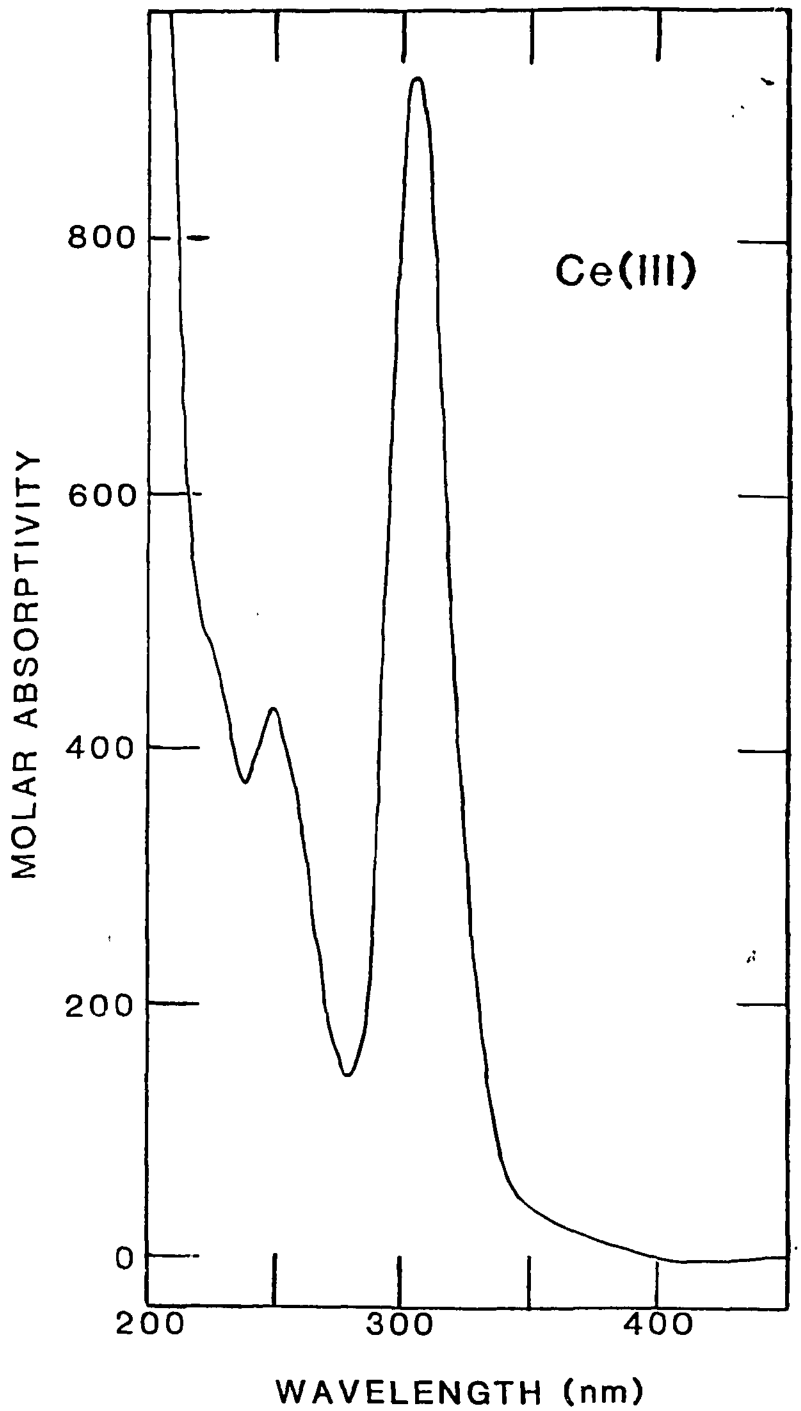

Figure 46. Absorption spectrum of $CeCl_3 \cdot 6H_2O$ in molten $DMSO_2$.

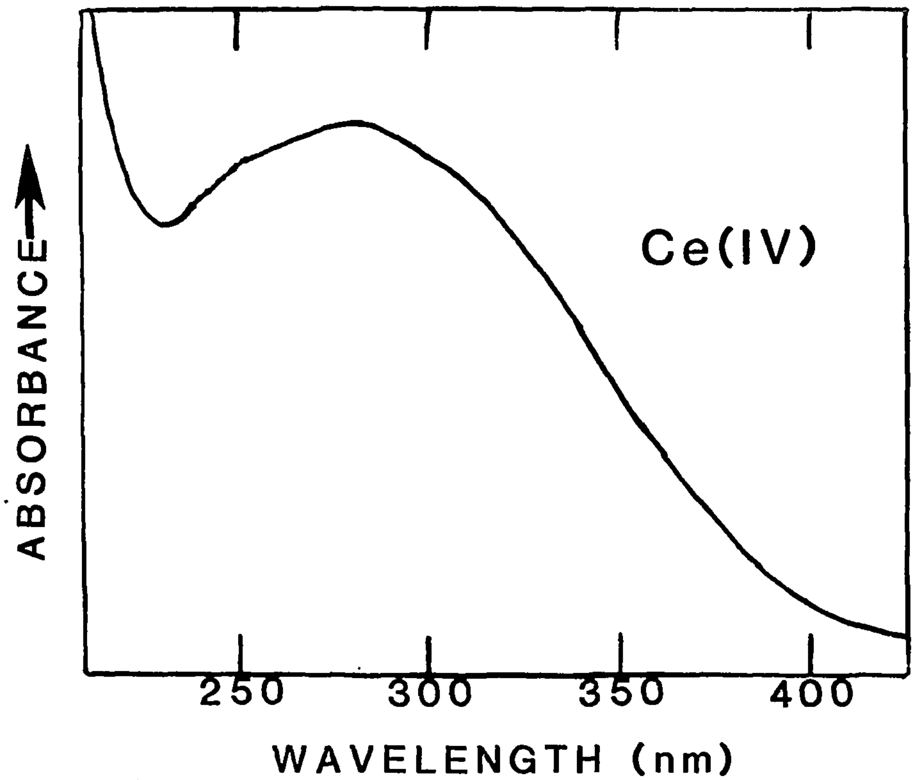

Figure 47. Absorption spectrum of Ce(IV) in molten $DMSO_2$.

The yellow tetravalent cerium solution was obtained by bubbling ozone through a solution of 10^{-3} M Ce(III) for 1 hr. Comparison of the spectral shifts of the f-d bands of Ce(III) and the charge-transfer band of Ce(IV) in $DMSO_2$ with those in aqueous acid solutions confirms the shift of the Ce(IV)/Ce(III) formal potential. The absence of similar shifts in the Ln(III)/Ln(II) formal potentials of Eu, Yb, and Sm indicates that the chloride complexation constant ratio of lanthanide(IV) to lanthanide(III) is much larger than the chloride complexation constant ratio of lanthanide(III) to lanthanide(II). It was impossible to oxidize electrochemically Ce(III) chloride to Ce(IV) in $DMSO_2$ due to oxidation of the chloride ion at potentials greater than about +0.2 V vs. a Ag/10^{-2} M $AgClO_4$, 2 M $LiClO_4$ reference electrode. Cerium(IV) was produced electrochemically from a solution containing 1 M $(NH_4)_2CO_3$, 1 M NH_4NO_3 and $Ce(NO_3)_3 \cdot 6H_2O$. Because of the strong complexation of Ce(IV) by carbonate ions, the Ce(IV)/Ce(III) couple was shifted sufficiently in the negative direction for Ce(IV) to be produced in bulk at +0.55 V vs. a Ag/10^{-2} M $AgClO_4$, 2 M $LiClO_4$ reference electrode. The NH_4NO_3 was present to prevent the precipitation of cerium carbonate when $Ce(NO_3)_3 \cdot 6H_2O$ was introduced into the $DMSO_2$ solution. If $(NH_4)_2CO_3$ was added to a solution of Ce(IV) in $DMSO_2$ (that did not contain NH_4NO_3), a dark purple precipitate was formed. The electrochemistry of this solution was complicated by the simultaneous presence of two oxidation states of nitrogen in solution. The electrochemical oxidation of Ce(III) and the electrochemical reduction of Ce(IV) in $DMSO_2$ were slow and were not well characterized.

A similar shift in the Ce(IV)/Ce(III) formal potential in aqueous carbonate solution was reported by Hobart *et al.*[4] In addition, Tb(IV) and Pr(IV) were generated in aqueous carbonate-hydroxide solutions.[4] Attempts in the present work to generate Tb(IV) and Pr(IV) in $DMSO_2$ electrochemically and by chemical oxidation with ozone were not successful. Failure to produce Tb(IV) and Pr(IV) was probably due to Cl^- ion oxidation for Cl^--$DMSO_2$ solutions and NH_4NO_3 oxidation for $(NH_4)_2CO_3$-NH_4NO_3-$DMSO_2$ solutions. In addition, cluster formation of Tb(IV) in aqueous carbonate-hydroxide solution, as mentioned earlier (see page 114), may not be possible in $DMSO_2$.

B. Actinides

1. Americium(III) Absorption Spectrum

In noncomplexing aqueous solution Am(III) exhibits a narrow, intense peak at 503 nm (ε = ca. 400 $\underline{M}^{-1}$ cm^{-1} in 0.1 $\underline{M}$ $HClO_4$).[96] No charge-transfer bands are seen in the aqueous UV spectrum of Am(III). An f-f band at 225 nm is seen for aqueous Am(III).[96] The absorption spectrum of $AmCl_3 \cdot nH_2O$ in $DMSO_2$ solution is presented in Figure 48. No charge-transfer band similar to those seen for Eu(III), Yb(III), and Sm(III) is observed. This is attributed to the relatively more negative reduction potential of the Am(III)/Am(II) couple as compared to the (III)/(II) reduction potentials of Eu, Yb, and Sm. The (III)/(II) standard reduction potentials of Eu, Yb, Sm, and Am are -0.35, -1.15, -1.55, and -2.3 V/NHE, respectively.[5] The

ORNL-DWG 84-15153

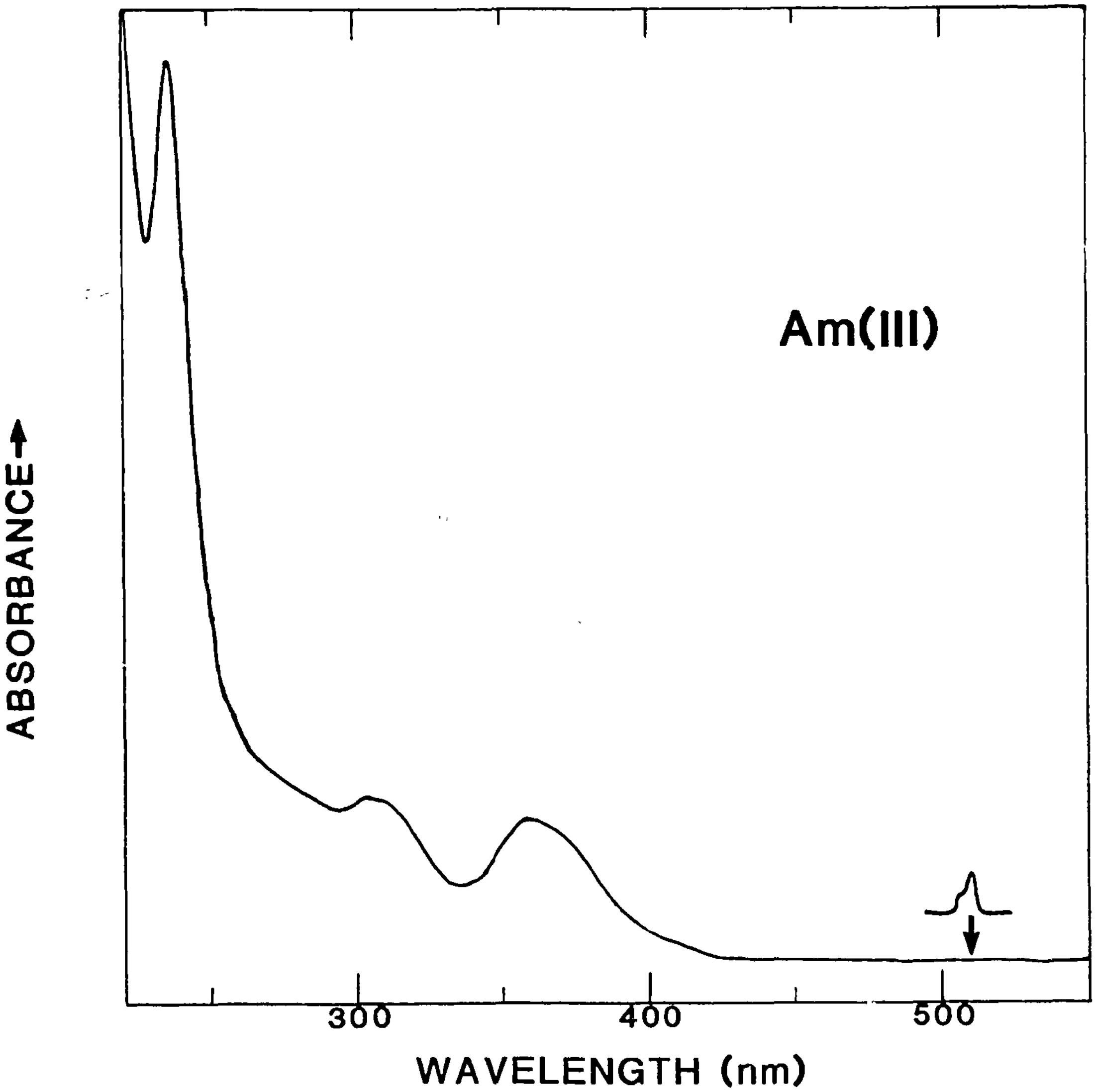

Figure 48. Absorption spectrum of $AmCl_3 \cdot nH_2O$ in molten $DMSO_2$. The 510 nm absorption peak was recorded using a more concentrated Am(III) solution.

ligand-to-metal charge transfer band for Am(III) occurs at too high an energy to be observed in the $DMSO_2$ spectra.

Absorption bands of $AmCl_3 \cdot nH_2O$ in $DMSO_2$ solution are seen at 305 and 358 nm. When aqueous HCl alone is injected into molten $DMSO_2$ and the water is driven off (with the aid of Ar gas bubbling), absorption peaks are seen at 272 and 357 nm. These peaks are attributed to Cl_2 and/or Cl_3^- ion. Bry et al.[50] reported that Cl_3^- ion is stable in $DMSO_2$. When the $DMSO_2$ solutions (that were injected with HCl) are bubbled with ozone gas instead of argon, the intensities of the 272 and 357 nm absorption peaks increase. Charge-transfer spectra involving Cl_2 and donor solvents have been studied.[112] Absorption spectra of $DMSO_2$ solutions of LiCl do not contain such peaks (at 272 and 357 nm), indicating that Cl^- ions from a dissolved salt remain unoxidized. In the Yb(III)-in-$DMSO_2$ solution spectrum (see Figure 42, page 128), a similar peak at ca. 359 nm is seen. Thus, the common shape and peak position of the 358 nm peak for Am(III) and the 359 nm peak for Yb(III) are proposed to arise from similar charge-transfer mechanisms involving complexed Cl^- ions (having Cl_2-like behavior) and the solvent molecules. The spectrum of $EuCl_3 \cdot 6H_2O$ in $DMSO_2$ solution (see Figure 40, page 126), may contain such a band around 360 nm, but the more intense absorbance arising from a ligand-to-metal charge-transfer band precludes detection of such a peak. The absorption spectrum of $SmCl_3 \cdot 6H_2O$ in $DMSO_2$ solution (see Figure 38, page 124) definitely does not contain a charge transfer peak around 360 nm. Thus, the metal ion plays some undetermined role in this charge-transfer band.

The 503 nm peak in the absorption spectrum of aqueous Am(III) is attributed to hydrated Am(III).[113] This band occurs at 510 nm in $DMSO_2$ and has a molar absorptivity value that appears to be much smaller (by at least a factor of ten) than the value in H_2O. This difference in molar absorptivities is attributed to the difference in water concentration between aqueous solution and $AmCl_3 \cdot nH_2O$-in-$DMSO_2$ solution. Marcus and Shiloh also noted a reduced intensity of this Am(III) absorption peak ($\varepsilon = 70\ \underline{M}^{-1}\ cm^{-1}$) in 13.7 $\underline{M}$ LiCl.[114] The 225 nm f-f peak of aqueous trivalent Am(III) occurs at 236 nm in $DMSO_2$ with a molar absorptivity enhanced in magnitude compared to that in H_2O. Shiloh and Marcus reported[114] an increase in this band's molar absorptivity in aqueous LiCl solution. The LiCl concentration needed to be in excess of 4 $\underline{M}$ before enhancement of this peak was seen.[114]

2. Actinide(VI) Absorption Spectra

A word of caution: the AnO_2^{2+}-in-$DMSO_2$ solutions discussed next are not anhydrous but contain some finite but undetermined amount of water (water of hydration plus that not driven off with time at 400 K). A cyclic voltammogram of Np(VI)/Np(V) in 0.1 $\underline{M}$ $LiClO_4$ in $DMSO_2$ is shown in Figure 49. The anodic background is an indication of water oxidation and/or platinum oxide formation at the Pt working electrode. The formal potential of the Np(VI)/Np(V) couple in $DMSO_2$ as determined from the average of the cathodic and anodic current peak potentials is $+1.22 \pm 0.02$ V vs. a Pt wire reference electrode. The quasi-reversible nature of the Np(VI)/Np(V) couple in $DMSO_2$ and the

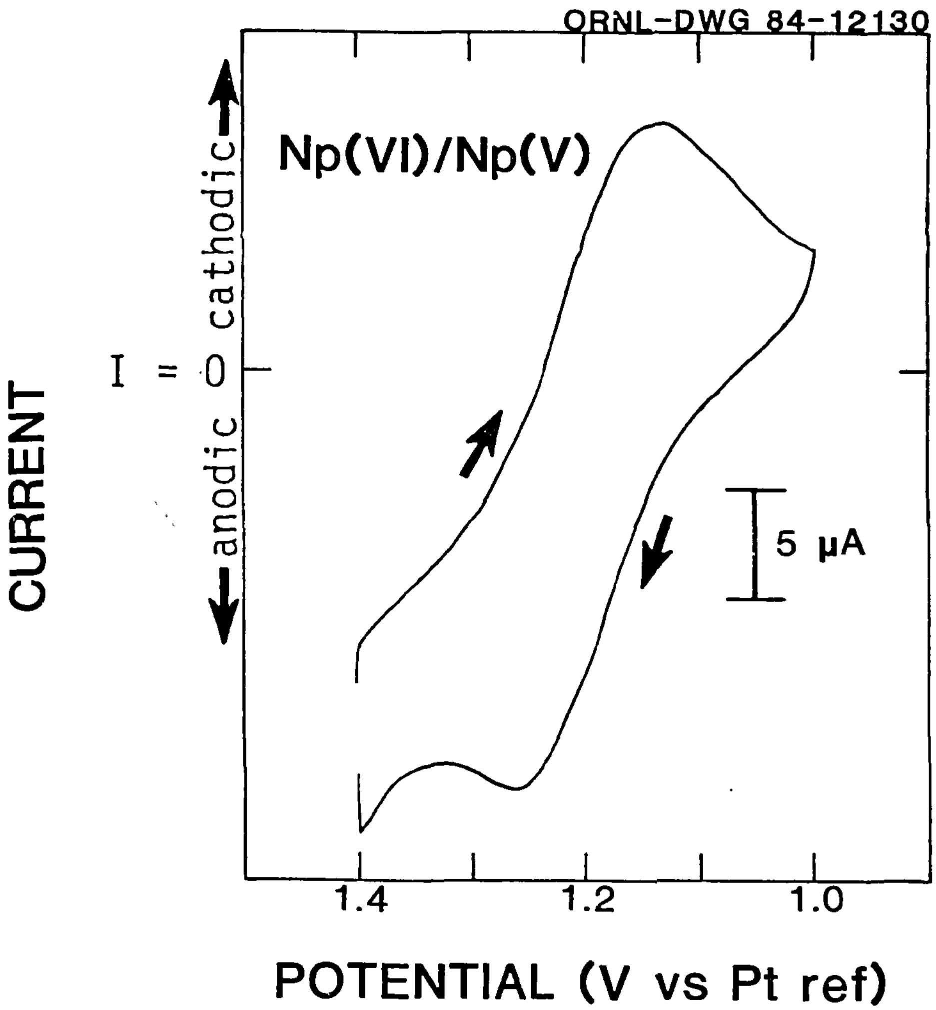

Figure 49. First scan cyclic voltammogram of Np(VI)/Np(V) in molten $DMSO_2$ (0.1 M $LiClO_4$). Scan rate = 50 mV/s; Pt electrode; [Np] = ca. 10^{-3} M.

similarity of the formal potential of the Np(VI)/Np(V) couple to that in aqueous acid solution ($E^{\circ\prime}$ = +1.14 V/NHE, 1 M $HClO_4$ solution)[115] suggest that Np(VI) and Np(V) exist as dioxy cations (NpO_2^{2+} and NpO_2^{+}, respectively) in $DMSO_2$ as they do in water. Similarly, U(VI) and Pu(VI) should exist in $DMSO_2$ solution as dioxy cations.

a. UO_2^{2+} absorption spectra. Numerous reports of the UV-VIS absorption spectrum of the uranyl ion in aqueous solution exist in the literature.[116-120] Changes in complexation in aqueous solution produce changes in the UO_2^{2+} spectrum. Similarly, changes in anions present affect the UO_2^{2+} spectrum in $DMSO_2$, as seen in Figures 50 and 51. However, the concentrations of complexing ions needed to produce changes in the aqueous UO_2^{2+} solution spectrum are much higher (orders of magnitude) than those necessary to produce changes in the $DMSO_2$ solution spectrum of UO_2^{2+}. This is a consequence of the poorer coordinating ability of $DMSO_2$ as compared to H_2O. The visible, vibrational-electronic absorption ($\pi \rightarrow n$ transition) band for yellow U(VI) obtained by dissolution of $UO_2(NO_3)_2{\cdot}6H_2O$ in $DMSO_2$ appears at higher energies than that for U(VI) derived from the dissolution of $UO_2Cl_2{\cdot}nH_2O$ in $DMSO_2$. This energy shift is due to differences in complexation of UO_2^{2+} by Cl^- and NO_3^- ions in $DMSO_2$. In addition, the vibrational substructure is not as well resolved in the spectrum of $UO_2(NO_3)_2{\cdot}nH_2O$ in $DMSO_2$ solution as it is in the spectrum of $UO_2Cl_2{\cdot}nH_2O$ in $DMSO_2$ solution. In both of these $DMSO_2$ solutions, the concentration of anion (Cl^- or NO_3^-) is about the same order of magnitude as that of UO_2^{2+} ion.

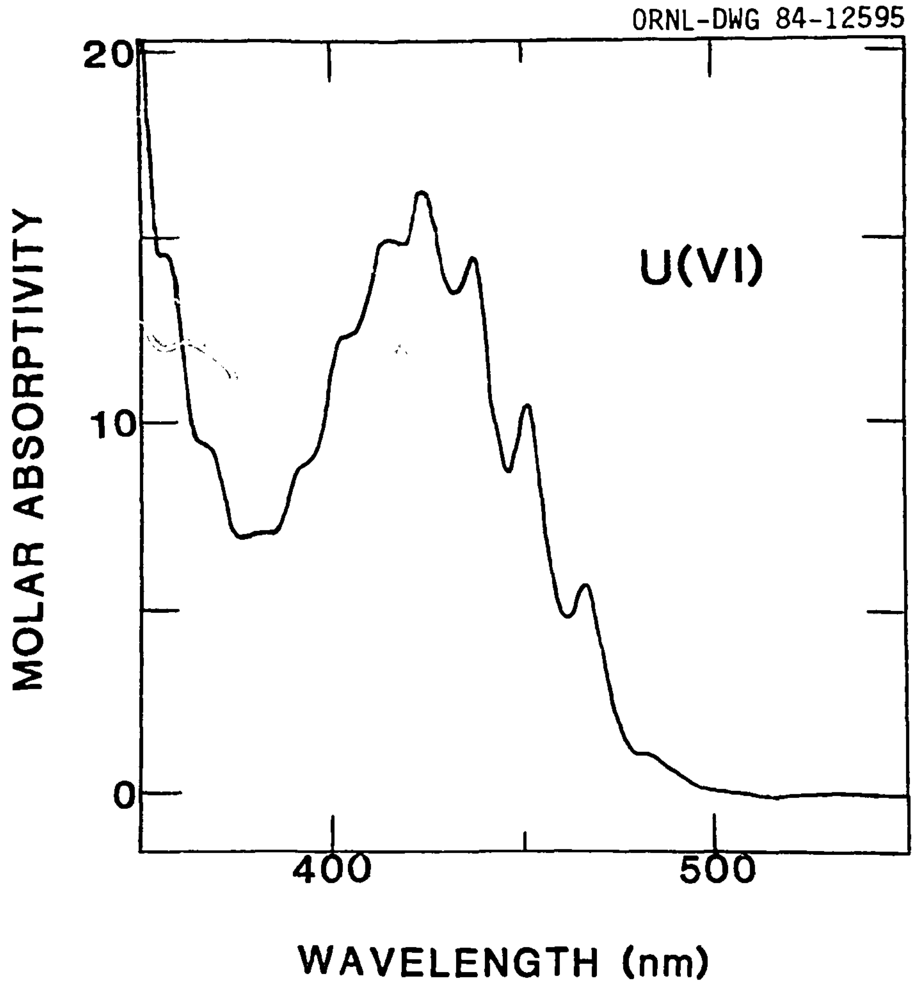

Figure 50. Absorption spectrum of $UO_2(NO_3)_2 \cdot 6H_2O$ in molten $DMSO_2$.

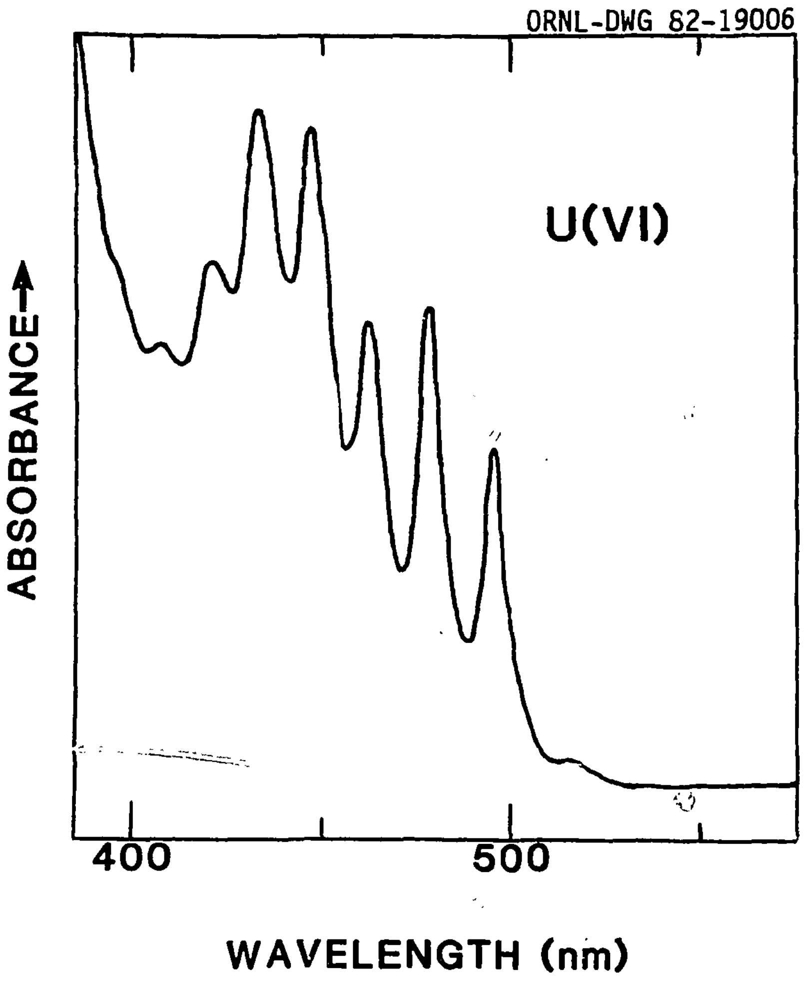

Figure 51. Absorption spectrum of $UO_2Cl_2 \cdot nH_2O$ in molten $DMSO_2$.

b. NpO_2^{2+} absorption spectra. As with UO_2^{2+}, the UV-VIS spectrum of NpO_2^{2+} in $DMSO_2$ solution is dramatically affected by the anion present. Solutions of Np(VI) in $DMSO_2$ are yellow-brown, green-brown, or green-brown with ClO_4^-, Cl^-, or NO_3^- ions, respectively. The UV-VIS absorption spectrum of $NpO_2(NO_3)_2 \cdot nH_2O$ in $DMSO_2$ is shown in Figure 52. The UV absorption "cut off" in the NpO_2^{2+} spectrum occurs at a higher wavelength with Cl^- ion in comparison to the UV "cut offs" in the NpO_2^{2+} spectra with ClO_4^- and NO_3^- ions. When frozen, solutions of $NpO_2Cl_2 \cdot nH_2O$ have a bright yellow-green fluorescent appearance. In contrast, frozen solutions of $NpO_2(NO_3)_2 \cdot nH_2O$ and $NpO_2(ClO_4)_4 \cdot nH_2O$ do not appear to fluoresce (under the illumination of the room fluorescent lights).

In 2 M $HClO_4$ solution, the principal absorption peak of NpO_2^{2+} occurs at 1223 nm (ε = 45 M^{-1} cm^{-1}).[121] A very similar spectrum of NpO_2^{2+} is obtained in aqueous HNO_3 solution.[122] No such near-IR peak is observed for $NpO_2(NO_3)_2 \cdot nH_2O$ in $DMSO_2$. The peak may be partially obscured by the background $DMSO_2$ absorption, but any such peak would have to have a molar absorptivity value considerably below that of the coresponding absorption peak in aqueous solution. This near-IR peak is, however, seen in the spectra of $NpO_2Cl_2 \cdot nH_2O$ and $NpO_2(ClO_4)_2 \cdot nH_2O$ in $DMSO_2$ solutions at 1245 and 1223 nm, respectively.

c. PuO_2^{2+} absorption spectra. The principal electronic absorption peak of PuO_2^{2+} in 1 M $HClO_4$ solution occurs at 831 nm (ε = 555 M^{-1} cm^{-1}).[123] This f-f absorption peak occurs at 846, 838, and 831 nm for Pu(VI) derived from the dissolutions of $PuO_2Cl_2 \cdot nH_2O$,

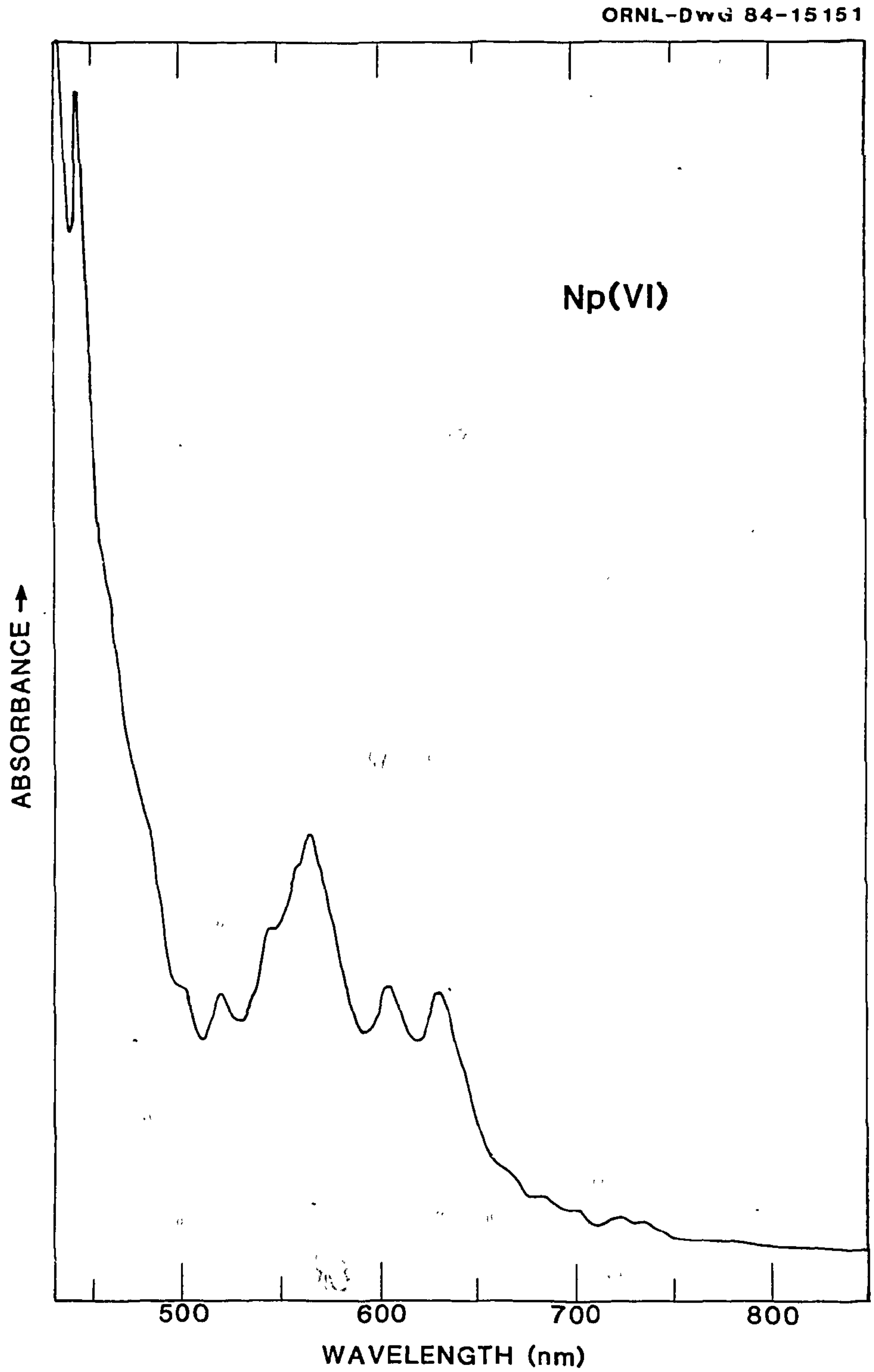

Figure 52. Absorption spectrum of $NpO_2(NO_3)_2 \cdot nH_2O$ in molten $DMSO_2$.

$PuO_2(NO_3)_2 \cdot nH_2O$, and $PuO_2(ClO_4)_2 \cdot nH_2O$ in $DMSO_2$, respectively. The spectrum of $PuO_2(NO_3)_2 \cdot nH_2O$ in $DMSO_2$ (turbid solution, see Chapter II, page 41) also exhibits an absorption peak at 817 nm that is not seen in the spectra of $PuO_2Cl_2 \cdot nH_2O$ and $PuO_2(ClO_4)_2 \cdot nH_2O$ in $DMSO_2$ solutions. Both $PuO_2(NO_3)_2 \cdot nH_2O$ and $PuO_2(ClO_4)_2 \cdot nH_2O$ in $DMSO_2$ solutions are light yellow. Solutions of $PuO_2Cl_2 \cdot nH_2O$ in $DMSO_2$ are a more intense yellow. The spectrum of $PuO_2Cl_2 \cdot nH_2O$ in $DMSO_2$ has an additional intense absorption peak at 393 nm (see Figure 53) that is not seen in the PuO_2^{2+} spectra with NO_3^- and ClO_4^- ions, which accounts reasonably well for the difference in color of the solutions. The source of this 393 nm absorption peak is not related to the oxidized Cl^- ion absorption peak described earlier (see page 142) since the latter occurs at ca. 360 nm.

3. Actinide(VI) Raman Spectra

The observed AnO_2^{2+} symmetric stretch frequencies (ν_1) for the hexavalent actinide perchlorates in $DMSO_2$ solution, along with those obtained by others[32] for actinyl ions in 0.01 M $HClO_4$ solution, are given in Table X. Both U(VI) and Pu(VI) exhibit the same ν_1 values (within experimental error) in $DMSO_2$ and in 0.01 M $HClO_4$ solutions. However, there is a 13 cm^{-1} difference between the ν_1 value for Np(VI) in molten dimethyl sulfone and that in 0.01 M $HClO_4$ solutions. A more linear relationship between ν_1 and atomic number is apparent in $DMSO_2$ than it is in 0.01 M $HClO_4$ for the three dioxy cations. The anion also has an effect on the value of ν_1. With NO_3^- ion, ν_1 = 866 $\pm$ 2

ORNL-DWG 84-15152

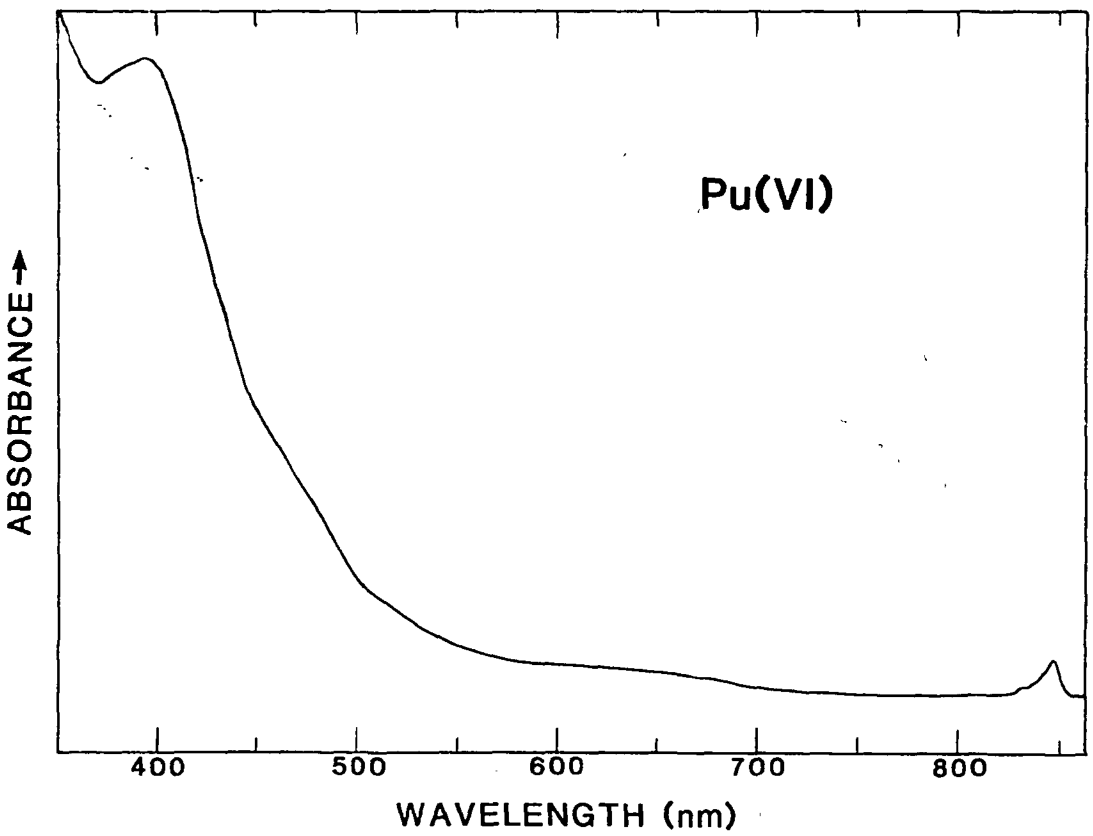

Figure 53. Absorption spectrum of $PuO_2Cl_2 \cdot nH_2O$ in molten $DMSO_2$.

TABLE X

AnO_2^{2+} SYMMETRIC STRETCH (ν_1) FREQUENCY (cm^{-1})

Solvent:	Molten $DMSO_2$[a]	0.01 M $HClO_4$
U(VI)	872 ± 2	872
Np(VI)	850 ± 2	863
Pu(VI)	834 ± 2	835

[a]The anion present is ClO_4^- ion.

cm^{-1} and 846 ± 2 cm^{-1} for U(VI) and Np(VI), respectively, in $DMSO_2$ solution.

Aqueous solutions of UO_2^{2+} fluoresce when excited by 514.5 Ar ion laser light. In molten $DMSO_2$, UO_2^{2+} fluoresces weakly when excited by 514.5 nm laser light, and no fluorescent background is noticed in the Raman spectrum of UO_2^{2+} (with 514.5 nm laser light excitation). However, in the frozen state, UO_2^{2+} in $DMSO_2$ solution exhibits a fluorescent background in its Raman spectrum. This background is not apparent at UO_2^{2+} concentrations of 0.1 <u>M</u> or lower; however, the fluorescent background at 1 <u>M</u> UO_2^{2+} concentration in frozen $DMSO_2$ is sufficiently large to obliterate the Raman signal of U(VI).

The Raman spectrum of $UO_2(NO_3)_2 \cdot nH_2O$ in molten $DMSO_2$ solution is presented in Figure 54. The depolarization ratio ρ [I_T (obs. ||)/I_T (obs. ⊥)] of the 695 cm^{-1} Raman peak (corresponding to the O=S=O symmetric stretch of $DMSO_2$) is dependent on the nature and concentration of the solute present. A noticeable effect on ρ (695 cm^{-1}) due to the presence of $UO_2(NO_3)_2 \cdot 6H_2O$ in $DMSO_2$ was observed. As seen in Table XI, the presence of 0.15 <u>m</u> $UO_2(NO_3)_2 \cdot nH_2O$ in $DMSO_2$ increases the value of ρ (695 cm^{-1}) from 0.052 (for pure $DMSO_2$) to 0.23 (an increase of greater than a factor of four). The amount of increase in ρ (695 cm^{-1}) is dependent on the concentration of the solute. At higher concentrations of $UO_2(NO_3)_2 \cdot 6H_2O$ in $DMSO_2$, the value of ρ (695 cm^{-1}) decreases (see Table XI). While $DMSO_2$ solutions containing only $LiNO_3$ or $NaNO_3$ have an effect on ρ (695 cm^{-1}), the

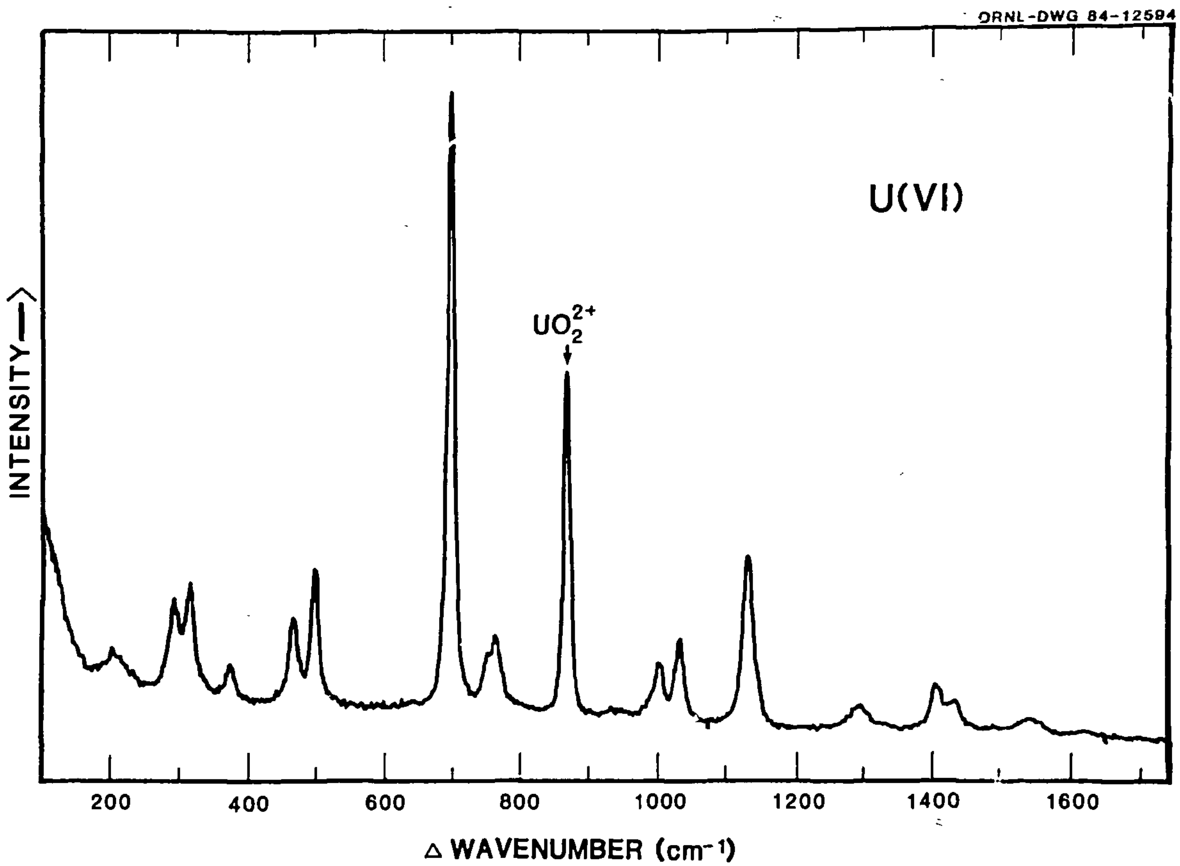

Figure 54. Raman spectrum of 1.0 m $UO_2(NO_3)_2 \cdot 6H_2O$ in molten $DMSO_2$. The 866 cm^{-1} peak is due to UO_2^{2+}. All other Raman peaks are due to vibrations of the solvent molecules. The nonpolarized 466 cm^{-1} $DMSO_2$ Raman peak was used as an "internal standard" (see Table XI, page 155).

TABLE XI

$DMSO_2$ DEPOLARIZATION RATIOS AT 695 cm^{-1}

Solute	ρ (695 cm^{-1})[a]
None	0.052
0.35 m $LiNO_3$	0.057
0.66 m $LiNO_3$	0.066
0.89 m $LiNO_3$	0.081
0.10 m $LiClO_4$	0.069
0.087 m $NaNO_3$	0.092
0.40 m $NaNO_3$	0.11
0.84 m $NaNO_3$	0.083
0.051 m $UO_2(NO_3)_2 \cdot 6H_2O$	0.16
0.15 m $UO_2(NO_3)_2 \cdot 6H_2O$	0.23
1.0 m $UO_2(NO_3)_2 \cdot 6H_2O$	0.093
0.089 m $UO_2(NO_3)_2 \cdot 6H_2O$ + 0.77 m $LiNO_3$	0.080

[a]The ρ values were multiplied by a correction factor to account for instrumental effects. The nonpolarized 466 cm^{-1} $DMSO_2$ Raman peak was used as an "internal standard." Ideally, ρ = 0.86 for a totally nonpolarized vibration (with the instrumentation used in this work). Thus, the correction factor was 0.86/ρ (466 cm^{-1}). No noticeable solute effect on ρ (466 cm^{-1}) was observed.

magnitude of the solute effect is not as large as it is with $UO_2(NO_3)_2 \cdot 6H_2O$.

The $DMSO_2$ depolarization ratio at 695 cm^{-1} increases by a factor of three with 0.051 m $UO_2(NO_3)_2 \cdot 6H_2O$ in $DMSO_2$ solution (see Table XI). It is surprising that such a significant change in ρ (695 cm^{-1}) occurs when the ratio of moles of solvent (dimethyl sulfone is 10.6 m) to moles of solute is over 200. When another source of NO_3^- ion is added to a solution of $UO_2(NO_3)_2 \cdot 6H_2O$ in $DMSO_2$, the effect on ρ (695 cm^{-1}) diminishes (with sufficiently high concentration of NO_3^- ion). Thus, this effect is dependent on both solute cation and anion concentrations. The mechanism of the solute effect does not appear to involve a simple coordination effect between $UO_2(NO_3)_2 \cdot 6H_2O$ and $DMSO_2$ based on the large concentration difference between the solute and the solvent. However, the effect is concentration dependent. Traces of water in $DMSO_2$ reduced the magnitude of the solute effect on ρ (695 cm^{-1}). Thus, actinide solutions prepared by injecting aqueous aliquots into $DMSO_2$ were not suitable for studies of the solute effect on ρ (695 cm^{-1}). The mechanism behind this solute effect on the depolarization ratio of the 695 cm^{-1} Raman peak is unknown at this time.

CHAPTER V

CONCLUSIONS

A. Aqueous Carbonate-Hydroxide Solution

1. Neptunium

Definite changes in the complexation of Np(V) in Na_2CO_3 solution as the pH is increased above 13 were indicated on the basis of absorption spectroscopic and potentiometric measurements. The exact nature of the Np(V) complexes in Na_2CO_3-NaOH solution are unknown and further studies are necessary. Neptunium(VI) is not stable in concentrated Na_2CO_3 solution as the pH is increased; it either forms a precipitate or is reduced to Np(V). Similarly, gray Np(IV) in 2 M Na_2CO_3 solution is not stable when the pH is increased above 11.7; it forms a gray precipitate. Neptunium(III) in carbonate solution is rapidly oxidized by water. This instability is expected, based on the strong complexation of actinides(IV) by carbonate ion and the concomitant shift of the formal potentials of An(IV)/An(III) couples to more negative values.[31,45]

Heptavalent neptunium cannot be produced in concentrated Na_2CO_3 solution unless the pH is ca. 14 or greater. The Raman spectrum of Np(VII) in Na_2CO_3-NaOH solution is quite similar to that of Np(VII) in NaOH solution, indicating that the complexation of Np(VII) is due principally, if not completely, to hydroxide ions.

2. Plutonium

Changes in the complexation of Pu(VI) and Pu(V) in carbonate solution as the pH was increased above 13 were seen based on spectrophotometric and potentiometric data. Plutonium(VI) oxidation to Pu(VII) in 2 M Na_2CO_3 solution requires at least 2.5 M OH^- ion. Carbonate ion seems to impede the oxidation of Pu(VI), and hydroxide ions seem to be responsible for the complexation of Pu(VII). The Raman spectrum of Pu(VII) in carbonate-hydroxide solution reveals a single plutonium peak at 703 ± 6 cm^{-1} that appears to be only moderately polarized. Plutonium(IV) is insoluble in Na_2CO_3 solution above pH 11.4 but is soluble in K_2CO_3 solution up to pH 12 or pH 13. Reduction of Pu(IV) in Na_2CO_3 solution yields a blue precipitate of Pu(III). In K_2CO_3 solution, however, reduction of Pu(IV) generates a blue solution of Pu(III) which is sensitive to air oxidation.

3. Americium

Evidence for the formation of hydroxo (and/or carbonato-hydroxo) complexes of Am(V) and Am(VI) in 2 M Na_2CO_3 solution was seen spectrally. The stability of Am(VI) in 2 M Na_2CO_3 solution decreases with increasing hydroxide ion concentration. More abrupt changes in the spectrum of Am(V) in 2 M Na_2CO_3 solution as the pH is increased are seen in comparison to the more gradual changes in the associated spectra of Np(V) and Pu(V). This suggests that Am(V) may be complexed by hydroxide ions in carbonate solution more strongly than are Np(V) and Pu(V).

4. Californium

Based on the similarity of the standard reduction potentials of the Cf(IV)/Cf(III)[5] and Tb(IV)/Tb(III)[5] couples and the stabilization of Tb(IV) in aqueous carbonate-hydroxide solution,[4] it was hoped that Cf(IV) could be stabilized in similar solutions. However, aqueous carbonate-hydroxide solution does not appear to provide a sufficient complexation environment for the stabilization of Cf(IV).

The inability to oxidize Cf(III) in carbonate-hydroxide solution suggests that the calculated value of the reduction potential of the Cf(IV)/Cf(III) couple may be too low. Alternatively, the shift in the formal potential of the Cf(IV)/Cf(III) couple provided by carbonate-hydroxide solution may not be sufficient to stabilize Cf(IV).

5. Terbium

Terbium(IV) does not appear to be similar to Ce(IV), Am(IV), and Bk(IV) in carbonate solution. The chemistry of the formation of Tb(IV) appears to be complicated. Since Cm(III) and Cf(III) could not be oxidized in carbonate-hydroxide solution,[94] the chemistry involved in the oxidation of Tb(III) in K_2CO_3-KOH solution is different from that of Cm(III) and Cf(III) in the same medium. Stabilization of Tb(IV) is provided not only by complexation with carbonate and hydroxide ions but also by the possible formation of a thermodynamically stable cluster involving Tb(IV and/or III), CO_3^{2-}, and OH^- ions. The exact nature of the Tb(IV) cluster is unknown.

Cluster formation involving Cm(IV) or Cf(IV) does not seem to take place in aqueous carbonate-hydroxide solution.

B. Molten Dimethyl Sulfone Solution

1. Lanthanide(III)/Lanthanide(II) Couples

Charge-transfer bands were observed in the $DMSO_2$ solution UV absorption spectra of chloro complexes of Sm(III), Eu(III), and Yb(III). These bands are shifted to lower energies in $DMSO_2$ solution compared to aqueous solution because $DMSO_2$ is a poorer coordinating ligand than is H_2O, thus making chloride ion complexation more favorable in $DMSO_2$.

Divalent Eu was stabilized in molten $DMSO_2$. Ytterbium(III) and samarium(III) in $DMSO_2$ solution could not be electrochemically reduced (in bulk) to their divalent oxidation states. The $DMSO_2$ purification method used (see Chapter II, page 32) may not be sufficient to stabilize Yb(II) and Sm(II) in molten $DMSO_2$. Anhydrous chloride and perchlorate salts of Yb(III) and Sm(III) are insoluble in $DMSO_2$. Dichloride salts of Yb and Sm are also insoluble in $DMSO_2$.

2. Cerium(IV)/Cerium(III) Couple

Cerium(IV) forms strong chloro complexes in $DMSO_2$ solution resulting in a large negative shift in the Ce(IV)/Ce(III) reduction potential in $DMSO_2$ solution compared with that in water. Cerium(III) was electrochemically oxidized to Ce(IV) in $DMSO_2$ solution containing 1 M $(NH_4)_2CO_3$ and 1 M NH_4NO_3. The NH_4NO_3 is necessary to prevent the precipitation of cerium(IV,III) carbonate.

3. Americium(III)

Ligand-to-metal charge-transfer bands observed in the $DMSO_2$ solution UV absorption spectra of $SmCl_3 \cdot 6H_2O$, $EuCl_3 \cdot 6H_2O$, and $YbCl_3 \cdot 6H_2O$ were not observed in the corresponding spectrum of $AmCl_3 \cdot nH_2O$. This is a result of the relatively more negative potential of the Am(III)/Am(II) couple compared to the (III)/(II) potentials of Eu, Yb, and Sm. Absorption bands of $AmCl_3 \cdot nH_2O$ in $DMSO_2$ solution are seen at 305 and 358 nm. These bands may result from charge-transfer between the complexed Cl^- ions and $DMSO_2$ molecules.

4. Actinides(VI)

Differences in the U(VI), Np(VI), and Pu(VI) absorption spectra in $DMSO_2$ solution with different anions (ClO_4^-, NO_3^-, and Cl^-) were seen and are attributed to complexation effects. Similarly, the anion present has an effect on the symmetric stretch frequency of the AnO_2^{2+} species. While complexation effects can also be observed in aqueous solution, the concentration of the complexing ions must be much higher than that in $DMSO_2$ to observe the same magnitude of spectral shifts/changes as seen in $DMSO_2$.

The concentration and nature of the solute affect the value of the depolarization ratio ρ of the O=S=O symmetric stretch (695 cm^{-1}) in $(CH_3)_2SO_2$. For example, the presence of $UO_2(NO_3)_2 \cdot 6H_2O$ in $DMSO_2$ solution produces an increase in ρ (695 cm^{-1}). The value of ρ (695 cm^{-1}) initially increases with increasing $UO_2(NO_3)_2 \cdot 6H_2O$ concentration and then decreases with larger concentrations (e.g., 1 M) of $UO_2(NO_3)_2 \cdot 6H_2O$ in $DMSO_2$ solution. This effect on ρ (695 cm^{-1}) depends on both the uranyl and nitrate ion concentrations.

LIST OF REFERENCES

LIST OF REFERENCES

1. T. Moeller, "The Chemistry of the Lanthanides," Reinhold Publ., New York, 1963.

2. F. A. Cotton and G. Wilkinson, "Advanced Inorganic Chemistry," 4th Ed., John Wiley and Sons, New York, 1980, Chpt. 23, p. 1002.

3. L. J. Nugent, J. Inorg. Nucl. Chem., 37, 1767 (1970).

4. D. E. Hobart, K. Samhoun, J. P. Young, V. E. Norvell, G. Mamantov, and J. R. Peterson, Inorg. Nucl. Chem. Lett., 16, 321 (1980).

5. L. J. Nugent, R. D. Baybarz, J. L. Burnett, and J. L. Ryan, J. Phys. Chem., 77, 1528 (1973).

6. G. R. Choppin, Radiochim. Acta, 32, 43 (1983).

7. C. Keller, "The Chemistry of the Transuranium Elements," Verlag Chemie, GmbH, Germany, 1971, Part 1, Chpts. 5 and 9.

8. J. C. Sullivan, S. Gordon, W. A. Mulac, K. H. Schmidt, D. Cohen, and R. Sjoblom, Inorg. Nucl. Chem. Lett., 12, 599 (1976).

9. B. F. Myasoedov, "Actinides in Perspective," N. Edelstein, Ed., Pergamon Press, Oxford, 1982, p. 509.

10. T. K. Keeenan, J. Am. Chem. Soc., 83, 3719 (1961).

11. V. P. Shilov, Sov. Radiochem. (Engl. Transl.), 18, 567 (1976).

12. W. T. Carnall, "Handbook on the Physics and Chemistry of Rare Earths," Vol. 3, K. A. Gschneider and L. Eyring, Eds., North-Holland Publishing Company, Amsterdam, 1979, Chpt. 24, p. 171.

13. S. Ahrland, J. O. Lijenzin, and J. Rydberg, "Comprehensive Inorganic Chemistry," Vol. 5, J. C. Bailar, Jr., H. J. Eméleus, R. Nyholm, and A. F. Trotman-Dickenson, Eds., Pergamon Press, Oxford, 1973, p. 477.

14. R. B. Heslop and K. Jones, "Inorganic Chemistry," Elsevier Scientific Publishing Company, Amsterdam, 1976, Chpt. 28.

15. T. Moeller, "Lanthanides and Actinides," Vol. 7, K. W. Bagnall, Ed., Butterworths and Co., London, 1972, Chpt. 7.

16. Ref. 7, Part 1, Chpt. 9.

17. C. Madic, D. E. Hobart, and G. M. Begun, Inorg. Chem., 22, 1494 (1983).

18. J. B. Headridge, "Electrochemical Techniques for Inorganic Chemists," Academic Press, London, 1969, Chpt. 8.

19. A. N. Kamenskaya, K. Bukietynska, N. B. Mikheev, V. I. Spitsyn, and B. Jezowska-Trzebiatowska, Russ. J. Inorg. Chem. (Engl. Transl.), 24, 633 (1979).

20. J. M. Cleveland, "Plutonium Handbook. A Guide to Technology," Vol. 2, O. J. Wick, Ed., Gordon and Breach, New York, 1967, Chpt. 14.

21. G. A. Burney, Nucl. Appl. Tech., 4, 217 (1968).

22. B. Allard, "Actinides in Perspective," N. Edelstein, Ed., Pergamon Press, Oxford, 1982, p. 553.

23. W. J. Deutsch and R. J. Serne, "Geochemical Behavior of Disposed Radioactive Waste," G. C. Barney, J. D. Navratil, and W. W. Schulz, Eds., American Chemical Society: Seattle, Washington, 1983, ACS Symp. Ser. No. 246.

24. L. Maya, Inorg. Chem., 21, 2895 (1982).

25. D. W. Wester and J. C. Sullivan, Inorg. Chem., 19, 2838 (1980).

26. S. O. Cinneide, J. P. Scanlan, and M. J. Hynes, J. Inorg. Nucl. Chem., 37, 1013 (1975).

27. J. P. Scanlan, J. Inorg. Nucl. Chem., 39, 635 (1971).

28. S. Casadio and F. Orlandini, J. Electroanal. Chem., 26, 91 (1970).

29. D. Cohen, J. Inorg. Nucl. Chem., 32, 3525 (1970).

30. D. W. Wester and J. C. Sullivan, J. Inorg. Nucl. Chem., 43, 2919 (1981).

31. A. M. Fedoseev, V. F. Peretrukhin, and N. N. Krot, Dokl. Phys. Chem. (Engl. Transl.), 244, 139 (1979).

32. L. J. Basile, J. R. Ferraro, M. L. Mitchell, and J. C. Sullivan, Appl. Spectrosc., 32, 535 (1978).

33. G.A. Simakin, Sov. Radiochem. (Engl. Transl.), 19, 424 (1977).

34. G. A. Simakin, Yu. F. Volkov, G. I. Visyashcheva, I. I. Kapshukov, P. F. Baklanova, and G. N. Yakovlev, Sov. Radiochem. (Engl. Transl.), 16, 838 (1974).

35. A. I. Moskvin, Sov. Radiochem. (Engl. Transl.), 13, 694 (1971).

36. K. Ueno and M. Hoshi, J. Inorg. Nucl. Chem., 33, 2631 (1971).

37. G. A. Simakin and I. V. Matyashchuk, Sov. Radiochem. (Engl. Transl.), 11, 472 (1969).

38. D. S. Gorbeko-Germanov, and V. C. Klimov, Russ. J. Inorg. Chem. (Engl. Transl.), 11, 280 (1966).

39. D. W. Wester and J. C. Sullivan, Radiochem. Radioanal. Lett., 57, 35 (1983).

40. M. Woods, M. L. Mitchell, and J. C. Sullivan, Inorg. Nucl. Chem. Lett., 14, 465 (1978).

41. S. Casadio and F. Orlandini, J. Inorg. Nucl. Chem., 34, 3845 (1972).

42. A. D. Gel'man, A. I. Moskvin, and V. P. Zaitseva, Sov. Radiochem. (Engl. Transl.), 4, 138 (1962).

43. A. I. Moskvin and A. D. Gel'man, Russ. J. Inorg. Chem. (Engl. Transl.), 4, 198 (1958).

44. J. Y. Bourges, B. Guillaume, G. Koehly, D. E. Hobart, and J. R. Peterson, Inorg. Chem., 22, 1179 (1983).

45. D. E. Hobart, K. Samhoun, and J. R. Peterson, Radiochim. Acta, 31, 139 (1982).

46. R. D. Baybarz, Atomic Energy Rev., 8, 327 (1970).

47. J. S. Coleman, T. K. Keenan, L. H. Jones, W. T. Carnall, and R. A. Penneman, Inorg. Chem., 2, 58 (1963).

48. J. R. Stokely, R. D. Baybarz, and J. R. Peterson, J. Inorg. Nucl. Chem., 34, 392 (1972).

49. R. D. Baybarz, J. R. Stokely, and J. R. Peterson, J. Inorg. Nucl. Chem., 34, 739 (1972).

50. B. Bry and B. Tremillon, J. Electroanal. Chem., 30, 457 (1971).

51. T. R. Griffiths, Chem. Commun., 23, 1222 (1967).

52. W. R. Feairheller, Jr. and J. E. Katon, Spectrochim. Acta, 20, 1099 (1964).

53. A. J. Bard and L. J. Faulkner, "Electrochemical Methods," John Wiley and Sons, New York, 1980, Chpt. 2, p. 52.

54. Ref. 53, Chpt. 10, p. 377.

55. G. M. Barrow, "Physical Chemistry," 3rd Ed., McGraw-Hill Book Co., New York, 1973, Chpt. 22, p. 629.

56. Ref. 53, Chpt. 6, p. 215.

57. W. R. Heineman, Anal. Chem., 50, 390A (1980).

58. Ref. 53, Chpt. 14.

59. Ref. 53, Chpt. 1, p. 23.

60. D. T. Sawyer and J. L. Roberts, "Experimental Electrochemistry for Chemists," John Wiley and Sons, New York, 1974, Chpt. 3, p. 118.

61. D. E. Hobart, V. E. Norvell, P. G. Varlashkin, H. E. Hellwege, and J. R. Peterson, Anal. Chem., 54, 1634 (1983).

62. V. E. Norvell and G. Mamantov, Anal. Chem., 49, 1470 (1977).

63. R. D. Baybarz, J. B. Knauer, and P. B. Orr, U.S. Atomic Energy Commission Document No. ORNL-4672, 1973.

64. J. Bjerrum and J. P. McReynolds, "Inorganic Syntheses," Vol. II, W. C. Fernelius, Ed., McGraw-Hill Book Co., New York, 1946, p. 217.

65. J. Kinnunen and B. Wennerstrand, Chemist-Analyst, 46, 92 (1957).

66. R. Goulden, "Comprehensive Analytical Chemistry," Vol. 1B, C. L. Wilson and D. W. Wilson, Eds., Elsevier Publ. Co, Amsterdam, 1960, p. 421.

67. J. Halperin, "CARBEX: A computer program to provide species concentrations in synthetic 'carbonate' containing solutions at selected temperatures and ionic strengths," Oak Ridge National Laboratory Internal Document No. ORNL/CF-82/36, 1982.

68. S. K. Ramalingam and S. Soundararajan, Curr. Sci., 35, 233 (1966).

69. Ref. 18, Chpt. 5, p. 45.

70. Ref. 53, Chpt. 6, p. 228.

71. Ref. 53, Chpt. 5, p. 160.

72. Ref. 53, Chpt. 6, p. 219.

73. Ref. 53, Chpt. 6, p. 229.

74. Ref. 60, Chpt. 2, p. 74.

75. Ref. 53, Chpt. 6, p. 230.

76. Ref. 60, Chpt. 1, pp. 14, 17, and 23.

77. Ref. 53, Chpt. 13, p. 571.

78. P. G. Varlashkin, D. E. Hobart, G. M. Begun, and J. R. Peterson, Radiochim. Acta, 35, 91 (1984).

79. D. Cohen and S. Fried, Inorg. Nucl. Chem. Lett., 5, 653 (1969).

80. Yu. F. Volkov, G. I. Visyashcheva, S. V. Tomlin, I. I. Kapshukov, and A. G. Rukov, Sov. Radiochem. (Engl. Transl.), 23, 191 (1981).

81. L. Maya, Inorg. Chem., 22, 2093 (1983).

82. C. Madic, G. M. Begun, D. E. Hobart, and R. L. Hahn, Inorg. Chem., 23, 1914 (1984).

83. I. M. Kolthoff and J. J. Lingane, "Polarography," Interscience Publishers, Inc., New York, 1941, Chpt. 10, p. 172.

84. L. J. Basile, J. C. Sullivan, J. R. Ferraro, and P. LaBonville, Appl. Spectrosc., 28, 142 (1974).

85. P. G. Varlashkin, G. M. Begun, and J. R. Peterson, Radiochim. Acta, in press.

86. U. Schedin, Acta Chem. Scand., Ser. A, A29, 333 (1975).

87. Ref. 7, Part 2, Chpt. 2, p. 421.

88. N. N. Krot and A. D. Gel'man, Dokl. Phys. Chem. (Engl. Transl.), 177, 987 (1967).

89. D. Cohen, J. Inorg. Nucl. Chem., 18, 211 (1961).

90. P. K. Bhattacharyya, R. Veeraraghavan, and R. D. Saini, Radiochim. Acta, 30, 217 (1982).

91. Yu. A. Komkov, V. P. Peretrukhin, V. P. Krot, and N. N. Gel'man, Sov. Radiochem. (Engl. Transl.), 11, 398 (1969).

92. V. I. Spitsyn, A. D. Gel'man, N. N. Krot, M. P. Mefodiyeva, F. A. Zakharova, Yu. A. Komkov, V. P. Shilov, and I. V. Smirnova, J. Inorg. Nucl. Chem., 31, 2733 (1969).

93. D. Cohen, Inorg. Nucl. Chem. Lett., 8, 533 (1972).

94. D. E. Hobart, P. G. Varlashkin, K. Samhoun, R. G. Haire, and J. R. Peterson, Rev. Chim. Minér., 20, 817 (1983).

95. J. G. Conway, S. Fried, R. M. Latimer, R. McLaughlin, R. G. Gutmacher, W. T. Carnall, and P. Fields, J. Inorg. Nucl. Chem., 28, 3064 (1966).

96. Ref. 7, Part 2, Chpt. 3, p. 516.

97. W. T. Carnall and P. R. Fields, J. Am. Chem. Soc., 81, 4445 (1959).

98. P. G. Varlashkin, G. M. Begun, and J. R. Peterson, J. Less-Common Metals, in press.

99. A. Saito and K. Ueno, J. Inorg. Nucl. Chem., 41, 507 (1979).

100. A. Saito and K. Ueno, J. Inorg. Nucl. Chem., 41, 513 (1979).

101. D. E. Hobart, Ph.D. Dissertation, University of Tennessee (Knoxville), 1981, U.S. Department of Energy Document No. DOE/ER/04447-124.

102. R. C. Propst, J. Inorg. Nucl. Chem., 36, 1085 (1974).

103. P. G. Varlashkin and J. R. Peterson, J. Less-Common Metals, 94, 333 (1983).

104. M. Machtinger, M. J. Vuaille, and B. Trémillon, J. Electroanal. Chem., 83, 273 (1977).

105. B. Bry and B. Tremillon, Electroanal. Chem., 46, 71 (1973).

106. C. H. Liu, J. Hasson, and G. Pedro Smith, Inorg. Chem., 7, 2245 (1968).

107. C. H. Liu, L. Newman, and J. Hasson, Inorg. Chem., 7, 1868 (1968).

108. C. Auerbach and D. K. McGuire, J. Inorg. Nucl. Chem., 28, 2659 (1966).

109. L. J. Nugent, R. D. Baybarz, and J. L. Burnett, J. Phys. Chem., 73, 1177 (1969).

110. J. L. Ryan and C. K. Jørgenson, J. Phys. Chem., 70, 2845 (1966).

111. J. P. Young, R. G. Haire, R. L. Fellows, and J. R. Peterson, J. Radioanal. Chem., 43, 479 (1978).

112. Ref. 2, Chpt. 17, p. 547.

113. M. Shiloh, M. Givon, and Y. Marcus, J. Inorg. Nucl. Chem., 31, 1807 (1969).

114. Y. Marcus and M. Shiloh, Israel J. Chem., 7, 31 (1969).

115. Ref. 7, Part 2, Chpt. 1, p. 297.

116. V. E. Komarov and N. P. Nekrasova, Sov. Radiochem. (Engl. Transl.), 22, 197 (1978).

117. J. T. Bell and R. E. Biggers, J. Mol. Spectry., 25, 312 (1968).

118. J. T. Bell and R. E. Biggers, J. Mol. Spectry., 22, 262 (1967).

119. J. T. Bell and R. E. Biggers, J. Mol. Spectry., 18, 247 (1965).

120. D. M. Gruen and R. L. McBeth, J. Inorg. Nucl. Chem., 9, 290 (1959).

121. P. G. Hagan and J. M. Cleveland, J. Inorg. Nucl. Chem., 28, 2905 (1966).

122. H. A. Friedman and L. M. Toth, J. Inorg. Nucl. Chem., 42, 1347 (1980).

123. T. W. Newton and F. B. Baker, J. Phys. Chem., 61, 934 (1957).

VITA

Peter Gregory Varlashkin was born in Johnson City, Texas on [redacted] He attended J. H. Rose High School in Greenville, North Carolina and graduated in June of 1976. He entered East Carolina University in Greenville, North Carolina in August of 1976. In 1977 he transferred to North Carolina State University, Raleigh, and graduated with a B.S. in Chemistry, summa cum laude, in May of 1980. He entered graduate school at the University of Tennessee, Knoxville, in September of 1980 and received a Ph.D. in Chemistry in March of 1985. Peter Varlashkin has co-authored papers appearing in Analytical Chemistry, Journal of the Less-Common Metals, Revue de Chimie Minérale, and Radiochimica Acta.